



Cite this: *Digital Discovery*, 2025, 4, 1685

## Democratizing self-driving labs: advances in low-cost 3D printing for laboratory automation

Sayan Doloi,<sup>a</sup> Maloy Das,<sup>a</sup> Yujia Li,<sup>a</sup> Zen Han Cho,<sup>a</sup> Xingchi Xiao,<sup>a</sup> John V. Hanna,<sup>ab</sup> Matthew Osvaldo<sup>a</sup> and Leonard Ng Wei Tat<sup>ab\*</sup>

Laboratory automation through self-driving labs represents a transformative approach to accelerating scientific discovery, particularly in chemical sciences, biological sciences, materials science, and high-throughput experimentation. However, widespread adoption of these technologies faces a significant barrier: the prohibitive costs of commercial automation systems, which can range from tens to hundreds of thousands of dollars. This financial hurdle has created a technological divide, limiting access primarily to well-funded institutions and leaving many research facilities unable to leverage the benefits of automated experimentation. 3D printing technology emerges as a democratizing force in this landscape, offering a revolutionary solution to the accessibility challenge. By enabling the production of customizable laboratory equipment at a fraction of the cost of commercial alternatives, 3D printing is transforming how researchers approach laboratory automation. This approach not only reduces financial barriers but also promotes innovation through open-source designs, allowing researchers to share, modify, and improve upon existing solutions. This review addresses a critical gap in the current literature by exploring both the transformation of low-cost Fused Deposition Modelling (FDM) 3D printers into sophisticated automation platforms and the use of FDM 3D-printed components to develop a broad

Received 30th December 2024  
Accepted 20th May 2025

DOI: 10.1039/d4dd00411f

rsc.li/digitaldiscovery

<sup>a</sup>School of Materials Science and Engineering (MSE), Nanyang Technological University, 50 Nanyang Ave, 639798, Singapore. E-mail: leonard.ngwt@ntu.edu.sg

<sup>b</sup>University of Warwick, Department of Physics, Millburn House, Coventry CV4 7AL, UK



From left to right: Yujia Li, Maloy Das, Sayan Doloi, Matthew Osvaldo, Zen Han Cho, Xingchi Xiao

The NGenuity Lab, led by Dr Leonard Ng, is based at the School of Materials Science and Engineering (MSE), Nanyang Technological University (NTU), Singapore. The group operates at the intersection of hardware, software, and materials science, and is focused on developing self-driving laboratories for photovoltaics research. Their work integrates advanced hardware for high-throughput experimentation, AI-driven software for data analysis and outcome prediction, and materials science expertise, aiming to accelerate the discovery of efficient, low-cost solar cell materials.

(From left) Yujia Li is a second year PhD student in the group and is working on hybrid perovskite solar cell devices. He received his bachelor's degree in engineering from the School of Materials Science and Engineering (MSE) at Nanyang Technological University (NTU) in 2023. Maloy Das is a second year PhD student in the group, working on organic photovoltaics (OPV) and hybrid perovskite solar cell devices. He received his master's degree from IIT Jodhpur in 2022. Sayan Doloi is a first year PhD student in the group and is working on the design and development of self-driving labs for OPV development. He received his master's degree from IIT Indore in 2024. Matthew Osvaldo is a final year bachelor's student at the School of Materials Science and Engineering (MSE), Nanyang Technological University (NTU). He is currently pursuing his final-year project on the development and integration of optimization algorithms in self-driving labs. Zen Han Cho is a first year PhD student in the group and is working on integrating both large language models and machine learning to optimize experimental processes in OPV development. He received his bachelor's degree in engineering from the School of Materials Science and Engineering (MSE) at NTU in 2024. Xingchi Xiao received his PhD degree from Nanyang Technological University (NTU) in 2024. He is now a postdoctoral researcher in the group, working on screen printing of carbon electrodes for perovskite and organic solar cells.



range of affordable laboratory automation systems. Furthermore, we explore how strategic modifications enable these systems to serve as automatic liquid handlers, robotic arms, automated sample preparation and detection systems, chemical reactionware, automated imaging systems and bioprinting units. The integration of these modified 3D-printed components with machine learning and artificial intelligence algorithms creates unprecedented opportunities for developing accessible, highly flexible self-driving laboratories.

## 1 Introduction

Self-driving laboratories (SDLs) represent a rapidly advancing field that integrates automated physical experimentation with intelligent, algorithm-driven decision-making. By combining robotics, artificial intelligence, and automation technologies, SDLs autonomously select and execute experiments without human intervention. These systems have the potential to transform research in chemistry,<sup>1</sup> materials science,<sup>2</sup> biology,<sup>3</sup> and beyond by enabling iterative experimentation at unprecedented speeds and scales. Through the automation of repetitive tasks and the integration of intelligent decision-making, SDLs enhance experimental efficiency, reproducibility, and scalability, paving the way for rapid advancements in scientific discovery.<sup>4–7</sup> SDLs are built on two foundational components: hardware infrastructure, encompassing modular workstations and robotic systems capable of executing complex workflows, and an AI “brain” capable of analysing incoming data and recommending the next experimental steps according to pre-defined goals.<sup>1,8–10</sup> Despite their potential, SDLs still face significant obstacles, including the high cost of proprietary hardware, limited accessibility, and difficulties in seamlessly integrating modular, customizable components into existing workflows.<sup>8,11–13</sup> Building a fully functional SDL involves confronting a range of hardware and integration challenges that extend well beyond data management and software development. Unlike data and algorithms, which are broadly reusable,

physical systems must be carefully adapted to the unique demands of each experimental context. Integration, rather than hardware construction alone, often proves to be the more formidable challenge.<sup>2,12,14,15</sup> SDLs integrate key components such as robotic systems for automated liquid handling,<sup>12</sup> advanced instrumentation for synthesis and characterization,<sup>16</sup> high-throughput imaging platforms<sup>17,18</sup> for real-time data acquisition, and sample preparation tools<sup>19</sup> like automated diluters, autosamplers and lab-on-a-chip systems *etc.*

However, widespread adoption of these technologies faces a significant barrier due to the prohibitive costs of commercial automation systems, which can range from tens to hundreds of thousands of dollars.<sup>12,15,20,21</sup> This financial hurdle has created a technological divide, limiting access primarily to well-funded institutions and leaving many research facilities unable to leverage the benefits of automated experimentation. In this context, 3D printing technology emerges as a democratizing force, offering a revolutionary solution to the accessibility challenge. With the rapid growth of 3D printing and the emergence of customizable, open-source, low-cost Fused Deposition Modelling (FDM) 3D printers, it is now possible to develop different components of SDLs as shown in the Fig. 1, tailored to specific needs and integrate them into SDLs. With the ability to fabricate intricate parts layer by layer, FDM stands out for its adaptability, low cost, and accessibility, making it ideal for the development of SDL hardware.<sup>22</sup> Recent advances in open-source 3D printing have further democratized access to



John V. Hanna

*Dr John V. Hanna is a Professor of Physics and Leader of the Materials Solid State NMR Group in the Centre for Magnetic Resonance at the University of Warwick since 2008. He previously served for 21 years in Australian Government Industrial Research Institutions (CSIRO and ANSTO). He earned his BSc from the University of Western Australia and completed his postgraduate studies at Griffith University in*

*Queensland. His research interests include solid state NMR spectroscopy, self-driving laboratories combining autonomous workflows with machine learning, X-ray/neutron diffraction, computational materials modeling, and the development of advanced materials for optoelectronics, energy storage, and sustainable applications.*



Leonard Ng Wei Tat

*Leonard Ng is an Assistant Professor of Materials Science and Engineering and Lead PI of the NGenuity Laboratory at Nanyang Technological University since 2023, Singapore. He also holds a Royal Academy of Engineering Enterprise Fellowship. He earned a PhD in Engineering from the University of Cambridge in 2019. His research interests include self-driving laboratories, printed electronics, roll-to-roll printed*

*photovoltaics, hybrid perovskite systems, non-fullerene acceptors, and self-driving labs for materials discovery and optimization.*



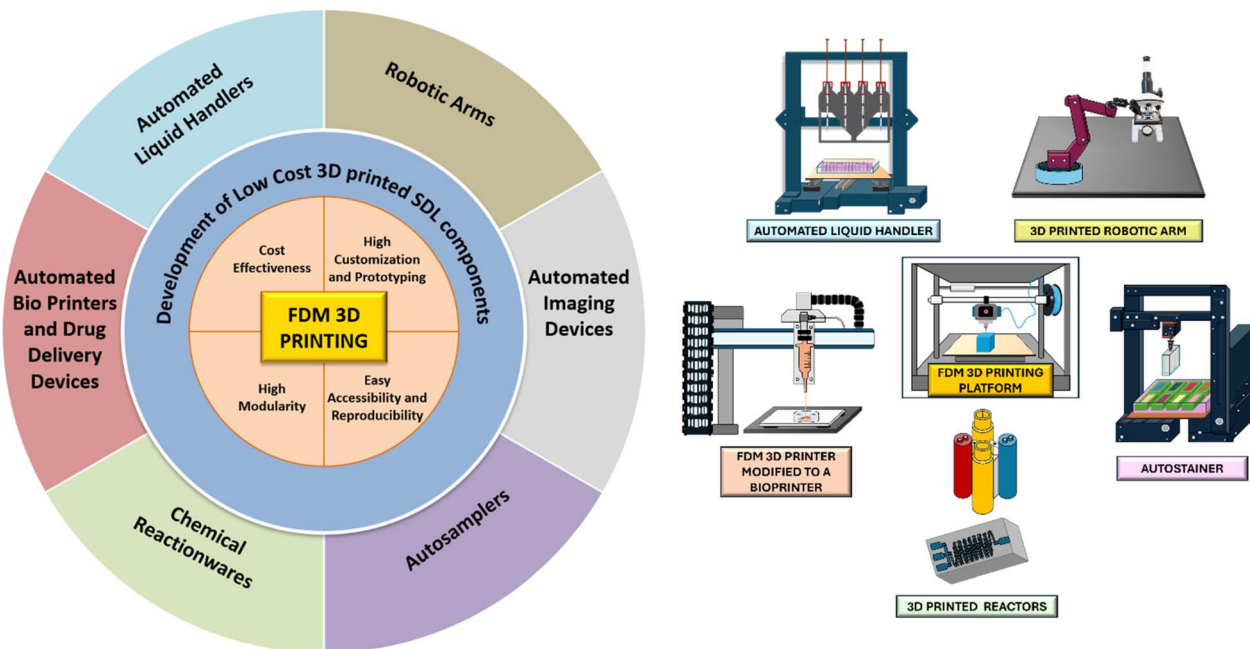


Fig. 1 Development of low-cost 3D-printed SDL components: a focus on affordable and accessible solutions for self-driving labs.

this technology, allowing researchers worldwide to design and share bespoke solutions tailored to their unique experimental needs. By enabling the production of customizable laboratory equipment at a fraction of the cost of commercial alternatives as shown in the Fig. 2, 3D printing is transforming how researchers approach laboratory automation. For example, traditional automated liquid handling systems, essential for high-throughput workflows, often cost between \$10 000 and \$60 000, making them unattainable for many smaller labs.<sup>23</sup> In contrast, 3D-printed solutions like the FINDUS liquid handler and the EvoBot platform offer comparable precision and functionality for tasks such as reagent dispensing, sample mixing,

and cell culture maintenance at costs as low as \$400.<sup>24,25</sup> In the realm of sample preparation, detection, and laboratory automation, 3D-printed innovations have led to the development of tools such as automated sampler, mixture and liquid handlers *etc.*<sup>24–36</sup> Similarly, affordable imaging solutions like FlyPi and OpenFlexure leverage modular components and open-source software to deliver advanced functionalities, including fluorescence and live-cell imaging, for under \$1000.<sup>37,38</sup> Additionally, 3D-printed alternatives to commercial robotic arms and grippers, such as the Soft Hand and Insta Grasp, provide cost-effective and adaptable solutions for tasks like pipetting, reagent mixing, and sample transfer.<sup>39,40</sup> The integration of 3D printing with open-source principles is pivotal to democratizing SDLs. Platforms like Arduino and Raspberry Pi enable the creation of low-cost, programmable devices that seamlessly integrate with 3D-printed hardware.<sup>41,42</sup>

This open-access, collaborative approach drives innovation by allowing researchers to rapidly prototype, share designs, and improve upon existing solutions.<sup>43,44</sup> Focusing on applications in chemistry, biology, and materials science, and as part of a broader effort to democratize low-cost SDLs, we explore topics related to the development of open-source, modular, and easily customizable laboratory automation equipment through 3D printing. First, we describe briefly the development of SDLs and its wide applications (Section 2). Thereafter, we explore the feasibility of 3D printing techniques which can be suited for the easy and low-cost manufacturing of laboratory automation tools (Section 3). Furthermore, we detail how FDM 3D printers can be used to produce different key hardware components of SDLs such as low-cost automated liquid handlers (Section 3.1), microscopic devices (Section 3.2), autosamplers (Section 3.3), automated sample preparation and detection devices (Section

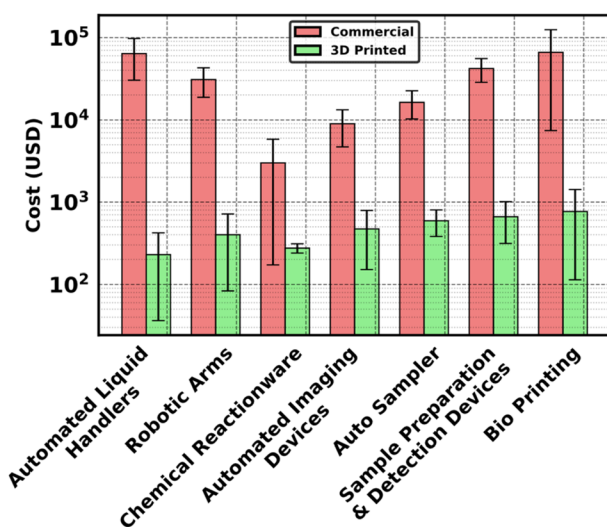


Fig. 2 Cost comparison between commercially available systems to 3D-printing alternatives.



3.4) robotic arms and grippers (Section 3.5). We also demonstrate how FDM 3D printers can advance chemical synthesis by enabling the development of low-cost chemical reactionware (Section 3.6), and we highlight how customizable FDM 3D printers can be used to develop automated, low-cost 3D bi-printers (Section 3.7). Finally, we discuss the feasibility of utilizing customizable, low-cost and highly modular 3D-printed equipment to develop hardware components for SDLs, highlighting its potential to democratize self-driving laboratories and make them accessible to a broader audience.

## 2 Overview of SDL

With the integration of Robotics and AI/ML, the growth of SDLs is inevitable in different fields of materials science, biology and chemistry *etc.* In the field of chemistry, significant advancements have been made in using SDLs to enhance reaction optimization and chemical discovery.<sup>1,4,19</sup> For example, Jeffrey A. Bennett *et al.* proposed a framework integrating machine learning and robotics to enable closed-loop autonomous experimentation, facilitating black-box optimization and surrogate modelling for chemical reaction mechanisms.<sup>46</sup> Similarly, Jaroslaw M. Granda *et al.* created an organic synthesis robot capable of autonomously performing and analysing chemical reactions, allowing rapid exploration of chemical reaction space and the discovery of novel reactions.<sup>47</sup> Complementing these efforts, Benjamin Burger *et al.* introduced a mobile robotic chemist that autonomously optimizes the photocatalyst systems.<sup>48</sup>

AI has brought transformative changes to laboratory research, particularly in high-throughput settings where it enhances the speed and efficiency of scientific discovery. Machine learning algorithms are used by artificial intelligence-powered platforms, such as Berkeley Lab's A-Lab, to automatically perform and improve chemical experiments, without human intervention while boosting throughput.<sup>49</sup> One active learning method that integrates computational reaction energies with experimental results is Autonomous Reaction Route Optimization with Solid-State Synthesis (ARROWS), which is part of A-Lab's AI framework.<sup>50</sup> By adapting to new data in real-time, ARROWS optimizes solid-state reaction pathways, improving the effectiveness of discovering new compounds.

Reinforcement learning has also been explored in closed-loop laboratories. For example, a self-driving enzyme engineering lab operated continuously for six months, employing an evolutionary AI algorithm to mutate and test proteins for enhanced thermal stability without human intervention.<sup>51</sup> These examples illustrate how AI agents can select optimal actions (*e.g.*, adjusting concentrations, choosing the next reactant, or tuning printer settings) based on real-time data (from images, spectra, *etc.*) to achieve specific goals. AI has also revolutionized structural biology beyond the synthesis of materials, with tools like DeepMind's AlphaFold being essential for making remarkably accurate protein structure predictions.<sup>52</sup> AlphaFold can be used as a sophisticated computational screening tool that can be easily incorporated into lab facilities,

significantly reducing the amount of time needed to determine protein structure before experimental validation.

In material science, SDLs have been instrumental in advancing materials discovery and optimization processes. Ryota Shimizu *et al.* developed a platform for autonomous material synthesis, leveraging machine learning and robotics to streamline experimental tasks, enabling efficient discovery and evaluation of new materials.<sup>53</sup> Similarly, Mikhail A. Soldatov *et al.* demonstrated how SDLs could integrate AI and robotics to conduct high-throughput experimentation, optimizing functional material synthesis.<sup>54</sup> In the polymer industry, SDLs can precisely control polymer synthesis by tailoring reaction conditions in real-time, addressing the high conversion requirements and viscosity challenges unique to polymers.<sup>45</sup> Automated modular systems in SDLs as shown in Fig. 3, are designed to handle the multipurpose processes.<sup>2</sup> This modular framework also lays essential groundwork for autonomous device fabrication and optimization. Aikaterini Vriza *et al.* developed PolyBot, a synthesis station equipped with an ISYNT platform from Chemspeed that enables chemical reactions to be conducted in highly controlled environments through a variety of modular components, including liquid and powder handling systems, parallel reactors, and purification units such as centrifuges.<sup>45</sup> Polybot as shown in Fig. 4 also features automated characterization tools, surface preparation and bond strength testing. Benjamin P. MacLeod *et al.* incorporated an SDL to autonomously map the Pareto front for thin film palladium (Pd) materials synthesized through combustion process.<sup>55</sup> SDLs have also made remarkable contributions to the biological sciences by streamlining processes in synthetic biology and regenerative medicine.<sup>3,56–58</sup>

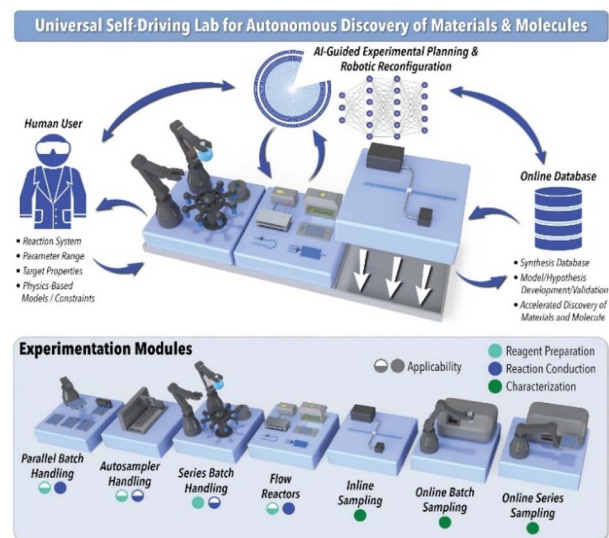


Fig. 3 Schematic Representation of a modular autonomous experimentation framework for a universal SDL. The generated experimental data can be utilized in decision-making algorithms and can be simultaneously stored in a centralized communal database. The human operator sets the operational constraints and defines the desired target properties or objectives for the system. Reproduced with permission. Copyright 2021, Elsevier.<sup>2</sup>



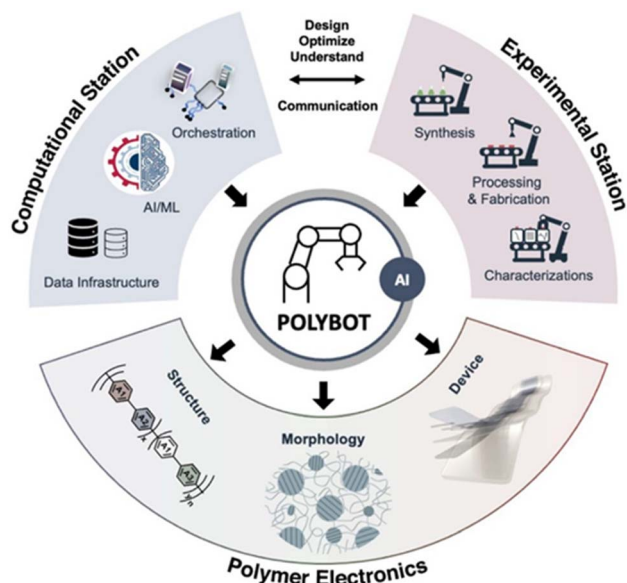


Fig. 4 Schematic representation of an SDL integrating AI/ML and automation for accelerating polymer electronics development. Reproduced with permission. Copyright 2023, American Chemical Society.<sup>45</sup>

However, as evident from the examples and current applications of SDLs, most rely on costly robotic arms, liquid handlers, and specialized commercial equipment, posing significant challenges to making SDLs widely accessible to all (Fig. 5–7). Most of the SDLs developed to date rely heavily on proprietary, high-cost equipment, which can limit their accessibility and scalability. Automated liquid handlers, widely used for pipetting and sample preparation, can cost anywhere from \$10 000 for entry-level systems like the Opentrons OT-2 to over \$60 000 for high-end integrated platforms such as the Tecan Fluent, Beckman Coulter Biomek, and Hamilton Microlab STAR, depending on throughput and add-ons.<sup>59,60</sup> Robotic arms, essential for inter-device transport and task automation, range from \$8000 to \$150 000, with costs increasing for collaborative features, cleanroom compatibility, and precision. Automated microscopes, especially those used in high-content imaging (e.g., Thermo CX7, Opera Phenix), fall between \$100 000 and \$500 000, depending on resolution, software, and environmental control.<sup>61</sup> Autosamplers, which automate sample introduction in analytical workflows such as gas chromatography (GC), liquid chromatography (LC), and mass spectrometry (MS), range in cost from approximately \$5000 to over \$100 000, especially for advanced modular systems like the PAL RSI and RTC series.<sup>62</sup> In addition, automated sample preparation platforms such as solid-phase extraction robots and magnetic bead handlers, typically cost between \$10 000 and \$150 000, with systems like the Thermo Fisher KingFisher Flex and Biotage Extrahera commonly used in omics laboratories. Detection and analytical instruments such as plate readers (\$10 000–\$60 000), mass spectrometers (\$100 000–\$500 000), HPLC/UPLC systems (\$30 000–\$150 000), and automated X-ray diffractometers (up to \$1 million or more), constitute a critical and often the most

expensive category in SDL infrastructure.<sup>63</sup> Over the past decade, commercial cloud laboratory platforms such as Emerald Cloud Lab (ECL) have offered researchers remote access to centralized, fully automated facilities.<sup>64</sup> While these platforms reduce upfront capital investment by shifting infrastructure costs to the provider, they impose substantial subscription and usage fees, making them more appealing to well-funded industrial clients. Accessing ECL typically requires a minimum financial commitment exceeding \$250 000, posing a significant barrier for academic researchers.

Over the past decade, growing awareness of the high costs associated with self-driving laboratories (SDLs) has spurred efforts to make them more affordable, driven by advances in modularity and scalability, which enable labs to start small and expand gradually, and open-source software ecosystems that lower development costs and facilitate the sharing of automation protocols. A collaborative open-source framework for AI-powered experimentation is emerging, integrating 3D-printed hardware, retrofitted printers, and open-source software to enable autonomous lab workflows.

AI and 3D printing synergize to accelerate scientific discovery, combining AI algorithms for designing, controlling, and optimizing experiments with 3D-printed tools. Materials science has been at the forefront of integrating AI with 3D printing, driven by the need to design complex material architectures and rapidly test their properties. Saldone *et al.* highlighted how 3D printing, especially polymer-based additive manufacturing, is shifting from a prototyping tool to a core technology for materials discovery.<sup>65</sup> Elbadawi *et al.* demonstrated a significant advancement in pharmaceutical materials development by employing conditional Generative Adversarial Networks (cGANs) to design novel formulations for FDM 3D printing.<sup>66</sup> Trained on 1437 pharmaceutical-grade formulations, the cGANs produced realistic, diverse, and 3D-printable drug formulations. This AI-driven approach not only expands the formulation space with greater diversity in composition and physical properties but also reduces reliance on traditional trial-and-error methods, highlighting its potential for high-throughput screening and accelerating the development of personalized medicines. A variety of AI methodologies facilitate real-time decision-making in autonomous experimentation. One common approach is Bayesian optimization (BO), where a probabilistic model, often a Gaussian Process Regression or Classification, is used to model the relationship between experimental inputs and outputs. As new data are generated, the model is iteratively updated to reflect current knowledge, guiding the selection of subsequent experimental parameters. This approach has been successfully applied in an autonomous additive manufacturing platform that employed BO alongside *in situ* imaging to dynamically optimize print parameters, achieving precise geometric control in real time.<sup>67</sup> Gongora *et al.* demonstrated how integrating 3D printing with AI, specifically Bayesian optimization, can revolutionize materials discovery and high-throughput experimentation. The researchers developed a fully automated system called BEAR (Bayesian Experimental Autonomous Researcher), which combines multiple FDM 3D printers, a robotic arm, and mechanical testing



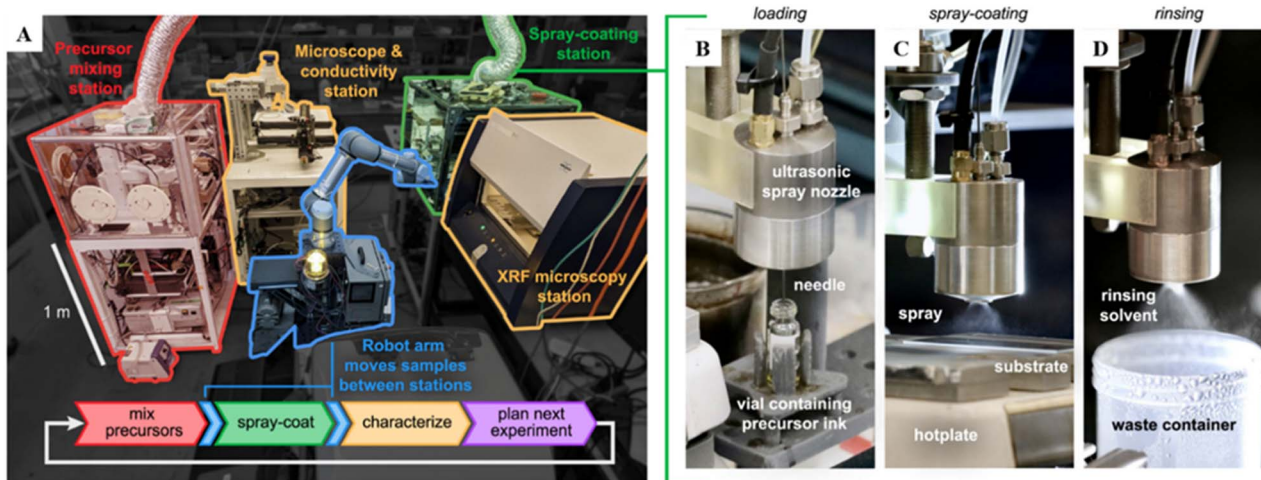


**Fig. 5** Framework of an SDL designed to automate the spray coating process. (A) The SDL is equipped with two synthesis stations (precursor mixing station and spray-coating station) and two characterization stations (Microscope, conductivity station and XRF microscopy station) all interconnected by a central six-axis robotic arm. (B–D) The spray-coating station is specifically designed with a retractable needle that extends through the nozzle for loading precursor inks (B). This front-loading design minimizes the required volume of precursor ink to prime the nozzle, enabling the use of small ink volumes (<1 mL) without waste. The loaded ink is sprayed onto a heated substrate to form a thin coating (C). Once spraying is completed, the system automatically performs a solvent rinse to clear any residual ink from the nozzle (D). Reproduced with permission. Copyright 2023, Elsevier.<sup>6</sup>

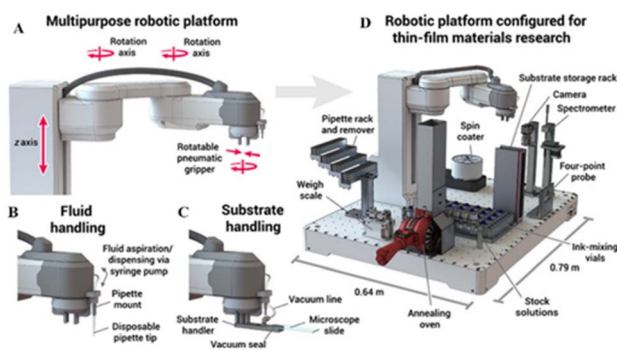


**Fig. 6** (A) Schematic representation of an SDL that operates on a modular robotic platform, featuring a polar robotic arm with a rotatable pneumatic gripper. (B) Fluid handling is facilitated by disposable pipette tips, which the robot can attach to and detach from the pipette mount via a press-fit mechanism. (C) Substrate handling is performed using a vacuum substrate handler, manipulated by the robotic arm. (D) The robotic platform is shown outfitted with experimental modules for thin-film materials research. Reproduced with permission. Copyright 2020, *Science Advances*.<sup>7</sup>

instruments to autonomously fabricate, test, and evaluate mechanical structures.<sup>68</sup>

In chemistry and chemical engineering, the integration of AI and 3D-printed equipment is driving a revolution in how reactions are performed and optimized.<sup>69,70</sup> A major trend is the development of autonomous synthesis platforms that combine robotics, microfluidics or modular 3D printed reactors and AI planning or optimization algorithms. Recent advances in AI and machine learning have revolutionized chemical synthesis optimization by enabling efficient exploration of complex reaction spaces and identification of optimal conditions with fewer

experiments. Manzano *et al.* developed a novel system that integrates AI and 3D printing to automate multistep chemical synthesis with high throughput and minimal human intervention.<sup>71</sup> Together, the 3D-printed reactor hardware and AI-driven automation enable the execution of over 24 000 base steps across 329 hours, including synthesis of APIs, peptides, and oligonucleotides. Van-Hao Vu *et al.* present an AI-integrated high-throughput experimental framework for green materials synthesis, combining Large Language Models (LLMs) for automated literature mining and CLIP-based image classification for identifying crystal formation.<sup>72</sup> The study features a custom 3D-printed 24-well plate, fabricated using PLA on an Ender 3

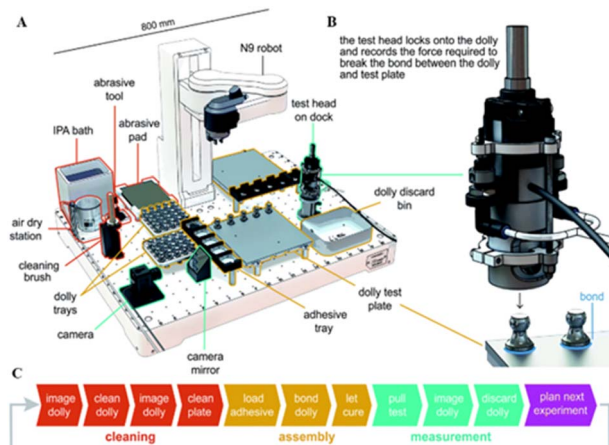


**Fig. 7** (A) Schematic of a self-driving laboratory operating on a N9 adhesive material testing. (B) A close-up view of the hydraulic strength testing tool utilized by the robot to measure bond strength. (C) Flow chart of the workflow sequence of the system. Reproduced with permission. Copyright 2022, Royal Society of Chemistry.<sup>16</sup>



printer, designed to fit the pipetting robot. The setup enabled precise, parallel synthesis of 22 different reaction conditions with minimal manual input. The integration of AI tools and 3D-printed labware demonstrates a scalable, low-cost approach to accelerating high-throughput experimentation in materials chemistry. The programmable microcontrollers and open-source, G-code-based control system support future integration with AI for automated optimization and data-driven experimentation, demonstrating how 3D printing and digital control can accelerate scalable, automated materials discovery.

### 3 Use of 3D printing for SDL applications

Over the last few decades, there has been significant growth in the development of additive manufacturing (AM) or rapid prototyping or 3D printing or digital manufacturing as a manufacturing method. This innovation has transformed the process of producing gadgets at lower costs and faster speeds compared to traditional manufacturing methods.<sup>41,42</sup> With the advancements in AM, a wide range of techniques has emerged based on material extrusion (Fused Filament Fabrication or Fused Deposition Modelling), vat photopolymerization (Stereolithography, Digital Light Processing), powder bed fusion (Selective Laser Sintering, Selective Laser Melting, Electron Beam Melting), binder jetting, material jetting, sheet lamination (Laminated Object Manufacturing), directed energy deposition (Laser Engineered Net Shaping, Electron Beam Additive Manufacturing, Wire Arc Additive Manufacturing) and many other hybrid additive manufacturing methods. These diverse methods highlight the adaptability and potential of AM in transforming industries.<sup>74,75</sup> However, Fused Deposition Modelling (FDM), a material extrusion-based 3D printing method invented by Scott Crump of Stratasys in 1989, is one of the most widely adopted AM techniques due to its affordability, versatility, and user-friendly operation, gaining momentum in subsequent years for its low cost and open-source accessibility. The process involves extruding thermoplastic materials in a semi molten state onto a stage, layer by layer, to build a 3D object as shown in the Fig. 8.<sup>73</sup> Thermoplastic filaments are fed through rollers to a heated nozzle where they are deposited according to the design's cross-sectional layers. Once one layer is completed, the stage lowers, and the process is repeated until the entire structure is fabricated. FDM's versatility is evident in its ability to process a wide range of materials, including acrylonitrile butadiene styrene (ABS), polylactic acid (PLA), nylon, polypropylene (PP), polycarbonate (PC), and composite polymers. In biomedical applications, materials like polycaprolactone (PCL) and poly lactic-co-glycolic acid (PLGA) are used to fabricate scaffolds for tissue engineering.

Despite the accessibility of FDM printers, the materials they use can impose significant limitations in laboratory settings. Standard thermoplastics such as PLA and ABS exhibit poor chemical resistance to many solvents and extreme pH conditions, leading to swelling, dissolution, or contamination in solvent-exposed applications.<sup>76</sup> More inert filaments *e.g.*

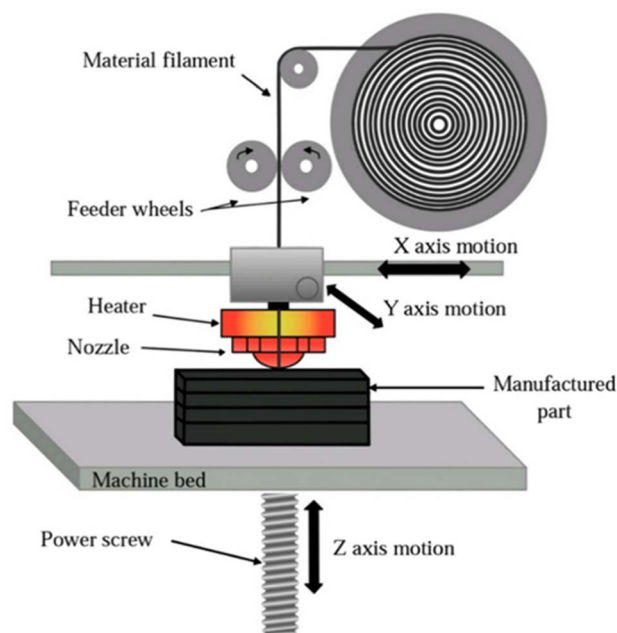


Fig. 8 A schematic representation of a Fused Deposition Modeling (FDM) 3D printing process. Reproduced with permission. Copyright 2023, Nature group.<sup>73</sup>

polypropylene or nylon can be used to improve chemical compatibility. Similarly, biocompatibility and sterility pose challenges because 3D-printed parts often have rough, layered surfaces that trap microbes and residues, making them difficult to clean and sterilize. This presents a limitation for sensitive biological applications, such as cell culture or clinical diagnostics.<sup>77</sup> One effective strategy to overcome this issue is surface finishing and post-processing.<sup>78–80</sup> Sanding and polishing with fine-grit sandpaper can significantly reduce surface roughness, though this approach is labour-intensive and impractical for intricate geometries.<sup>78</sup> Chemical smoothing, such as acetone vapor treatment for ABS, reflows the outer layers to produce a glossy, sealed finish, but it is limited to specific materials and requires careful handling due to solvent hazards.<sup>80</sup> Alternatively, applying a thin layer of biocompatible epoxy or UV-curable resin can seal the surface, improving cleanability and enhancing chemical resistance.<sup>78</sup>

Another general limitation of low-cost FDM printers is their limited resolution and precision.<sup>76</sup> Typical layer heights (100–300  $\mu\text{m}$ ) and nozzle diameters ( $\geq 0.4$  mm) constrain the fineness of features, which can be problematic for applications requiring high precision, including microfluidics, fine pipette tips (needing sub-millimetre accuracy), optical components (such as lenses or mounts requiring smooth surfaces), and high-precision positioning systems (like linear stages or micromanipulators demanding micron-scale accuracy). To overcome this, researchers often adopt hybrid approaches, using higher-resolution Stereolithography Apparatus (SLA) prints or commercially manufactured components for fine-detail parts such as microchannels, lenses, or pipette interfaces, while relying on FDM for structural elements. Precision can also be



enhanced through calibration and software compensation, including backlash correction and motor tuning. Adaptive slicing algorithms can also dynamically adjust layer heights and print speeds based on part geometry, prioritizing finer resolution for critical components. Additionally, integrating off-the-shelf components such as linear rails or lead screws can significantly improve accuracy without greatly increasing costs.

Durability presents a significant challenge when using 3D-printed apparatus for long-term or repetitive laboratory tasks. FDM-printed plastics, particularly PLA, ABS, are prone to creep and fatigue under continuous stress and can become brittle over time, especially in warm or humid environments. Functional components such as gears, sliders, and threads wear faster than metal equivalents, risking mechanical failure after repeated cycles. In robotics applications, the limited stiffness of printed parts can compromise both accuracy and load capacity, making them unsuitable for tasks requiring force application such as press-fitting pipette tips in liquid handlers or extruding viscous bio-inks in bioprinters.

An effective approach is adopting hybrid designs, where high-stress or load-bearing components such as joints, rails, or mounting points are made from metal, while less critical parts remain 3D-printed to retain cost-efficiency and design flexibility. Material selection also plays a crucial role: replacing PLA with more robust filaments like PETG, nylon, PEEK or carbon-fiber-reinforced composites can significantly improve mechanical strength, temperature resistance, and fatigue life.<sup>73,81</sup> Additionally, design optimization can extend component lifespan for example, increasing wall thickness, adding fillets to reduce stress concentrations, or using wear-resistant bushings and inserts in moving parts. By adopting modular design strategies, laboratories can ensure quick replacement of worn components while minimizing downtime. Maintaining a digital library of standardized, optimized parts enables on-demand reprinting and seamless system maintenance.

Mechanical properties of printed objects can be enhanced by incorporating natural fillers, metals, wood, or graphite, improving strength, flexibility, and conductivity. Additionally, embedding conductive materials, such as metals or carbon-based nanomaterials, enables the fabrication of sensors, circuits, and batteries, further broadening the scope and application potential of FDM technology.<sup>22,76,81</sup> While 3D printing enables customizable structural components, open-source lab devices also reliant on off-the-shelf electronics and mechanical parts, which often become bottlenecks for reproducibility. Challenges such as hard-to-source or proprietary components, supply chain disruptions, and the rapid obsolescence of electronics can render even well-documented designs difficult to rebuild. To enhance the sustainability and reproducibility of open-source labware, developers should prioritize modular designs with interchangeable components, create adaptable parametric models for supply chain flexibility, foster community-driven part sourcing and knowledge sharing, and leverage open hardware standards and widely supported platforms to reduce reliance on any single vendor. These strategies collectively future-proof designs and help maintain long-term accessibility. Collectively, these solutions enhance the

reliability and longevity of 3D-printed systems in demanding laboratory environments.

The advent of affordable, open source FDM 3D printers marks a pivotal role in the ongoing “maker movement”.<sup>82</sup> Researchers and educators can now fabricate essential laboratory automation tools and components at a fraction of the cost of commercial equipment.<sup>22,41,42,82–84</sup> When combined with off-the-shelf electronics, low-cost microcontrollers (like Arduino), and single-board computers (such as Raspberry Pi or Beagle-board), FDM 3D printing unlocks possibilities ranging from custom labware to fully automated laboratory workflows.<sup>42</sup> The initial investment in a printer, typically under \$350 can yield functionally sophisticated devices that once would have required specialized, expensive machinery.<sup>84</sup> For example, FDM 3D printers can be repurposed as versatile robotic platforms, reducing the need for expensive proprietary automation systems. The linear motion components of an FDM 3D printer can be repurposed into liquid-handling systems and automated sample preparation units.<sup>24</sup> The development of 3D printing has been closely intertwined with the rise of open-source hardware and software communities. A wide array of designs is made freely available under flexible licenses on platforms like the NIH 3D Print Exchange, GitHub, and in open-hardware focused journals (e.g., HardwareX). Online collaboration allows scientists and enthusiasts to share CAD files and firmware modifications, fostering a global culture of innovation and enabling automated laboratories to build on each other's advancements.

As 3D printers evolve from mere fabrication tools into multi-purpose robotic platforms, their integration with machine learning (ML) algorithms can create self-driving labs capable of autonomously optimizing protocols, adjusting parameters based on sensor feedback, and improving experimental throughput and data quality over time. Such innovation can dramatically reduce human labour and accelerate scientific discovery. However, precision and material properties of 3D-printed parts can be limited, restricting their suitability for highly specialized or sensitive applications. Ensuring reproducibility and quality control across different labs, printers, and material batches is not always straightforward, potentially impacting the reliability of shared designs. Despite these drawbacks, the collective benefits of accessibility, customization, and knowledge exchange continue to drive the widespread adoption of open-source 3D-printed labware. In this review, we have delved into the vast potential of FDM 3D printing for creating diverse, low-cost laboratory automation equipment, showcasing its transformative role in enhancing accessibility and innovation in scientific research.

### 3.1 3D printed automated liquid handlers

Effective liquid handling devices are crucial for ensuring precision and efficiency in laboratory works, particularly across a wide range of scientific disciplines such as chemical engineering, materials science, biomedical research, pharmaceutical laboratories, biochemistry, environmental science, point-of-care diagnostics, and microbiology.<sup>23,24</sup> In this regard, automated liquid handling systems, especially when incorporated



into self-driving lab environments, can enable high-throughput experimentation by rapidly processing numerous samples, thereby accelerating both research and discovery processes.<sup>9</sup> These systems can also be integrated seamlessly with different analytical instruments, enabling continuous, end-to-end automation of experimental workflows.<sup>3</sup> By minimizing human intervention, automated liquid handling reduces the risk of errors and contamination, enhancing the overall quality of experimental results. However, the high cost of commercial liquid handling robots and the limitations in customization are significant barriers for many research facilities. For example, the traditional commercial liquid handlers, like the Opentrons OT-2, are priced around \$10 000, while higher-end systems such as the Hamilton Microlab STAR, Beckman Coulter Biomek i7, and Tecan Freedom EVO can range from \$50 000 to \$60 000. These costs make laboratory automation unaffordable for many academic and smaller labs, particularly those with limited budgets.

3D printing provides a viable solution to these challenges by enabling the creation of customizable, modular, and cost-effective devices. Open-source liquid handlers built using 3D printing like FINDUS (Fully Integrable Non-commercial Dispensing Utility System), Sidekick, FAST Pump, Open-Source Peristaltic Pump, DIY Syringe Pump, OTTO, PHIL, Large Volume Extruder (LVE) and Belt-Driven Syringe Pump *etc.* drastically lower these costs as shown in the Table 1.<sup>85–89</sup> In

addition to cost constraints, commercial liquid handling systems often feature rigid designs and limited adaptability. However, these issues can be addressed with FDM 3D printing, as it not only enables flexible, customizable designs but also allows for modifications to the printers due to the open-source nature of the FDM 3D printers. 3D-printed automated liquid handlers can be tailored to perform different tasks, such as serial dilutions, sample mixing, or cell culture maintenance, which are common needs in high-throughput experiments.<sup>85,90–92</sup> This flexibility is particularly advantageous in academic research, where experimental conditions and protocols can vary widely. BioCloneBot developed by Ke'Koa CDH Wells *et al.* is an open source, highly accurate, low-cost alternative to the commercial liquid handlers, capable enough to accommodate up to four tip boxes, tube stands and 96 well plate, working in the range of 1 micro-litres to 200 micro-litres.<sup>92</sup> Barthels *et al.* developed the FINDUS as shown in the Fig. 9(C), an open-source liquid-handling workstation designed for flexibility, accessibility, and affordability, with a construction cost under \$400.<sup>24</sup> It utilizes an XYZ gantry system to precisely control pipettes, achieving pipetting errors below 0.3%, making it suitable for high-precision tasks. Emphasizing a low-budget approach, FINDUS is ideal for routine laboratory applications and features open-source components that allow easy customization and adaptation to specific experimental needs. Additionally, FINDUS supports integration with various modules for

**Table 1** Cost of 3D-printed alternatives to effective automated liquid Handling

| S/N | Device name  | Category                          | Cost (USD) | Specific use   | References |
|-----|--|-----------------------------------|------------|--|------------|
| 1   | FINDUS   | Automated liquid handler          | \$400      | Laboratory automation for biology and chemistry  | 24         |
| 2   | Automated liquid handler from a 3D printer             |                                   | \$325      | Laboratory automation for chemistry and biology pipetting tasks                              | 93         |
| 3   | Sidekick   |                                   | \$710      | Low-cost liquid dispensing, lab automation   | 86         |
| 4   | EvoBoT   |                                   | \$500      | Basic liquid handling, nurturing of microbial fuel cells, and droplet chemotaxis experiments | 25         |
| 5   | Open-source peristaltic pump                           | Peristaltic pump                  | \$120      | Point-of-care diagnostics, flow control in microfluidics                                     | 87         |
| 6   | PiFlow   |                                   | \$350      | Biocompatible dynamic flow pumping system  | 94         |
| 7   | Open-hardware wireless controller and 3D-printed pumps | Peristaltic pump/<br>syringe pump | \$50       | General purpose liquid handling  | 95         |
| 8   | Ender 3 syringe pump                                   | Syringe pump                      | \$170      | Programmable syringe pump for microfluidics  | 96         |
| 9   | Programmable dual-syringe pump                         |                                   | \$100      | Precise addition of reagents in chemistry laboratories                                       | 32         |
| 10  | Smartphone-controlled 3D-printed syringe pump          |                                   | \$100      | Point-of-care biosensing applications  | 97         |
| 11  | Low-cost infusion pump                                 |                                   | \$113      | <i>In vivo</i> imaging, controlled infusion for ERI studies                                  | 98         |
| 12  | Large volume syringe pump extruder                     |                                   | \$49       | Bioprinting and paste extrusion  | 88         |
| 13  | Cost-effective belt-driven syringe pump                |                                   | \$41       | Precise fluid transfer in biomedical applications  | 89         |
| 14  | Feedback-controlled syringe pressure pump              |                                   | \$110      | Microfluidics applications   | 99         |
| 15  | Touchscreen dual syringe pump                          |                                   | \$347      | Cell homogenization, programmable liquid handling  | 100        |



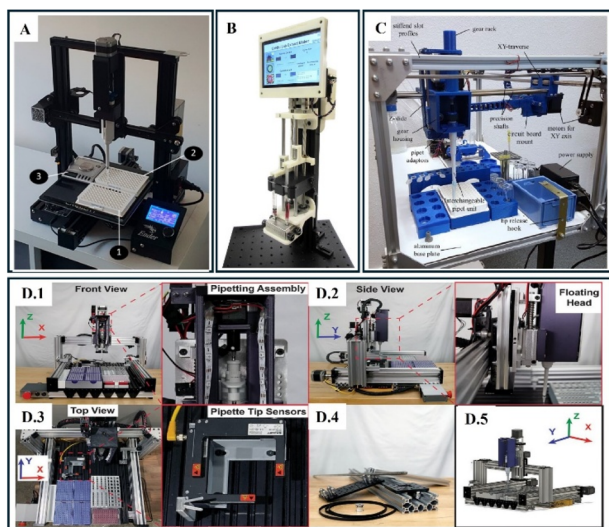


**Fig. 9** (A) Modified FDM 3D printer repurposed as an automated liquid handling system. Key components include: (1) a standard 96-well plate for liquid dispensing, (2) a mounted syringe or pipette for dispensing liquids, and (3) a platform with customized attachments enabling precise liquid handling. Reproduced with permission. Copyright 2024, *Journal of Chemical Education*.<sup>93</sup> (B) Photographic view of a low-cost, touchscreen-driven programmable dual syringe pump. This device features a user-friendly touchscreen interface for controlling volume and cycles, dual syringe holders for precise dispensing of liquids, and a modular design suitable for a variety of laboratory applications, exemplifying cost-effective automation in scientific research. Reproduced with permission. Copyright 2018, Elsevier.<sup>100</sup> (C) Photographic view of FINDUS (fully integrable noncommercial dispensing utility system). It includes an interchangeable pipet unit for versatile liquid handling, a motorized XY-traverse system for precise movement across the workspace, a Z-slide with gear housing for vertical adjustments, and a modular design with stiffened slot profiles, tip release hooks, and a circuit board mount for enhanced functionality. Reproduced with permission. Copyright 2020, Elsevier.<sup>24</sup> (D) Photographic view of a computer-controlled linear motion automated liquid handling system. (D.1) Front view showing the pipetting assembly integrated with an X, Y, Z axis system, (D.2) side view highlighting the floating head mechanism for precise liquid dispensing, (D.3) top view demonstrating the arrangement of sample plates and pipette tip sensors, (D.4) disassembled components, including modular aluminum extrusions, belts, and pulleys, emphasizing the system's customizable design, (D.5) 3D schematic of the system, illustrating the linear motion principles across X, Y, Z axes for automation. Reproduced with permission. Copyright 2020, *Nature Scientific Reports*.<sup>101</sup>

functions such as pipetting and transport, enabling a fully automated and customizable workflow as research requirements evolve. Michael R. Behrens *et al.* developed an open-source peristaltic pump which can be widely used as point of care diagnostic tool as shown in the Fig. 10(E), in different clinical settings.<sup>87</sup> Kopyl *et al.* replaced the extrusion head of a Creality Ender 3DM printer with a 3D printed liquid handling setup as shown in the Fig. 9(A).<sup>93</sup> It utilizes the cartesian system of the 3D printer to deliver the liquid into different positions.<sup>93</sup> Bass *et al.* modified the Creality Ender 3 3D printer as shown in the Fig. 10(C) to a modular and programmable syringe pump setup for around \$170.<sup>96</sup>

Unlike typical DIY setups requiring multiple vendors, the Ender 3 approach consolidates parts within a 3D printer kit, minimizing the need for external components. Its modularity and low cost make it highly accessible, though it's limited in scalability and relies on manual G-code programming. Similarly, Kessay *et al.* developed the Sidekick with a focus on simplifying hardware, software, and assembly.<sup>86</sup> Unlike most open-source liquid handlers that utilize Cartesian gantry systems like 3D printers, are often complex to build and reliant on commercial micropipettes, which raise maintenance and hidden costs. The Sidekick adopts an armature-based design as shown in the Fig. 10(D). This design reduces part count, increases reliance on 3D-printable components, and streamlines planar motion mechanics. Consequently, it minimizes assembly complexity, reduces machine size, and lowers material costs. The motion system is priced at around \$152, requiring only 19 parts, and can be assembled in less than four hours, excluding printing time. Using 3D printing, liquid handlers can be customized to perform multidimensional tasks. For example, Faiña *et al.* developed EvoBot, that allows researchers to customize its configuration for diverse tasks, including droplet placement and mixing, due to its highly adaptable design that supports modifications in both hardware and software, with modules for functions such as droplet manipulation, pipetting, and even biological material handling.<sup>25</sup> A notable feature of EvoBot is its feedback control system, allowing real-time adjustments during experiments, which is especially beneficial for applications requiring dynamic interaction, like monitoring chemical reactions or maintaining specific conditions for biological samples. Eggert *et al.* advanced the Open Workstation concept, further demonstrating customization through a modular approach with flexible hardware elements, including transport and pipetting modules that can be reconfigured without altering the entire system, enhancing its versatility and future-proofing capabilities.<sup>34</sup> Open Workstation provides modular components, such as pipetting, transport, and photo-crosslinking modules, allowing for adaptable configurations to meet evolving research needs.

The integration of 3D printing, microcontrollers and data analysis is revolutionizing low-cost automated liquid handlers, driving the vision of self-driving labs capable of independent, data-driven experimentation.<sup>42</sup> Microcontrollers like Arduino and Raspberry Pi provide customizable control, allowing for precise programming of tasks and real-time adjustments, while open-source software enables integration with data analysis tools for monitoring and dynamic feedback. This synergy allows for automated systems that not only perform high-precision liquid handling tasks but also respond to experimental data in real time. For example, Garcia *et al.* developed the programmable, 3D printed dual syringe pump (PDSP) as shown in the Fig. 9(B) which allows high customization *via* Python script, making it useful in repetitive laboratory tasks like cell homogenization.<sup>100</sup> Its unique configuration allows it to perform simultaneous or sequential fluid dispensing operations which is beneficial in experiments that require multiple reagents or buffers to be introduced in a controlled manner.



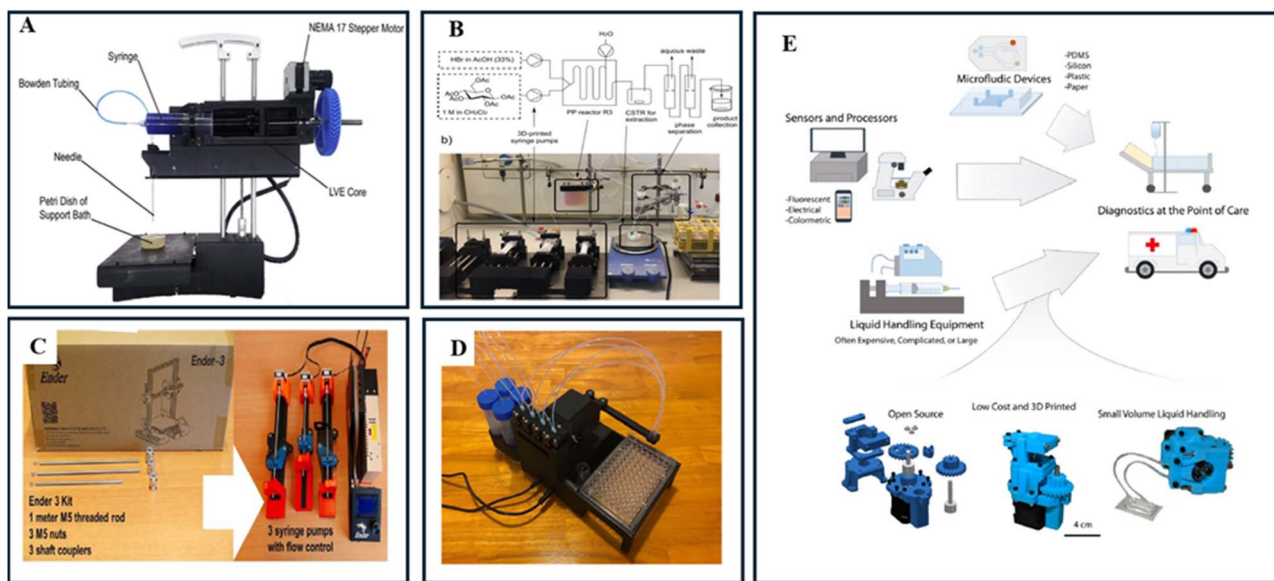


**Fig. 10** (A) Pictorial view of 3D printed Large Volume Extruder (LVE) to print wide range of materials. Reproduced with permission. Copyright 2018, Elsevier.<sup>88</sup> (B) Schematic and photographic view of a typical 3D printed liquid handling setting for continuous flow reaction. Reproduced with permission. Copyright 2019, *Beilstein Journal of Organic Chemistry*.<sup>102</sup> (C) An Ender 3 3D printer kit repurposed to build a three-channel syringe pump system. All custom parts are 3D printed. Reproduced with permission. Copyright 2021, Elsevier.<sup>96</sup> (D) Pictorial view of the 3D printed Sidekick liquid handler. Reproduced with permission. Copyright 2022, Elsevier.<sup>86</sup> (E) Integration of sensors, processors, and microfluidic devices for point-of-care diagnostics often relies on costly liquid handling equipment. A low-cost, open-source, 3D-printed peristaltic pump provides a compact solution for precise liquid handling. Reproduced with permission. Copyright 2020, *Nature Scientific Reports*.<sup>87</sup>

The microcontroller-based systems enable users to program and adjust key parameters such as flow rate, infusion volume, and timing, providing a high degree of control over the dispensing process. The user-friendly interface further simplifies operation, making it suitable even for those with minimal technical experience. The PiFlow system developed by Kassis *et al.* presents a low-cost, customizable solution for liquid handling in laboratories, utilizing 3D printing and a Raspberry Pi Zero microcontroller to provide an open-source alternative to commercial flow systems at an affordable cost of \$350.<sup>94</sup> PiFlow's programmability, enabled by Python scripting, allows for precise control over flow rates and dynamic concentration profiles, which are critical for controlled environments such as cell culture and drug delivery experiments. The system's modular design includes a 3D-printed micromixer for generating concentration gradients, facilitating biological applications like organ-on-a-chip and micro physiological studies. Gervasi *et al.* presented a new wireless controller tailored for precise liquid manipulation tasks, designed to work with 3D-printed peristaltic and syringe pumps, and capable of handling volumes from microliters to litres with a relative error below 1%.<sup>95</sup> It offers a low-cost and flexible approach to liquid handling, ideal for experiments needing repeatability and adaptability. Using ESP32 microcontrollers, it can be remotely controlled and configured, making it suitable for high-precision and low-cost setups in biological and biochemical applications. Similarly, Rogosic *et al.* developed a 3D-printed, smartphone-controlled syringe pump which is designed for flexibility in lab environments and point-of-care applications.<sup>97</sup> David C.

Florian developed an open source automated liquid handler from the off shell components and the 3D printed parts.<sup>101</sup> As shown in the Fig. 9(D) the 3D linear motion platform is capable of positioning the micro-pipette anywhere within its work envelope. The pump's cost is around \$110, and it includes customization options, such as flow rate adjustment for various experimental needs. Kujawa *et al.* developed a low-cost Arduino controlled infusion pump designed specifically for biomedical research, with a focus on precise fluid delivery for *in vivo* imaging applications.<sup>98</sup> The main components are 3D-printed, and the pump is controlled by an Arduino microcontroller, which allows researchers to program various infusion parameters such as flow rate, volume, and timing. This capability is essential for experiments requiring controlled dosing, such as pharmacokinetic studies and drug testing in animal models. Research efforts to control liquid volumes from nanolitres to litres have led to innovative solutions that combine precision with scalability. This is demonstrated in studies such as Councill *et al.*'s adaptation of low-cost pipetting robots for nanolitre handling,<sup>91</sup> which is ideal for high-precision applications in proteomics and cell analysis at a reduced cost compared to commercial systems, as well as Pusch *et al.*'s development of a 3D-printed large-volume syringe pump<sup>88</sup> extruder as shown in the Fig. 10(A), which manages fluid volumes up to 60 mL, catering to bioprinting and paste extrusion needs. These studies collectively illustrate how combining open-source accessible for various research applications and supporting the development of low-cost, self-driving laboratories.



Table 2 Cost of 3D-printed alternatives to effective microscopy

| S/N | Device name                         | Category                          | Cost (USD)     | Applications   | References |
|-----|-------------------------------------|-----------------------------------|----------------|--|------------|
| 1   | FlyPi                               | Microscope                        | \$200 to \$300 | It is an affordable and adaptable solution for education, research, and medical diagnostics  | 37         |
| 2   | UC2 modular microscope              |                                   | <\$400         | It enables diverse imaging modalities like brightfield microscopy for long-term <i>in vitro</i> cell culture observation, fluorescence imaging for biological samples, and light sheet microscopy for 3D imaging | 104        |
| 3   | PHIL (pipetting helper imaging lid) |                                   | <\$600         | It is useful for both microscopy imaging and high-throughput fluorescence-based analysis. It provides live cell time lapse microscopy with automated media exchange  | 105        |
| 4   | Incubot                             |                                   | \$1000         | It leverages a modified 3D printer for motion control and is designed for long-term live-cell imaging in incubators, offering flexibility for reflected, oblique, and fluorescence imaging                       | 106        |
| 5   | EnderScope                          |                                   | \$300          | The ender 3D printer has been transformed into an automated scanning microscope designed for detecting and imaging microplastics in seawater   | 107        |
| 6   | Microscopi                          |                                   | \$300–\$400    | It has modular design which is adaptable for different imaging modalities. It can deliver accurate fluorescence microscopy. It is used as a diagnostic tool for identifying pathogens                            | 108        |
| 7   | Octopi                              |                                   | \$250–\$500    | It can perform automated slide scanning for diagnosis with high-throughput imaging of 1.5 million cells per minute, integrated with machine learning for automated and accurate detection                        | 109        |
| 8   | Portable fluorescence microscope    |                                   | \$240          | It is suitable for fluorescence imaging to detect pathogens  | 110        |
| 9   | OpenStage motorized stage           | Positioning stage                 | <\$1000        | It provides automated 3-axis positioning for microscopy, supporting applications like time-lapse imaging, 3D data acquisition, and image mosaicking. It produces micron positioning accuracy in X, Y, and Z axes | 111        |
| 10  | Flexure translation stage           |                                   | <\$50          | High precision sample positioning for microscopy, capable of sub-micron motion range   | 112        |
| 11  | Handheld microplate reader          | Detection tool <i>via</i> imaging | <\$100         | It provides point-of-care ELISA testing for disease diagnostics in resource-limited environments. It can enable high-throughput analysis of multi-well plates with quick results                                 | 113        |

### 3.2 3D printed microscope

Automated microscopy is a critical component in the development of SDLs enabling high-throughput imaging, real-time data acquisition, and the integration of *in situ* image analysis.<sup>17,18</sup> However, commercial automated microscopy systems face significant limitations due to their proprietary and non-customizable nature, which restricts modifications to hardware and software and may void warranties if alterations are attempted.<sup>103</sup> The extremely high costs make them inaccessible to many laboratories, especially those in low-resource settings or educational institutions. The options for interfacing with third-party systems are also limited due to undocumented I/O ports and closed-source software, hindering compatibility with other tools and technologies. In case of hardware defects, repairs or replacements can take weeks to months, leading to long downtimes that disrupt research activities and potentially cause significant delays. 3D printing offers innovative solutions

to overcome the limitations of commercial systems by making advanced microscopy equipment more affordable and accessible as shown in Table 2. The wide applications of 3D printing in Microscopy are shown in Fig. 11. The 'Makers' approach facilitated by 3D printing democratizes access to advanced technologies, with equipment that can be built and shared through 'Fab labs' and other collaborative platforms, promoting wider participation in scientific research. The 3D-printed devices can also be integrated with open-source microcontrollers like Arduino and software, adaptability with 3D printing can address a vast volume range in liquid handling, making advanced fluid management enhancing compatibility with other systems and enabling seamless integration into existing laboratory setups.

Several researchers have contributed to this movement by developing innovative microscopy platforms and complementary technologies that collectively expand the capabilities of low-cost and high-precision imaging.<sup>109,112</sup> Andre Maia Chagas *et al.*



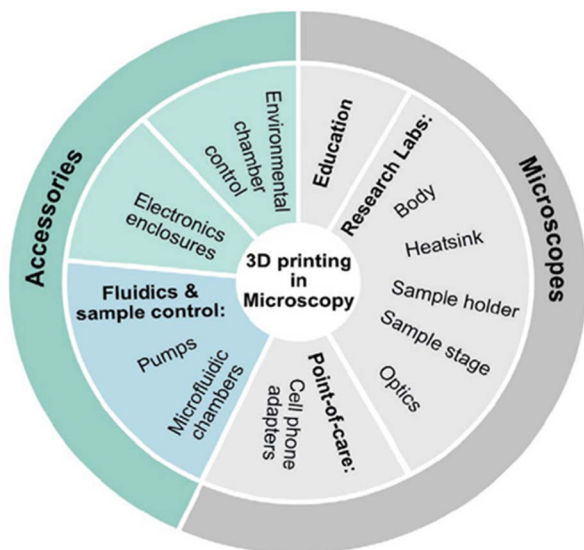


Fig. 11 Application of 3D printing in different fields. Additive manufacturing has become a key component in numerous open-source projects focused on modular microscope designs. It enables the fabrication of complete microscope structures at relatively low costs, with only a few components requiring alternative manufacturing methods. Reproduced with permission Copyright 2021, *Advanced Biology*.<sup>103</sup>

developed a modular, open-source fluorescence microscopy and optogenetic platform known as FlyPi, costing under \$100.<sup>37</sup> Designed to make advanced research accessible, FlyPi supports fluorescence microscopy, optogenetics, thermogenetics and behavioural tracking.

Despite its affordability and versatility, the system is constrained by its optical setup, performing well for basic tasks but struggling to resolve fine details such as malaria parasites within blood cells. Complementing this approach, Diederich *et al.* presented UC2, a modular, open-source microscopy platform as shown in Fig. 12 which is capable of supporting various imaging modalities, including light-sheet and fluorescence microscopy.<sup>104</sup> Costing as little as \$400, UC2 allows users to easily toggle between configurations, making it suitable for prototyping and scalable research. Yujin Lee *et al.* further contributed by 3D printing low-cost optofluidic blocks and a slide-scanning microscope stage.<sup>114</sup> Users can download digital design files, assemble components, and modify the systems as needed, fostering an environment of shared innovation and adaptability in microscopy technology. In the realm of automated microscopy, Philip Dettinger and his team developed PHIL (Pipetting Helper Imaging Lid), a low-cost (\$600) device that combines pipetting, incubation, and microscopy functionalities as shown in Fig. 13(C).<sup>105</sup> By enabling real-time data acquisition during experiments, PHIL allows continuous, unsupervised experimentation. Addressing the need for live-cell imaging under physiological conditions, George O.T. Merces *et al.* developed the Incubot, a 3D printer-based microscope as shown in Fig. 13(A) for long term live-cell imaging within a tissue culture incubator.<sup>106</sup> Constructed

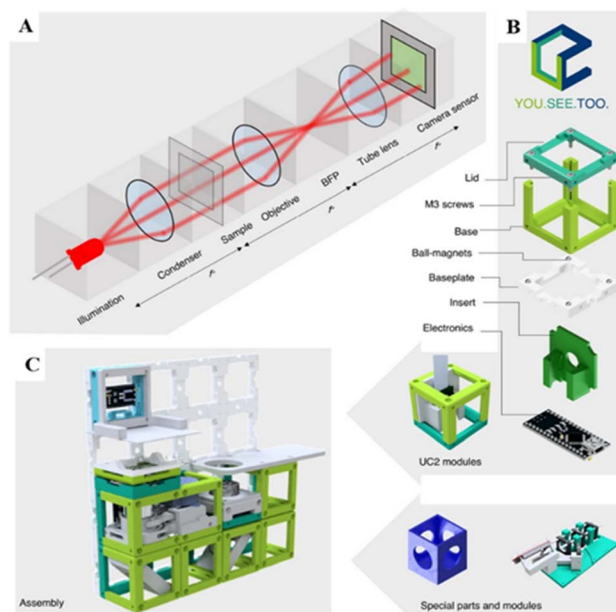
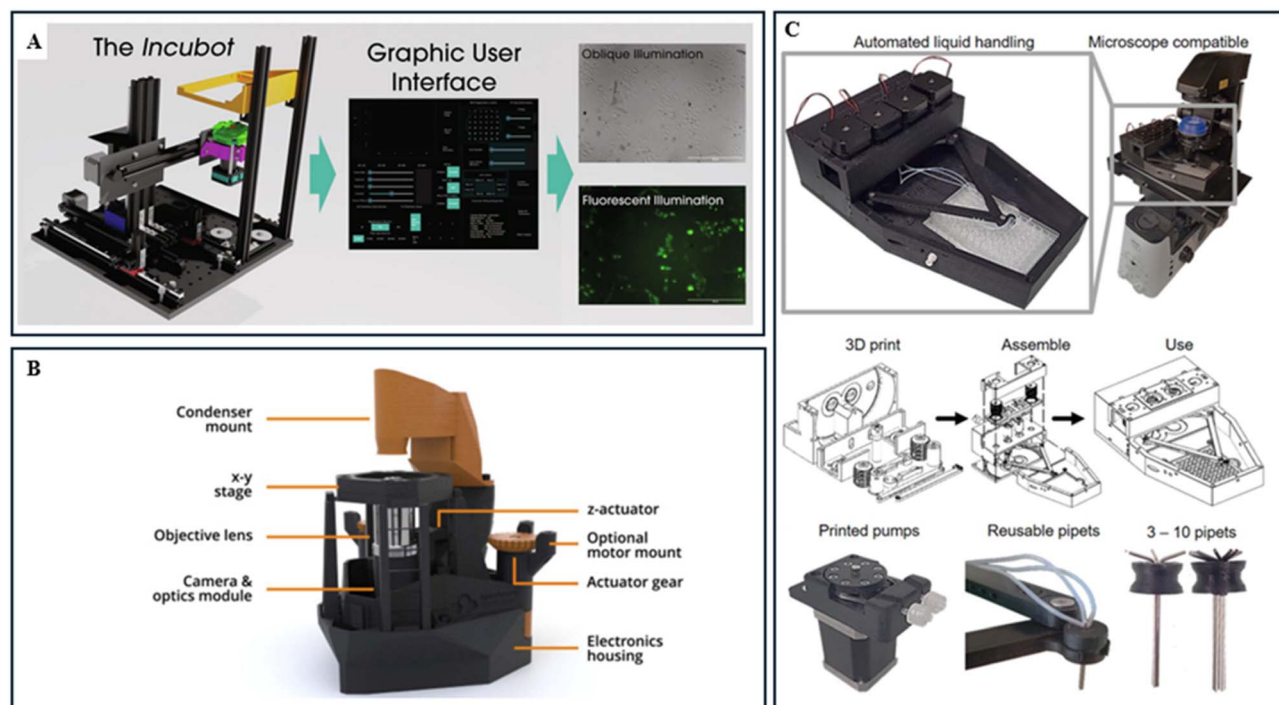


Fig. 12 Overview of the UC2 (You-See-Too) 3D-printed modular optical platform. (A) Schematic representation of the optical pathway in a modular microscopy system, illustrating the components from illumination to the camera sensor, including the condenser, sample, objective, back focal plane (BFP), and tube lens. The  $4f$  system segments Fourier-optical configurations into distinct functional units, where  $f$  represents the focal lengths. (B) Breakdown of the UC2 modules, featuring key components such as the cube base, lid, baseplate, ball magnets, inserts, and electronics. (C) Assembly of the UC2 system, demonstrating its modular structure and integration of optical and electronic components, along with special parts for additional customization. Reproduced with permission Copyright 2020, *Nature Communications*.<sup>104</sup>

at approximately \$1000, the Incubot is significantly cheaper than commercial systems, making advanced imaging accessible to underfunded labs and educational institutions. Its open-source nature eliminates licensing fees and promotes free access to upgrades and modifications. Operating within standard incubators, it avoids temperature gradients that could affect live-cell behaviour. However, limitations include data transfer issues during imaging and imaging times that may disrupt certain experimental workflows, requiring further refinements. Niamh Burke *et al.* modified the commercially available Creality Ender 3 FDM 3D printer into a fluorescence and white-light microscope, enabling automated scanning and detection of microplastics in seawater.<sup>107</sup> A Raspberry Pi camera, a NeoPixel LED ring for illumination, and 3D-printed mounts and filters are all part of a modular optics system that replaces the printer's hot end module. This system allows for automated scanning over areas as large as  $20 \times 20$  cm, greatly lowering the amount of work needed for microplastic analysis. However, its performance may not match high-end fluorescence microscopes, restricting its use for advanced imaging, and it is limited to detecting fluorescently labelled particles, potentially overlooking non-fluorescent microplastics. Enhancing precision in microscopy, Dominik Schneider *et al.* introduced





**Fig. 13** (A) Pictorial view of the modular Incubot setup, built using a 3D printer framework and equipped with essential optical and mechanical components for live-cell imaging. It is incorporated with the graphical user interface (GUI) that allows users to control imaging parameters such as frame rate, brightness, and magnification, as well as manage scanning and recording functionalities. It can produce cellular imaging under different illumination modes: oblique illumination for structural visualization and fluorescent illumination for identifying labeled cellular components. Reproduced with permission Copyright 2021, Elsevier.<sup>106</sup> (B) Pictorial view of the OpenFlexure Microscope design in its transmission bright-field configuration: the condenser mount includes an illumination LED and a plastic condenser lens. Below the stage, the optics module contains the objective lens, tube lens, and camera, and it is connected to the z-actuator to enable adjustable focus. The x-y stage and optics module are operated using actuator gears located at the rear of the microscope, with the option to integrate stepper motors for precise control. Additionally, a removable electronics housing accommodates optional components such as motor controllers and a Raspberry Pi, allowing for automation. Reproduced with permission Copyright 2020, Optica Publishing Group.<sup>38</sup> (C) Photographic view of PHIL (Pipetting Helper Imaging Lid), a compact automated liquid handling system integrated with microscope to enable precise and automated pipetting for live-cell experiments. Key components of the system, including 3D-printed pumps, reusable pipettes, and interchangeable pipette tips (ranging from 3 to 10 tips). Reproduced with permission copyright 2022, *Nature Communications*.<sup>105</sup>

a cost-effective (\$250), open-source motorized positioning stage for automated high-content microscopy.<sup>115</sup> Lightweight and compact, the device demonstrated a spatial resolution of 5  $\mu\text{m}$  and repeatability of  $\pm 5 \mu\text{m}$ , comparable to commercial instruments. Although scanning speed is limited due to software bottlenecks and some components may lack durability, it reduces reliance on expensive proprietary systems and can be further developed for improved performance. Similarly, Campbell *et al.* introduced OpenStage, a low-cost (under \$1000) motorized stage providing sub-micron positioning accuracy with repeatability of approximately 1  $\mu\text{m}$  in *X/Y* and 0.1  $\mu\text{m}$  in *Z*.<sup>111</sup> Sharkey *et al.* focused on precision applications by introducing a monolithic 3D-printed flexure translation stage that enables sub-micron positioning accuracy over an  $8 \times 8 \times 4 \text{ mm}$  range.<sup>112</sup> Exhibiting high stability with minimal drift (less than 20  $\mu\text{m}$  over a week without temperature stabilization), this stage is ideal for time-lapse measurements in containment facilities or incubators. It demonstrates how 3D-printed mechanisms can achieve precise control in microscopy applications. Wincott *et al.* created Microscopi, a 3D-printed fluorescence imaging system using open-source hardware such as Raspberry Pi and

Arduino, for educational applications.<sup>108</sup> Leveraging smartphone technology, Berg *et al.* created a handheld ELISA reader utilizing 3D-printed optomechanical attachments integrated with smartphones.<sup>113</sup> Capable of processing 96-well plates and achieving over 98% accuracy for diseases such as measles and herpes simplex, the device offers rapid diagnostic results. Its portability and affordability make it promising for high-throughput disease screening and vaccine campaign monitoring. However, reliance on smartphone-based computational support and potential connectivity challenges in remote areas are notable drawbacks. To support the data-intensive needs of automated microscopy, Hilsenbeck *et al.* developed FastER, a robust, trainable cell segmentation software tailored for large-scale microscopy.<sup>116</sup> By significantly reducing analysis time while maintaining high accuracy, FastER is especially valuable in high-content screening and time-lapse imaging experiments, complementing the capabilities of low-cost, automated microscopes. Collins *et al.* developed the OpenFlexure Microscope, a fully automated, 3D-printed laboratory-grade microscope featuring motorized sample positioning and focus control using a flexure mechanism.<sup>38</sup> Achieving sub-micron precision with



Table 3 Cost of 3D-printed alternatives to autosamplers

| S/N | Device name                     | Cost (USD)    | Applications  | References |
|-----|---------------------------------|---------------|---|------------|
| 1   | Osmar microsyringe autosampler  | \$700         | It performs automated sampling for gas chromatography and liquid handling in biochemistry and chemistry labs  | 30         |
| 2   | BioSamplr                       | \$700         | It provides automated sampling for bioreactors with precise timing and temperature control  | 28         |
| 3   | RotoMate Autosampler            | \$550         | It is a fully open-source, 3D-printed system for automated sample handling in NMR spectrometers, capable of processing 30 samples per batch with integrated data processing and a web interface for remote monitoring       | 31         |
| 4   | Automated fluid delivery system | <\$500        | It performs automated fluid delivery from multiwell plates to microfluidic devices  | 117        |
| 5   | Low-cost universal autosampler  | <\$500        | It conducts automated liquid sampling for potentiometric titrations and water quality analysis  | 27         |
| 6   | Miau (microbalance autosampler) | \$900         | It provides a pick-and-place operation with a dual-function gripper capable of transferring tin capsules and dispensing powder from a container into the capsules, offering accurate and precise handling of sub-mg samples | 26         |
| 7   | micrIO                          | Not specified | It combines 3D-printed AutoSipper and fraction collector to automate fluid input-output for microfluidic experiments, enabling high-throughput sample handling  | 29         |
| 8   | 3-Axis autosampler              | \$335         | It can perform automated sampling for 96-well plates and microfluidic workflows   | 118        |
| 9   | Portable water autosampler      | \$850         | It employs a syringe pump and a 3D-printed gantry robot with android-based control for field sampling of water in environmental analysis  | 119        |

step sizes of 50 nm in the z-axis and 70 nm in the x and y axes, this microscope supports various imaging modalities such as brightfield and fluorescence as shown in the Fig. 13(B).

These low-cost, open-source developments collectively demonstrate a dramatic shift towards easily accessible, affordable, and customizable microscopy solutions, effectively democratizing the self-driving laboratory. By utilizing open-source hardware, 3D printing, and modular designs, researchers are overcoming resource limitations and enabling wider participation in scientific discovery and education.

### 3.3 3D printed auto sampler

Autosamplers play a crucial role in laboratory automation by automatically handling sample collection, preparation, and transfer.<sup>26</sup> Commercial autosamplers, while advantageous for laboratory automation, have notable limitations that hinder their broader adoption. Their high cost, often reaching tens of thousands of dollars which makes them inaccessible to smaller labs or institutions with limited budgets.<sup>26,30</sup> These devices typically operate within proprietary ecosystems, requiring specific software and hardware integrations, which restrict flexibility and complicate their adaptation to unique workflows or non-compatible instruments. Furthermore, they are often designed for specialized tasks, making customization or modification challenging and costly. 3D printing significantly lowers the cost of developing autosamplers as shown in the Table 3. The modularity of 3D-printed systems supports easy adaptation for various tasks, as seen in designs like Osmar and BioSamplr, which handle liquid, gas, or powder sampling.<sup>28,30</sup> This accessibility democratizes automation, particularly in smaller organizations. Dyga *et al.* developed RotoMate, a 3D

printed autosampler designed for benchtop nuclear magnetic resonance (NMR) spectrometers, specifically the Magritek Spinsolve series.<sup>31</sup> This device automates the insertion, ejection, and data processing of up to 30 samples. By integrating with spectroscopy software, RotoMate enables real-time reaction monitoring and automated yield calculations. Constructed from 3D-printed components and controlled by an Arduino, it provides a low-cost alternative to commercial NMR autosamplers. Ross C. Lagoy *et al.* developed a robust, open-source robotic system for automated fluid delivery from multiwell plates to microfluidic devices, addressing key challenges in high-throughput biological and chemical experimentation.<sup>117</sup> The system integrates inexpensive components, such as stepper motors, 3D-printed parts, and Arduino-based controls, to achieve sequential delivery of liquids with high precision and minimal cross-contamination. This design bridges the gap between static multiwell plate assays and dynamic microfluidic environments, enabling complex protocols such as dose-response curves, compound screening, and multi-step cell staining. The authors demonstrate the system's versatility through three case studies: odor-response analysis in *C. elegans*, solvent screening for neural activity modulation, and automated staining of human mesenchymal stem cells. Carvalho *et al.* developed a low-cost, universally adaptable autosampler for liquid handling using a robotic arm kit and simple software integration.<sup>27</sup> The system is designed to be compatible with various analytical instruments and supports automation in multi-parameter water analyses, including alkalinity, pH, carbon, and nitrogen content. By utilizing GUI-based controls, the autosampler simplifies operation for users without advanced programming expertise. It is also highly



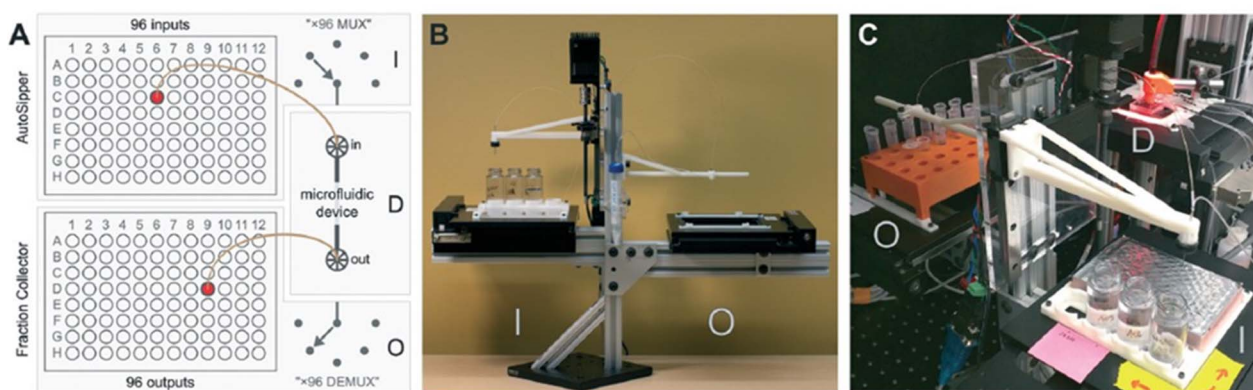


**Fig. 14** Overview of the micrIO platform: (A) A schematic illustration of the experimental setup, where the ‘AutoSipper’ module [I] sequentially draws input samples from a multiwell plate and directs them into a microfluidic device [D]. The Fraction Collector [O] then routes the output effluent from the microfluidic device into another multiwell plate. (B) A photograph showcasing the entire platform, with the AutoSipper [I] and Fraction Collector [O] clearly labeled. (C) A closer view of the AutoSipper [I] and Fraction Collector [O] integrated into an experimental setup, featuring a valved microfluidic device [D] being monitored using a microscope. Reproduced with permission. Copyright 2020, Royal Society of Chemistry.<sup>29</sup>

customizable, enabling integration with equipment from different manufacturers. However, the system’s reliance on GUI compatibility and scripting can limit its integration with non-compatible hardware, while its performance depends on the precision and reliability of the robotic arm. Efromson *et al.* developed “BioSamplr”, an open-source, 3D printed, low-cost system for automated sampling of bioreactors, addressing sterility, reproducibility, and labour reduction.<sup>28</sup> The device can collect up to ten samples at programmable intervals while maintaining sample integrity through cooling. Carvalho introduced Miao, a microbalance autosampler optimized for weighing powders in the sub-mg range.<sup>26</sup> This Cartesian robot features a dual-function gripper for tin capsule manipulation and powder transfer, making it well-suited for preparing working standards for isotopic and elemental analyses. Although it performs exceptionally well in repetitive weighing tasks, its applicability is restricted to powder-related use cases, and it has trouble with heterogeneous materials, which can affect the accuracy of some applications. Scott A. Longwell *et al.* introduced micrIO, an open-source autosampling platform for high-throughput microfluidic input–output operations.<sup>29</sup> As shown in the Fig. 14, the platform consists of an “AutoSipper” which enables pressure-driven, contamination-minimized sample introduction from multiwell plates, and a “Fraction Collector” which ensures efficient, cross contamination-free output collection using a sheath flow system. This low-cost, modular platform, built with 3D-printable components and Python-based software, is validated through applications like DNA sampling and spectrally encoded bead generation, demonstrating reliability and minimal cross-contamination. Carvalho and Murray developed Osmar, a microsyringe-based autosampler using G-code mechanics from 3D printers.<sup>30</sup> The device features a movable gantry for precise liquid and gas sampling, controlled *via* open-source software. Osmar offers high precision and movement accuracy, at an affordable cost (\$700). The system is also adaptable for various laboratory tasks, including gas chromatography and liquid handling. Despite its

versatility, Osmar’s reliance on linear motion systems restricts its application to tasks requiring strict syringe manipulation, and its scalability for industrial use remains a challenge. Růžička *et al.* presented a compact autosampler for portable capillary electrophoresis, designed to monitor gamma-hydroxybutyric acid (GHB) in biological fluids such as saliva.<sup>120</sup> The device employs peristaltic pumps and solenoid valves for liquid flow control and integrates these components with a capillary electrophoresis system to enable miniaturization and portability. However, it is specialized for capillary electrophoresis and lacks the ability to handle multiple sample types or high-throughput workflows, which limits its applicability beyond specific scenarios like drug monitoring. Gregory Murray and his team developed and compared a low cost 3-axis stepper motor (\$335) based autosampler and a SCARA based auto sampler (\$300) made of 3D printed parts and servomotors.<sup>118</sup> 3-axis autosampler adapts a Cartesian movement system commonly seen in 3D printers, offering precise motion control. The SCARA autosampler employs rotational movement with a series of linked arms, enabling compact designs but with reduced precision. Both systems are designed for use with 96-well plates, enabling high-throughput liquid handling for chemical analysis. However, the SCARA system suffers from reduced positioning precision due to its reliance on angular rotation and servomotors. Collectively, these innovations demonstrate how 3D printing revolutionizes laboratory automation by making it accessible, customizable, and cost-effective, overcoming the limitations of commercial devices, and promoting enhanced efficiency and precision across diverse scientific disciplines.

#### 3.4 3D printing in automated sample preparation and detection

Researchers worldwide have increasingly leveraged 3D printing and open-source hardware to democratize access to laboratory automation and develop cost-effective, customizable tools



Table 4 Cost of 3D-printed alternatives to automated sample preparation and detection devices

| S/N | Device name  | Category                  | Cost (USD)    | Applications  | References |
|-----|--|---------------------------|---------------|---|------------|
| 1   | HistoEnder   | Sample preparation device | \$200         | It can perform automated staining of histological slides for biological and material sciences, with the ability to perform automated dip-coating and histological staining, making it highly accessible for low-budget laboratories   | 123        |
| 2   | Magnetic particle-based nucleic acid extraction device repurposed from a 3D printer                        |                           | \$400–\$750   | It automates complex nucleic acid extraction (DNA/RNA) and PCR cycles for diagnostic applications, integrating both processes into a single multifunctional device for seamless extraction and amplification  | 124        |
| 3   | Archerfish retrofitted 3D printer  |                           | \$500         | Enables high-throughput combinatorial experimentation for material science, facilitating rapid material composition screening and deposition for applications such as nanoparticles and semiconductors. Supports up to 250 unique samples per minute, significantly reducing the time required for material screening and experimentation | 125        |
| 4   | Nutating mixer (3D-printed desktop mixer)  |                           | \$37          | A 3D-printed nutating mixer for gentle gyrating agitation of samples such as DNA and blood, ideal for sensitive procedures  | 36         |
| 5   | Rotator shaker mixer (Arduino-controlled)  |                           | \$50          | A 3D-printed mixer combining rotator and shaker functionality, customizable for different mixing angles and speeds  | 35         |
| 6   | MVO automation platform  |                           | Not specified | It provides a modular platform for automating repetitive clinical assay procedures  | 126        |
| 7   | Repurposed 3D printer as a cost-effective high-performance liquid chromatography (HPLC) fraction collector | Detection device          | \$1400        | It performs fraction collection for HPLC-separated compounds, enabling downstream analysis such as stable isotope measurements  | 127        |
| 8   | Microextraction platform   |                           | \$600–\$700   | Automation of liquid and solid phase microextraction integrated with chromatography and mass spectroscopy analysis  | 128        |
| 9   | Fully automated spotting device  |                           | \$500         | Automates the spotting process for thin-layer chromatography (TLC) plates, increasing throughput, reducing preparation time, and supporting various plate and rack sizes using a repurposed 3D printer  | 129        |
| 10  | High-throughput reaction screening system using a modified 3D printer                                      | Reaction screening device | \$400–\$500   | It employs a delta 3D printer to dispense reaction mixtures into a 96-well plate for simultaneous screening   | 130        |

suitable for automated sample preparation, detection and point-of-care diagnostics leading to high-throughput experimentation as shown in the Table 4. For instance, Akhil Chaturvedi *et al.* designed a low-cost Automated Blood Sample Preparation Unit (ABSPU) that automates critical processes such as blood sample dilution, mixing, and staining for flow cytometry.<sup>131</sup> This device utilizes a miniature vibration motor to prevent cell settling, ensuring uniform sample quality, and its compact, electricity-independent design makes it ideal for point-of-care diagnostics. However, its focus on microfluidic flow cytometry limits its applicability across broader diagnostic workflows. Similarly addressing nucleic acid extraction challenges, Samantha Byrnes and her team developed an open-source system as shown in the Fig. 15(B) that enables nucleic acid extraction from blood using

a room-temperature, pressure-driven method, effectively removing the need for cold chain logistics.<sup>122</sup> This system achieves clinically relevant limits of detection for HIV, demonstrating significant utility in global health diagnostics, though manual interventions like cartridge handling limit full automation, and its adaptability to other biomolecules or diagnostic applications remains unproven. Expanding on high-throughput analytical capabilities, Mariusz Belka and his team introduced a 96-blade sorbent system for simultaneous extractions using chemically active 3D-printed materials.<sup>132</sup> Their system effectively demonstrated steroid analysis from human plasma, including hormones like cortisol and testosterone, utilizing LAY-FOMM-based sorbents.



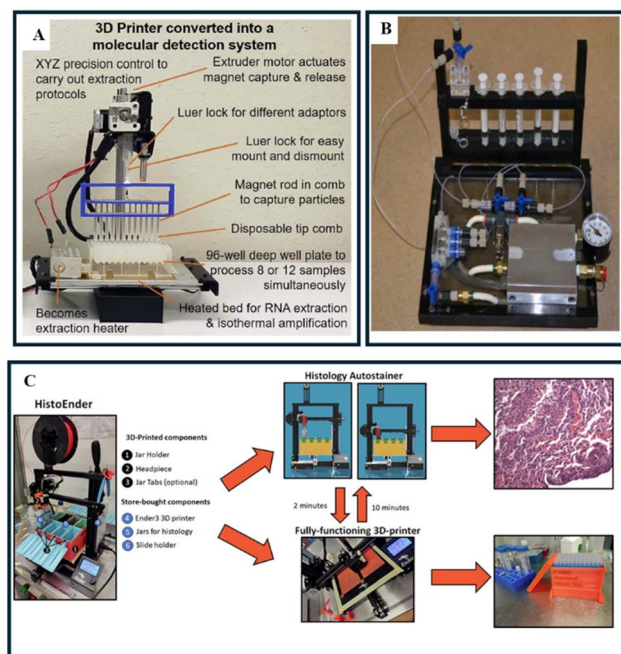


Fig. 15 (A) The transformation of a 3D printer into a molecular detection device. The printer's extruder was removed to allow for the mounting of adaptors via a luer lock mechanism. A Magnetic Particle Processor Attachment (MPPA) was then connected to this adaptor. The vertical movement of the MPPA is controlled by the Z-motor, while lateral movements are managed by the X and Y platform controls. A disposable tip comb, equipped with magnetic rods controlled by the extruder motor, is used to perform magnetic particle (MP) capture and resuspension. The printer bed accommodates either a 96-well deep-well microplate or pre-loaded cartridges, enabling simultaneous processing of 8 or 12 samples, depending on the plate orientation. The heated bed provides the necessary elevated temperatures for isothermal amplification. Reproduced with permission. Copyright 2018, Elsevier.<sup>121</sup> (B) Pictorial view of a portable, pressure driven room temperature nucleic acid extraction and storage system. Reproduced with permission. Copyright 2013, Royal Society of Chemistry.<sup>122</sup> (C) Pictorial view of adaptation of a 3D printer (Ender 3) into a functional histology autostainer using a combination of 3D-printed and commercially available components. The system retains its original 3D printing capabilities while also functioning as a histology autostainer. Reproduced with permission. Copyright 2022, Elsevier.<sup>123</sup>

The innovation of 3D-printed scabbard-like sorbents represents a breakthrough in bioanalysis, particularly for high-throughput formats, by significantly reducing production costs compared to traditional manufacturing methods and providing unmatched design flexibility that enables the creation of customized shapes and functional geometries tailored to specific analytical needs. However, the recovery rates for the 3D-printed sorbents were lower than those of commercial C18 sorbents, and performance validation was limited to a narrow range of steroids without testing broader chemical classes, highlighting areas for future improvement. In the realm of solution mixing, Tiffany M. Farris and her team utilized the design flexibility of additive manufacturing to develop two innovative 3D-printed tools for effective and simultaneous mixing of reactant solutions.<sup>133</sup> The first device, called “Flip Lead”, is designed for commercially available 96-well plates and

enables simultaneous mixing of reactants in adjacent wells through simple inversion. The second device, named “Mix-Bricks”, consists of two 3D-printed components: an interlocking brick with a customizable number of wells of specific volumes and a lid that facilitates the mixing of solutions in neighbouring wells by inversion. These devices are inexpensive to produce, making them ideal for resource-limited laboratories, and they offer high reproducibility with relative standard deviations below 5%, enhancing the reliability of experimental results.

Transforming standard 3D printers into multifunctional laboratory equipment has been a significant focus for several research teams. For example, Marco Ponzetti and his colleagues transformed a Creality Ender 3 3D printer as shown in the Fig. 15(C) into an automated slide stainer for histology, supporting protocols like hematoxylin and eosin (H&E) staining.<sup>123</sup> This adaptation is particularly ideal for laboratories with intermittent staining needs, offering a cost-effective alternative to commercial autostainers by costing under \$200 compared to the \$2000 to \$10 000 price range of commercial systems, and it retains the printer's original functionality, allowing quick reversion for standard 3D printing tasks. However, the system has limited capacity due to its bed size and slow Z-axis movement. In a similar vein, Kamfai Chan and his team explored the modification of entry-level 3D printers as shown in the Fig. 15(A) and 16 to perform nucleic acid extraction and amplification, aiming to address the high costs and complexity associated with conventional methods.<sup>121,124</sup> By replacing the printer's extruder with a magnetic particle processor attachment for automated nucleic acid extraction and utilizing the heated bed for thermal control tasks like DNA denaturation, enabling polymerase chain reaction (PCR), they significantly lowered the entry barrier for automated diagnostics. However, the system is currently limited to processing 12 samples per run due to the bed size, which could be addressed in the future by increasing the work envelope of the 3D printing setup. Similarly, Robert L. Schrader and his team modified an Anycubic Kossel 3D printer for automated liquid handling by replacing the hot end module of the printer with a glass syringe controlled by a stepper motor.<sup>130</sup> This configuration enabled the preparation of reaction mixtures in 96-well plates within approximately 40 minutes and completed the screening process within 105 minutes, with conditions optimized through electrospray ionization mass spectrometry (ESI-MS) analysis. The system effectively screened chemical reactions such as *N*-alkylation, Katritzky transamination, and Suzuki cross-coupling, providing heat-map visualizations of product distributions to facilitate rapid optimization of reaction conditions. By using open-source firmware and affordable hardware, the platform significantly reduced costs compared to commercial high-throughput systems and achieved precise liquid handling with a coefficient of variation of less than 3% in dispensed volumes. However, its use is restricted to reactions suitable for ESI-MS analysis. Broadening its compatibility with alternative detection methods could transform it into a universal tool for reaction optimization.



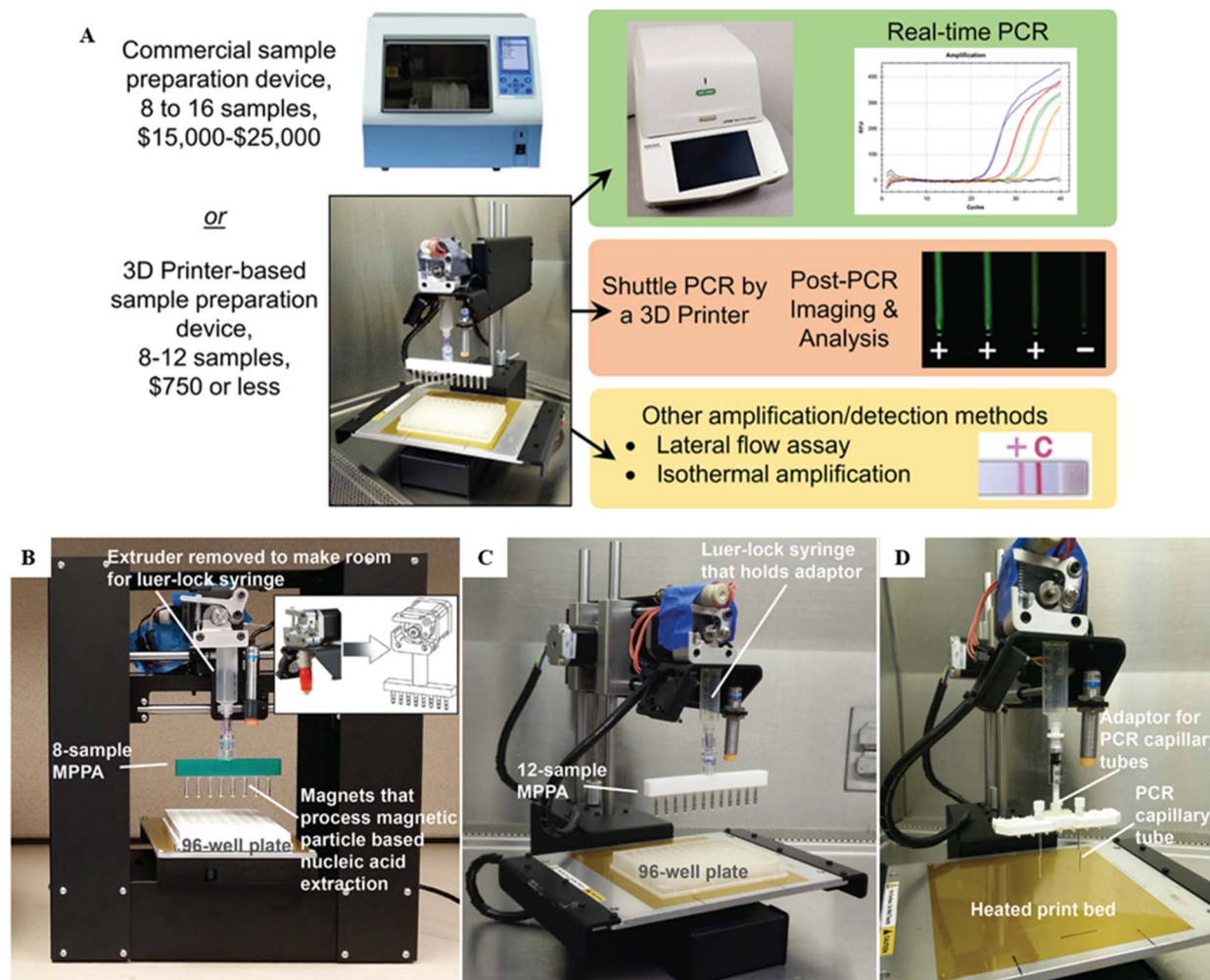


**Fig. 16** (A) Comparison of commercial sample preparation devices (8–16 samples, \$15 000–\$25 000) with a 3D printer-based sample preparation system (8–12 samples, \$750 or less). The modified 3D printer is shown performing multiple tasks, including shuttle PCR for thermal cycling, post-PCR imaging, and analysis, as well as alternative amplification/detection methods such as lateral flow assays and isothermal amplification. (B) The modified Printbot Play 3D printer (base footprint: 5" × 11") with the extruder replaced by a luer-lock syringe for magnetic particle-based nucleic acid extraction. The 8-sample Magnetic Particle Processor Attachment (MPPA) operates with a 96-well plate, and magnets are housed in PCR tubes to prevent direct contact with samples. (C) The Printbot Simple 3D printer (base footprint of 11" × 13") configured with a 12-sample MPPA and a 96-well plate setup, small enough to be fit inside a biosafety cabinet. (D) Adaptation of the 3D printer for thermal cycling, including an adaptor for PCR capillary tubes and a heated print bed for precise temperature control. Capillary tubes are shuttled between temperature zones for denaturation and annealing phases. Reproduced with permission. Copyright 2016, *PLOS One*.<sup>124</sup>

In the field of chromatography, Matheus C. Carvalho and Joanne M. Oakes modified a standard 3D printer to function as a high-performance liquid chromatography (HPLC) fraction collector for compound-specific isotope analysis (CSIA).<sup>127</sup> The adapted system enables heating of collected fractions, beneficial for rapid solvent evaporation which is not commonly available in commercial fraction collectors and it supports the analysis of compounds such as carbohydrates, amino acids, and fatty acids. The cost of adapting a 3D printer is significantly lower compared to purchasing commercial HPLC fraction collectors, which are often prohibitively expensive for smaller laboratories. Addressing the need for portable and versatile fluid handling, Deyber Arley Vargas Medina and his team developed a new class of movable 3D-printed microfluidic components, including torque-actuated pumps, rotary valves,

and pushing valves that operate manually without the need for bulky off-chip equipment such as syringe pumps or pressure sources.<sup>128</sup> The proof-of-concept demonstrated its effectiveness in protein quantification using artificial urine samples *via* colorimetric analysis, and the system is adaptable to a wide range of point-of-care analyses, making it a versatile tool for clinical diagnostics and environmental testing in field. In the domain of high-throughput experimentation, Alexander E. Siemenn and his team developed Archerfish, a retrofitted standard 3D printer capable of fluid mixing and high-speed material deposition, combining stepper motors and low-cost syringe pumps for precise control and achieving speeds of 250 unique compositions per minute.<sup>125</sup> The system demonstrates utility in fields like perovskite semiconductor development for automated characterization of band gap and stability, nanoparticle



synthesis, and pigment mixing, showcasing its versatility in material science and chemistry. Archerfish offers a transformative approach to material science experimentation by democratizing access to high-throughput tools, though future iterations should focus on improving uniformity in material deposition and expanding its functionality to include controlled-environment printing.<sup>125</sup> Low-cost mixing devices were also developed by researchers like Dhvani K. Trivedi and colleagues, who 3D-printed a desktop nutating mixer with a fixed 20-degree tilt angle, enabling gentle gyrating agitation of samples such as DNA and blood.<sup>36</sup> Suitable for foam-free mixing in sensitive procedures like protein purification or DNA extraction, the system costs just \$37. Similarly, Karankumar C. Dhankani and his team combined a rotator mixer and shaker into a single system, operating on an Arduino microcontroller that allows users to customize mixing angles and speeds.<sup>35</sup> Ideal for gentle mixing across various tube sizes with applications in biochemistry and molecular biology, it can be used in diverse laboratory settings, including glove boxes and cold rooms, and at a cost of under \$50, it offers savings of over 90% compared to commercial systems. Furthermore, platforms like the Minimum Viable Option (MVO) automation system developed by Brian Iglehart leverage open-source hardware and software combined with 3D-printed components to democratize laboratory automation.<sup>126</sup> Its iterative prototyping process has resulted in high precision, achieving linear motion accuracy of less than 0.1 mm and pipetting performance comparable to commercial systems. With Internet of Things integration *via* Raspberry Pi, the platform enables remote monitoring and data logging, making it particularly appealing for resource-constrained laboratories. Additionally, Gerald C. Anzalone and his colleagues developed a 3D-printed colorimeter built on open-source principles using an Arduino microcontroller for low-cost chemical oxygen demand analysis.<sup>134</sup> The platform demonstrated performance equivalent to commercial colorimeters at a fraction of the cost, making it suitable for applications such as monitoring wastewater quality and other environmental or educational uses. Its affordability and adaptability facilitate widespread adoption and customization, particularly in under-resourced settings. While it is currently optimized for chemical oxygen demand analysis, adapting it for other assays would require further development, presenting opportunities for broader applicability in the future.

Collectively, these advancements highlight the transformative potential of 3D printing and open-source technology in creating cost-effective, customizable laboratory tools. They facilitate applications ranging from sample preparation and diagnostics to high-throughput experimentation, addressing challenges in affordability and accessibility of sophisticated laboratory equipment. While these innovations offer significant benefits, challenges remain in ensuring scalability, full automation, and broader applicability across diverse analytical and diagnostic workflows. Future developments may focus on expanding compatibility with various assays, improving sample throughput, and enhancing user-friendliness to further democratize laboratory automation and make advanced scientific tools accessible to a wider range of researchers globally.

### 3.5 3D-printed robotic components for laboratory automation

With the rapid advancements in Robotics, robotic arms, grippers and manipulators have become critical components for Self-Driving Laboratories (SDLs), particularly in automating repetitive laboratory tasks such as liquid handling, object sorting, equipment operation, and sample management.<sup>3,6,45,48,135</sup> Robots are contributing remarkably to high throughput experiments by automating the repetitive tasks, thereby reducing human error and allowing researchers to focus on complex experimental design.<sup>2,10,136</sup> Integrating robotics with artificial intelligence (AI) enables real-time data analysis and autonomous decision-making, thereby optimizing research pathways.<sup>1,5,137</sup> Additionally, robots can safely perform tasks in hazardous environments, expanding the scope of feasible research without compromising human safety. Commercial robots such as Articulated Robots (*e.g.*, KUKA KR 6 R900, ABB IRB 120, FANUC LR Mate 200iD), Cartesian Robot (*e.g.*, Yamaha XY-X Series, IAI IK2-P6XB, Festo YXCR), SCARA Robots (*e.g.*, Epson LS3-B, Yamaha YK400XR, Toshiba TH650A, DOBOT M1 Pro) and Delta Robots (*e.g.*, ABB FlexPicker IRB 360, FANUC M-1iA, OMRON Quattro) are often prohibitively expensive ranging approximately between \$20 000 to \$40 000, thus limiting their accessibility for research and educational purposes in cost-sensitive SDLs. However, recent advancements in FDM 3D-printed robotic hands and arms are revolutionizing affordable, accessible solutions for SDLs. Table 5 presents a curated list of low-cost, 3D-printed robotic manipulators, arms, and grippers that have potential in Self-Driving Laboratories (SDLs). These devices were selected based on criteria such as affordability, adaptability, ease of integration, and relevance to lab automation tasks like sample handling, object transfer, or equipment operation. While some of these designs were originally developed for broader robotics contexts, they offer clear features that support SDL workflows, especially when customized for specific laboratory needs.

By leveraging 3D printing technology, researchers are developing adaptive, modular robotic hands that provide the dexterity and functionality necessary for various tasks in SDLs.<sup>39,138</sup> Notably, Haoran Li *et al.* introduced the SoftHand, an underactuated, tendon-driven robotic hand with both soft and adaptive synergies.<sup>39</sup> Costing around \$65, this hand exemplifies affordability in design. Its underactuated, tendon-driven structure allows it to grasp objects of different shapes and sizes by adapting its grip, making it suitable for simple material handling, such as transferring Petri dishes or cuvettes, within automated chemical or biological SDLs. The modular design also facilitates easy assembly and maintenance, and its open-source model encourages widespread adoption and further customization. However, as it relies on a single actuator, its performance in complex tasks is somewhat limited. Future enhancements could incorporate multi-actuator setups, like those seen in other designs, to expand its adaptability and control. A more advanced robotic arm, Reachy, developed by Sébastien Mick and his team, further demonstrated 3D printing's role in creating low-cost robotic solutions for SDLs.<sup>139</sup> As



Table 5 Cost of 3D-printed alternatives to effective robotic manipulators, grippers and arms

| S/N | Device name  | Category    | Cost (USD)    | Applications   | References |
|-----|--|-------------|---------------|--|------------|
| 1   | SoftHand   | Gripper     | \$65          | It is ideal for grasping experiments and dexterity research. It can perform various grasping tasks with a single actuator  | 39         |
| 2   | Print-N-Grip 3D printed robotic hand                     |             | Not specified | One-shot 3D printing eliminates complex assembly and reduces the cost. It is suited for hazardous material handling in chemical plants, radioactive environments, and bio-contaminated zones   | 140        |
| 3   | Wireless-controlled robotic hand with flex force sensors |             | \$100–\$150   | It is 3D printed with biodegradable PLA material. It offers flexible and precise control through glove-based wireless transmission, making it ideal for hazardous environments and remote operations, such as handling dangerous materials | 141        |
| 4   | InstaGrasp adaptive gripper                              |             | \$100         | It is fully 3D printed with minimal parts and fast assembly (<10 minutes). It can be used as an adaptive gripper in automated laboratories   | 40         |
| 5   | Modular, open-source 3D printed underactuated hand       |             | \$500         | It is designed for experimentation and easy integration into new systems due to modular components   | 138        |
| 6   | 3D printed robotic gripper                               |             | \$150         | It is suitable for manipulation tasks involving small and delicate objects. Its 3D-printed, open-source design makes robotics more accessible to a wider audience  | 142        |
| 7   | Reachy   | Arm         | Not specified | 7-DOF anthropomorphic robotic arm for delicate lab manipulations   | 139        |
| 8   | 3D printed robotic arm with elements of AI               |             | \$350         | It is ideal for small-scale assembly lines and testing AI based closed loop algorithms for precise robotic control. The six degrees of freedom enable versatile movement   | 137        |
| 9   | 3D-printed anthropomorphic arm                           |             | \$700         | It is suitable for performing automated experiments requiring gasping operations. Integrated vision-based manipulation with closed-loop deep learning enables adaptive tasks and high grasp success rates                                  | 143        |
| 10  | PyRobot  | Manipulator | Not specified | It is designed for mobile manipulation in research and education. It can be used for basic pick-and-place tasks  | 144        |
| 11  | 3D printed DeltaZ robot                                  |             | \$50          | It is suitable for basic manipulation tasks in small scale. The robot's affordability creates an opportunity to make manipulators more accessible for research applications  | 145        |

shown in the Fig. 17(D), its human-mimicking structure with seven degrees of freedom makes it ideal for SDL applications requiring delicate manipulations, such as adjusting instrumentation or conducting experiments where anthropomorphic motion is advantageous. Despite its flexibility, Reachy lacks a poly-articulated hand, which limits its capabilities for intricate grasping tasks. Integrating a versatile, low-cost gripper, like Soft Hand or Insta Grasp, could enhance Reachy's application in SDLs by providing it with the capability to handle a broader range of laboratory objects.<sup>39,40,139</sup> Similarly Alon Laron and his

team developed a 3D printed tendon based human like robotic arm which follows underactuated mechanism to adapt the shape of the object.<sup>140</sup> The hand is created using single-step 3D printing without the need for additional engineering and can support a varying number of fingers based on the user's requirements as shown in the Fig. 17(C). It can be easily detached from a universal base for disposal if contaminated and quickly replaced with a newly printed version. Alejandro Canizares and his team focused on developing cost-effective, 3D-printed prosthetic hand prototypes, with one controlled



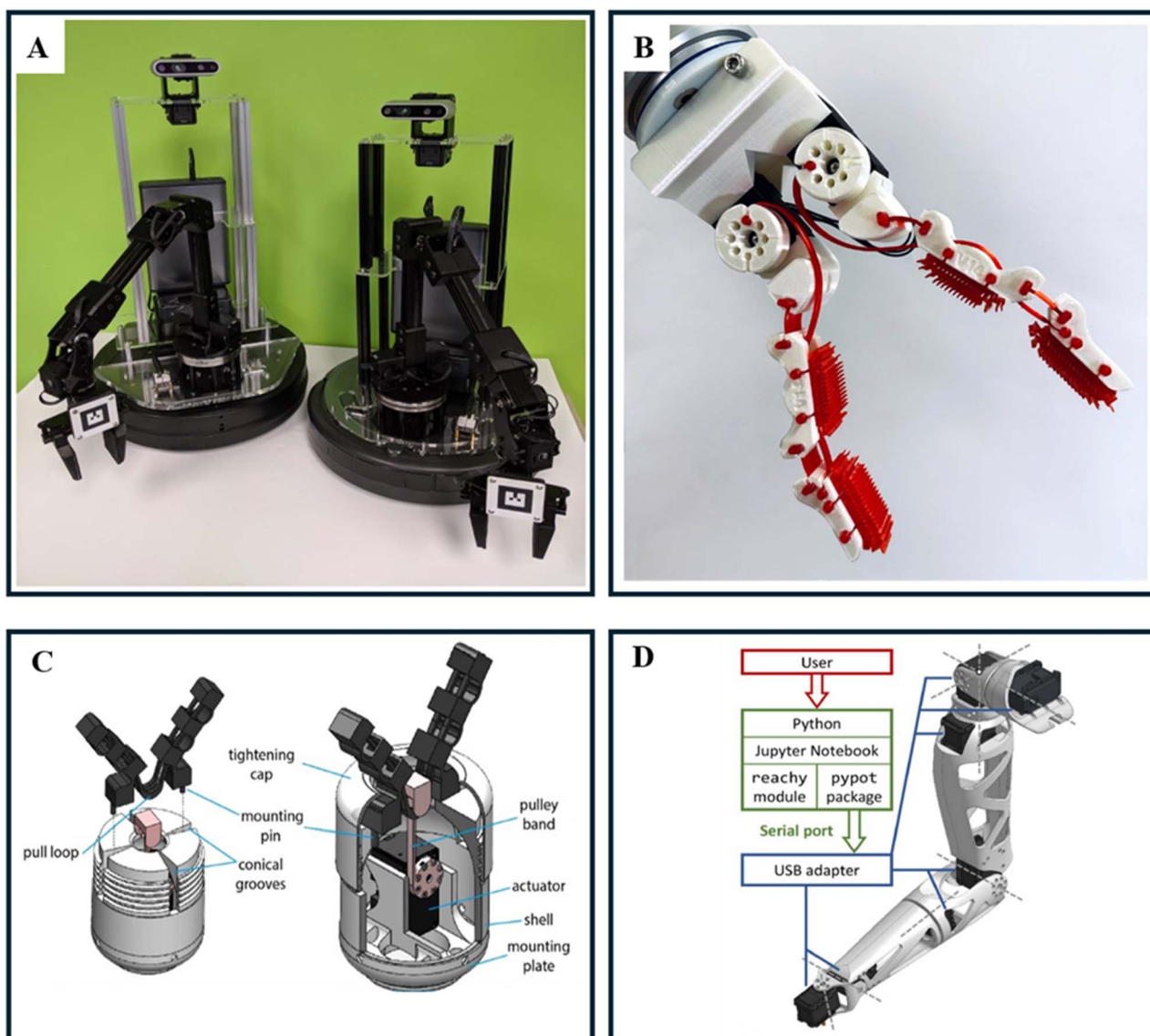


Fig. 17 (A) Dual robotic systems equipped with articulated arms and integrated sensors. Two mobile robotic platforms featuring robotic arms with grippers and depth cameras mounted on top. These systems demonstrate modular design suitable for tasks involving manipulation and perception in controlled environments.<sup>144</sup> (B) Pictorial view of an entirely 3D printed Adaptive gripper. Reproduced with permission. Copyright 2022, *IEEE*.<sup>40</sup> (C) A universal base designed for attaching the 3D-printed hand. The hand is secured to the base by aligning the mounting pins with the conical grooves and fastening them using the tightening cap. For smaller-scale hands, a reduction sleeve is employed to ensure a proper fit. Reproduced with permission. Copyright 2024, *Journal of Mechanical Design*.<sup>140</sup> (D) Architectural diagram illustrating the control stack of the Reachy robotic arm, detailing the high-level software interface (Python with Jupyter Notebook, reachy module, and pypot package) communicating via a serial port to the hardware through a USB adapter. Reproduced with permission. Copyright 2019, *Frontiers in Neurorobotics*.<sup>139</sup>

via a wearable glove equipped with flex sensors and another through EMG (myoelectric) sensors.<sup>146</sup> These designs, controlled through user gestures, highlight the accessibility and adaptability of 3D-printed prosthetics, capable of accurately replicating human hand movements at a fraction of the cost of commercially available alternatives. Although originally developed for prosthetics, can be adapted for SDL scenarios requiring intuitive remote operation of lab tools in biohazardous settings. However, the lack of structural durability could limit this prosthetic's functionality in rigorous lab environments.

Insta Grasp, developed by Xin Zhou *et al.*, provides a unique approach to adaptive grippers, aiming to reduce costs (\$100) and simplify assembly.<sup>40</sup> This fully 3D-printed gripper, as shown in Fig. 17(B), utilizes a push-fit assembly system enabling rapid setup in under 10 minutes, making it ideal for repetitive sample transfers, tube manipulation, and quick tool swaps in SDLs. Constructed with rigid PLA for durability and TPU for flexible components, it demonstrated exceptional durability, with TPU tendons enduring over 86 000 stress cycles without significant wear, proving its reliability for continuous use in lab environments. While Insta Grasp is highly adaptable for various



grasping tasks, it lacks advanced control features and could benefit from integrating control sensors like EMG, as seen in Canizares's work, to broaden its application range.<sup>40,146</sup> The hybrid actuation system developed by Florin-Felix Răduică offers a novel approach to prosthetic and robotic hands.<sup>147</sup> Combining body-powered and motorized mechanisms, this design provides flexibility for tasks requiring varied control methods. At around \$260, it presents a cost-effective solution for SDLs looking to prototype adaptable robotic elements for both simple and complex tasks. Future adaptations could involve incorporating Reachy's customizable components to enhance its versatility, while also benefiting from Insta Grasp's push-fit system for simplified maintenance and part replacement.<sup>40,139</sup>

Henning Zwirnmann *et al.* developed adaptive, dual-material fingers for parallel robotic grippers using FDM 3D printing, combining rigid PLA structures with soft TPU coatings to mimic the compliant touch of human skin and enhance grip.<sup>148</sup> They introduced a practical taxonomy of lab containers (micro-centrifuge tubes, cryotubes, centrifuge tubes, Petri dishes, cell culture flasks, well plates, disinfectant and glass bottles), to guide the design of versatile gripper fingers, enabling stable grasping through passive underactuation and mechanical compliance. These grippers were integrated with a tool exchange system which can facilitate multi-step lab automation workflows in SDLs. While the finger size may limit their effectiveness in miniaturized or densely packed environments, and durability under sterilization remains to be fully validated, the design stands out for its use of off-the-shelf filaments and consumer-grade printers, offering a low-cost, rapidly customizable solution. Fazil Salman *et al.* introduced a wireless-controlled 3D-printed robotic forearm, operated *via* flex sensors embedded in a glove, making it suitable for remote use in hazardous environments. This system enables the remote handling of infectious or toxic substances in SDLs, thereby minimizing human exposure risk.<sup>141</sup> The biodegradable PLA construction adds an environmentally conscious aspect, while the low-cost components like Arduino Nano controllers and NRF24L01 modules make the design accessible and easy to replicate. The system's high responsiveness (0.133 milliseconds) allows it to mimic real-time human gestures, making it an ideal tool for SDLs. The integration of artificial intelligence (AI) with robotics is essential for advancing self-driving laboratories (SDLs), enabling automation, precision, and adaptive experimentation. Sainul Islam Ansary *et al.* introduced the design and development of an adaptive gripper capable of grasping objects with varied geometric shapes. The design uses movable pulleys and tendon wires to ensure stable grasping of various objects.<sup>149</sup> The gripper design is optimized and developed using 3D printing, and its effectiveness is validated through experiments with common household objects. Its open, adaptable structure aligns with DIY and open-source automation efforts, helping to lower the entry barrier for SDL implementation in resource-constrained environments. However, the study does not address key considerations such as material compatibility, or integration with broader robotic systems, which may limit its applicability in more demanding laboratory contexts. Rafał

Siemasz *et al.* has integrated the elements of artificial intelligence in a cost-effective 3D printed robotic arm combining affordability with modularity for easy customization and repair.<sup>137</sup> In SDLs, it can automate sample pick-and-place tasks, integrate with sensors for real-time process adjustments, and streamline repetitive tasks. Although this arm, costing around \$350, offers flexible manipulation for tasks like sample handling, its 750-gram payload limit and reliance on stepper motors can restrict precision and durability, particularly in complex SDL tasks requiring real-time feedback and corrections.

Pavlo Tymkiv's IoT-enhanced 3D-printed robotic arm focuses on real-time tactile feedback, with the resulting data capable of being fed into SDL software to iteratively optimize delicate handling tasks.<sup>150</sup> With AI-driven adaptive control, the arm can mimic human movements for fine handling, beneficial for SDL applications involving sensitive materials. However, the FDM 3D-printed materials' durability limits its use in extreme environment. Adithyavairavan Murali *et al.* designed PyRobot as a high-level interface built on top of ROS (Robot Operating System), enabling researchers and students to control different robots without needing deep expertise in robotics.<sup>144</sup> As shown in the Fig. 17(A), PyRobot possess articulated arms and built in sensors which simplifies the process of commanding robots, making it accessible to those outside the field and expanding the usability of robotics in various research and educational settings. PyRobot is optimized to work with affordable, open-source platforms such as LoCoBot and Sawyer, reducing financial barriers to entry for robotics experimentation. By democratizing access to robotics hardware and software, PyRobot enables non-experts to program SDL tasks like object placement, material delivery, and feedback-driven sorting. Pragna Mannam *et al.* designed a 4-axis robotic gripper with two 3D-printed mini delta robots and linear actuators, priced at around \$300, significantly lower than commercial alternatives.<sup>142</sup> Using neural networks, they modelled the gripper's forward and inverse kinematics to achieve repeatable, precise movements. This approach allows for fine motor tasks, making it ideal for SDLs requiring precise, small-scale handling. Similarly, DeltaZ robot developed by Sarvesh Patil and his team, is an affordable, modular delta robot made from 3D-printed materials, costing around \$50.<sup>145</sup> Its compliant design ensures safe interactions, making it suitable for automated pipetting, weighing, and mixing tasks in microfluidic or chemical SDL setups. With three degrees of freedom, DeltaZ can handle a range of dynamic and precise pick-and-place tasks. Tamás Bárány *et al.* developed a low-cost 3D-printed robotic arm which is designed for educational use and offers four degrees of freedom and a budget-friendly build utilizing micro-servos.<sup>151</sup> This robot is accessible and suitable for classroom settings or simple SDL automation tasks. However, the low-cost micro-servos limit its precision and load-carrying capacity to approximately 140 grams, restricting its application to basic tasks that do not demand high accuracy or heavy lifting. The Óscar Delta Robot, developed by César M. A. Vasques, has a modular structure that supports simple pick-and-place tasks in educational settings.<sup>152</sup> This 3D-printed delta robot offers



performance comparable to more expensive models while remaining a low-cost, entry-level solution for straightforward pick-and-place tasks or demonstration-scale SDL experiments. However, it lacks real-time control and advanced software capabilities, limiting its application to basic tasks. Future upgrades could include a more sophisticated control interface, allowing Oscar to handle more complex SDL manipulations that require precision and adaptability.

So, it is evident that the recent developments in affordable, 3D-printed robotic arms, grippers, and integrated systems are transforming the landscape of SDLs. Moreover, integrating AI-driven control and easily upgradable modular architectures further reduces the barriers to entry, empowering a wider array of laboratories and educational institutions to adopt SDL technologies. Although challenges remain, such as durability limitations, precision constraints, and the need for more user-friendly software ecosystems, the convergence of 3D printing, low-cost electronics, and intelligent control systems heralds a future where SDL automation is both highly capable and broadly accessible.

### 3.6 Chemical synthesis

The rapid advancement of 3D printing technology in recent decades has emerged as one of the most transformative innovations in the chemical sciences, particularly through its ability to create low cost “reactionware” *i.e.* customized chemical reactors that harness 3D printing’s precision in shaping topology, geometry, and composition to significantly influence reaction outcomes.<sup>153,154</sup> This technology has demonstrated utility in a range of applications, including inorganic and organic synthesis, hydrothermal synthesis, flow chemistry, and analytical chemistry. As a result, the field of chemical synthesis is being revolutionized by the adoption of 3D-printed reactionware, which provides customizable, affordable, and scalable solutions for laboratory automation.<sup>155,156</sup> This shift is evident in the work of Philip J. Kitson *et al.*, who demonstrated the use of low-cost 3D printing to fabricate hydrothermal reactors, designed for high-throughput synthesis.<sup>157</sup> These 3D-printed reactors allow for easy customization in design, scale, and geometry to meet specific experimental needs, from small-scale testing to preparative-scale synthesis. As shown in the Fig. 18, the reactionware includes a 5 × 5 array of reactors that enables 25 simultaneous reactions. The study successfully synthesized two coordination polymers (one cadmium-based and one copper-based) and optimized the synthesis conditions for scale-up, showcasing the practical application of 3D-printed reactors in chemical synthesis. Due to less cost of the 3D printed reactors, the reactors are designed to be used for single use hence minimizing the contamination risks from prior reactions. Unlike traditional, fixed-geometry apparatus, 3D-printed reactors can be tailored to specific experimental requirements, allowing for innovative design features like spherical voids.

3D printed polypropylene based reactionware allowed the creation of hydrothermal reactors with internal voids, eliminating the need for costly stainless-steel equipment and

enabling high-throughput synthesis at temperatures up to 140 °C. However, the polypropylene material used limits the reactors to temperatures below 150 °C, restricting their use for high-temperature reactions. The reactors may deform at higher temperatures and pressures due to the softening of thermo-plastic materials. To address this problem, several studies have focused on developing hybrid multi-material 3D-printed reactors to enhance the mechanical strength necessary for operation under high-temperature conditions.<sup>70</sup> Reactionware designed with polypropylene (PP) structures combined with acetoxy-silicone components can endure challenging chemical environments. The acetoxy-silicone polymer also acts as a matrix for embedding catalysts, allowing for sequential reactions and applications in electrochemical and catalytic synthesis.<sup>154,155</sup> This multi-material approach also supports sequential, multistep syntheses within a single device by using separate reaction chambers, enabling different, often incompatible, reactions to occur independently. Additionally, the introduction of silicone rubber in the reactionware functions as a self-sealing membrane for introducing reagents, while the reactor’s geometry allows control over reaction stoichiometry.<sup>154</sup> Chang-Gen Lin *et al.* expanded on this concept by introducing 3D-printed reactionware with compartmentalized chambers, enabling modular control over reaction pathways.<sup>158</sup> This setup allows for precise timing in the mixing of different reaction mixtures, offering flexibility in managing reaction intermediates and creating compounds otherwise inaccessible with conventional single-chamber reactors. By allowing sequential multi-stage hydrothermal synthesis, the 3D-printed reactors expand the synthetic parameter space, facilitating high-throughput exploration of novel compounds.

While 3D printing holds transformative potential for lab automation, challenges related to print quality can impact the utility of reactionware. Various issues can arise during 3D printing, each with potential solutions to improve print quality.<sup>76,159–161</sup> Delaminating layers may result from a large step size along the z-axis or low extrusion temperatures, which can be resolved by reducing layer thickness or slightly increasing the hot-end temperature.<sup>76</sup> High flow rate can result in over-extrusion, closing small voids, which can be managed by decreasing the flow rate in print settings.<sup>161</sup> Incorrect filament diameter selection often leads to inner dimensions printing smaller than intended, so ensuring the filament diameter matches the actual size can prevent this issue.<sup>154</sup> Low extrusion temperature or incorrect nozzle size can lead to layered outer boundaries or gaps in extruded filaments, which can be fixed by adjusting the nozzle size and increasing the temperature.<sup>160</sup> Under-extrusion, incorrect infill structure, or too few solid layers can cause leaks in printed reactionware.<sup>154</sup> Increasing the flow rate, choosing a denser infill, or adding more solid layers can resolve this issue. Incompatible bed surface or poorly calibrated z-height may lead to detachment from the print bed.<sup>160,161</sup> Applying glue or tape to the bed or setting the nozzle 100–200 μm from the surface can improve adhesion. Damaged filament from the feed wheel or low pressure can result in filament feed issues, such as slipping or blockage.<sup>76</sup> Checking and adjusting



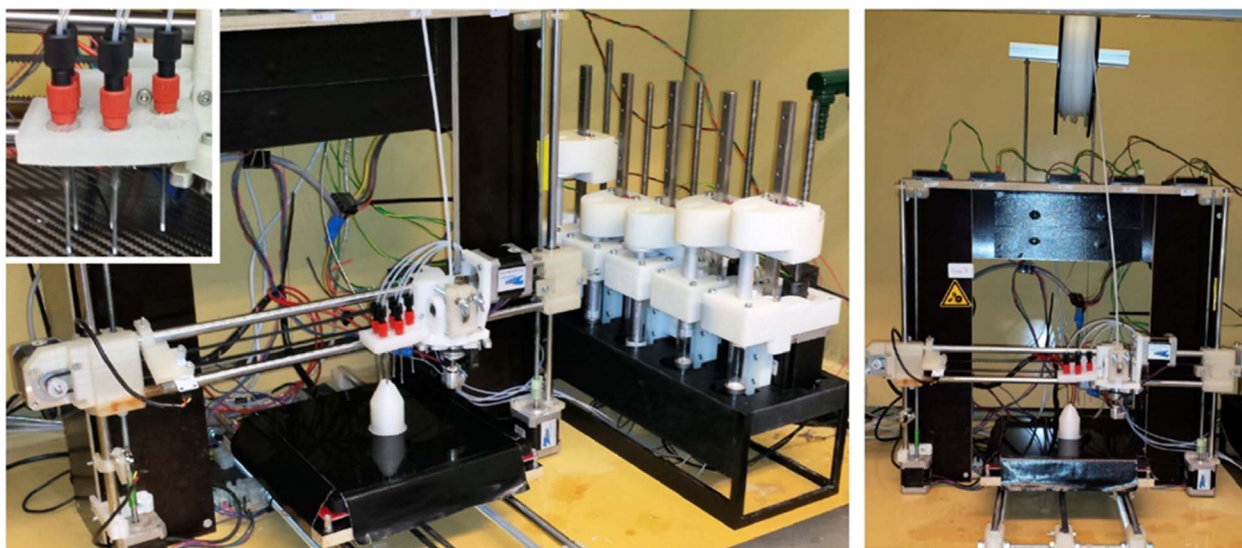


Fig. 18 Photographic view of a Prusa i3 RepRap printer modified into a robotic platform set-up with a 3D-printed reaction for the automated synthesis of ibuprofen. Reproduced with permission. Copyright 2016, *Beilstein Journal of Organic Chemistry*.<sup>157</sup>

feed wheel settings helps maintain consistent filament movement.

In pursuit of real-time monitoring in synthesis, Jennifer S. Mathieson *et al.* developed a low-cost, custom 3D-printed device designed to continuously monitor reactions in real-time through electrospray ionization mass spectrometry (ESI-MS).<sup>162</sup> The setup allows simultaneous, real-time analysis with ESI-MS, while also splitting the reaction stream to collect products for further examination. By coupling the device with ESI-MS, reactions can be observed as they progress, allowing for dynamic adjustments to optimize conditions and product yields without interrupting the flow. The reactionware features adaptable fittings and flow paths, making it reusable and versatile for different chemical reactions and experimental setups. This approach aligns with continuous flow chemistry setups, paving the way for automated, scalable processes in synthetic chemistry and high-throughput analysis. Future research could expand on this work by incorporating more advanced designs that include more variety of in-line characterizations. These enhancements would enable more comprehensive real-time analysis of reaction pathways, providing a fuller understanding of reaction dynamics and product formation.

Vincenza Dragone *et al.* demonstrated that the 3D printed reactionware can be efficiently designed and fabricated for continuous-flow reactions.<sup>163</sup> The study incorporates in-line ATR-IR spectroscopy, a non-invasive real-time monitoring method within the flow system. The ability to monitor reactions continuously allows for rapid optimization and troubleshooting, which is essential in producing a feedback loop in controlling the reactions. For self-driving labs, real-time data collection is essential, as it allows machine-learning algorithms to adjust parameters dynamically based on real-time feedback. Integrating in-line analytical tools with 3D-printed devices

makes high-frequency data collection possible in smaller, lower-cost setups. This accessibility to real-time monitoring means that self-driving labs can be more effective in fine-tuning reaction parameters in continuous-flow settings, enhancing the autonomy and accuracy of automated processes. Precise control over reaction kinetics is essential for self-driving labs as it allows for high-throughput experimentation with various flow rates and residence times to optimize yields. The ease of adjusting flow dynamics in 3D-printed devices facilitates this experimentation, making it feasible to explore a wide range of conditions affordably. By modifying RepRap 3D printer, Philip J. Kitson and his team developed a unified synthesis robot that autonomously builds reaction vessels and performs the necessary liquid handling steps to synthesize the common painkiller ibuprofen.<sup>164</sup> This project showcases the remarkable flexibility of today's open-source consumer robotic equipment when adapted for laboratory automation at an affordable cost. Future progress in this area may lead to further open-source solutions that enable robotic platforms to handle more routine chemical synthesis tasks, such as work-up and purification steps.

The rapid expansion of open-source software and affordable 3D printers supports a vision where researchers can quickly download, customize, and fabricate tools, democratizing access to sophisticated lab equipment. This approach enables individuals to access tools for chemical synthesis and discovery without relying on expensive laboratory infrastructure. Mark D. Symes and his team illustrated this with a low cost 3D printed robotically controlled syringe to produce self-healing, reusable reactionware which can be used for automated synthesis as well as spectroscopy characterization.<sup>155</sup> By integrating reagents directly into a 3D-printed matrix, the setup allows chemical reactions to be precisely initiated and controlled through digital means. This highlights the transformative potential of integrated, 3D-printed reactionware to democratize chemical



synthesis and analysis, creating opportunities for labs to perform sophisticated chemical processes affordably and accessibly. Furthering the concept of self-driving labs, Kitson and his team explored a unique approach in creating low cost self-contained reactionware for multi-step chemical synthesis and purification by combining solid and liquid handling directly in 3D-printed devices.<sup>153</sup> The inclusion of liquid handling automation marks a step forward in creating self-driving labs, where reactions can be carried out without manual reagent transfer, increasing precision and reducing variability. The reactionware incorporates reagents, catalysts, and purification systems, making the process accessible even outside a traditional lab setting and to users without extensive chemical expertise. While yields in these 3D-printed reactors were slightly lower than in traditional glassware due to incomplete transfers and potential reagent loss, this design marks a significant step in automated lab processes. However, relying on gravity to move reagents between chambers may limit applications where precise flow rates are needed, as gravity-driven movement lacks the fine control of actively pumped systems.

Extensive research has also been conducted to showcase the potential of 3D printing in making configurable lab-on-a-chip devices more accessible, offering a flexible, fast, and cost-effective solution for performing complex chemical synthesis in compact environments.<sup>163,165</sup> The capability to rapidly design, produce, and modify reactor configurations customized for specific reactions brings a new dimension of accessibility and adaptability to micro and milli fluidic devices.

However, a significant challenge to adopting 3D printing in synthetic chemistry labs is the need to design reactors from scratch for each synthesis. Typically, this design process relies on general-purpose 3D CAD software like AutoCAD, SolidWorks, or OnShape, which are not tailored for reactionware creation. As a result, chemists need CAD skills to produce digital reactor designs suited to their specific needs. To overcome this barrier, Wenduan Hou *et al.* developed the ChemSCAD specifically to simplify and streamline the reactor design process for chemists, eliminating the need for CAD expertise and focusing on chemically relevant parameters for synthesis.<sup>70</sup> Traditional reactor design is labour-intensive, and creating custom reactionware for each synthesis is time-consuming. ChemSCAD automates the design process, enabling standardized, modular reactors that are easily customizable for different synthesis pathways. By generating digital reactor designs that can be used in automated systems, it facilitates streamlined workflows and optimizes the chemical discovery process. ChemSCAD enables the storage of synthesis designs and analytical data in a digital repository, which can be shared and versioned, facilitating easy access to reactor designs and reproducibility of synthesis procedures. For comprehensive, digitizing automated chemical synthesis requires capturing all relevant parameters and processes in a modular, precise, and unambiguous way. Recording reaction steps, times, and reagent information alone is insufficient because chemical synthesis often relies on tacit knowledge about specific reactions, reagents, and chemotypes, affecting reproducibility. Therefore, to successfully digitize

reactions, all unit operations (such as heating, stirring, and transfers) must be defined and organized. This level of detail is common in process chemistry and helps reduce challenges in developing automated synthesis platforms.

Andrius Bubliauskas *et al.* presents a new approach to digitizing organic synthesis by using 3D-printed reactionware to perform multi-step reactions in a modular, controlled manner.<sup>156</sup> Reactionware devices are divided into modules based on unit operations, like heating, stirring, and filtering, enabling complex chemical processes to be broken down and performed in separate steps. The study successfully digitized the synthesis of various compounds, including MIDA boronate esters, sulphanilamide, and products from reactions like ester hydrolysis and Wittig olefination, showcasing the versatility and reliability of the reactionware approach. The modular design makes advanced synthesis techniques more accessible, even to users with limited expertise, by reducing the need for tacit knowledge typically required in traditional synthesis. This approach is suitable for instructional labs, where students can learn organic synthesis through structured, reproducible protocols that illustrate key chemical processes in a controlled environment. Defining reactions in modular, machine-readable formats allows reactionware to lay the groundwork for AI-driven synthesis and optimization. This approach could lead to the automation of complex chemical processes with minimal human intervention, a promising area for future research.

As open-source FDM 3D printing and accessible software continue to evolve, they present a transformative pathway for democratizing chemical research and development, opening high-throughput, customizable synthesis to a broader community and accelerating innovation in synthetic chemistry. FDM 3D printing is also set to play a pivotal role in material discovery by serving as a rapid testing ground for AI and machine learning, which will inform material design and provide insights for scaling from lab to industrial manufacturing.<sup>65</sup> Many researchers have leveraged this technology to produce lab tools and structural models for educational purposes, benefiting from its low cost and ease of use.<sup>164,166</sup> This easy availability and low cost allow synthetic chemists to test large-scale implementations of molecular designs and enables engineers to fabricate diverse structures using a wider array of materials than previously possible. Despite its potential to revolutionize areas like large-scale manufacturing and regenerative medicine, FDM 3D printing still faces significant limitations. Many polymers were not originally designed for FDM 3D printing, resulting in defects that reduce the mechanical strength of printed parts, especially when compared to parts made with conventional injection moulding.<sup>76,161</sup> Extensive research in polymer chemistry now makes it possible to 3D-print a wider range of materials, enabling the creation of advanced chemical instruments from diverse compositions that can operate reliably under extreme conditions.<sup>81,183,184</sup>

### 3.7 3D bio printing

The significance of 3D bioprinting lies in its transformative impact on the medical and biomedical fields, offering a highly



Table 6 Cost of 3D-printed alternatives to custom made Bio Printers

| S/N | Device name                               | Cost (USD)   | Applications   | References |
|-----|---|--------------|--|------------|
| 1   | Low-cost hybrid 3D bioprinter             | \$300        | It is capable of simultaneous printing of thermoplastics and hydrogels for multi-material designs, retaining FDM printing capabilities with the integration of a syringe-based extruder  | 167        |
| 2   | Open-source biofabricator                 | \$1000       | It combines extrusion and electrohydrodynamic printing technologies in a single system, enabling multi-material and multi-technology scaffold fabrication for advanced tissue engineering applications   | 168        |
| 3   | Dual-mode hybrid bioprinter               | \$1000       | It is capable of developing hybrid constructs for regenerative medicine and tissue engineering by seamlessly alternating between plastic and hydrogel extrusion within a single print  | 169        |
| 4   | Versatile open-source printhead           | \$2000       | Conventional FDM 3D printer is repurposed into a microextrusion bioprinters capable of handling bioinks like gelatin, alginate, and poloxamer, while maintaining compatibility with existing FDM systems and enabling multi-material printing capabilities | 170        |
| 5   | Hackable modular printer                  | \$900–\$1900 | This printer is designed for soft material applications like printing hydrogels, automated liquid dispensing, non-planar printing, and pick-and-place operations for meso-objects  | 171        |
| 6   | Thermosensitive hydrogel printer          | \$800        | It is capable of printing cell-laden hydrogels for tissue engineering using a customizable extruder capable of handling both light-sensitive and thermo-sensitive bioinks  | 172        |
| 7   | Hybrid droplet-and-extrusion bioprinter   | \$1370       | It is capable of fabricating high-resolution microstructures <i>via</i> inkjet printing and larger 3D constructs with extrusion printing   | 173        |
| 8   | Ultra-low-cost 3D bioprinter              | \$150        | It is a modified off-the-shelf desktop FDM 3D printer designed to accommodate bioprinting functionalities, capable of printing both cell-free and cell-laden hydrogels for biological studies  | 174        |
| 9   | DIY 3D bioprinter                         | \$500        | Adaptation of a desktop FDM printer with a syringe-based extruder for large-volume printing, enabling cost-effective tissue scaffold bioprinting through accessible open-source design   | 175        |
| 10  | Multimaterial high-throughput DIW printer | \$250        | It is a custom-built printer with active mixing, multi-nozzle, and multi-material gradient capabilities  | 176        |
| 11  | Accessible bioprinter for stem cells      | \$300        | Adapts a low-cost 3D printer for precise cell placement and stem cell differentiation  | 177        |
| 12  | Open-source multihead bioprinter          | \$400        | Uses motor-driven volumetric extrusion with multiple print heads for multimaterial bioprinting   | 178        |
| 13  | LEGO-based 3D bioprinter                  | \$250        | It is constructed using LEGO mindstorm and technic for modular and reconfigurable bioprinting, enabling the creation of 3D hydrogel structures with live human cells for tissue models and artificial skin   | 179        |
| 14  | High-performance open-source bioprinter   | \$900        | FlashForge finder FDM 3D printer is converted into a bioprinter using the 4-syringe pump and open-source components, enabling the printing of collagen-based scaffolds and complex 3D anatomical models  | 180        |
| 15  | Quad-extrusion bioprinter                 | \$297        | Features a quad-extrusion head supporting multi-material and support bath printing modes   | 181        |
| 16  | Nydus one syringe extruder bioprinter     | \$100        | It is a modification of prusa i3 printer with mechanical syringe extrusion for the FRESH method, enabling the printing of geometrically complex cell-laden constructs with high reproducibility for tissue and organ modelling                             | 182        |

versatile and efficient method for fabricating customized medical products, such as prosthetics, implants, scaffolds, and even tissues and organs, with enhanced accuracy, resolution, and cost-efficiency.<sup>185–188</sup> The ability to tailor designs based on patient-specific data, such as CT or MRI scans, has revolutionized personalized medicine, reduced surgery and recovery times and improving clinical success rates.<sup>187,188</sup> However, the

widespread adoption of 3D bioprinting has been substantially impeded by the high cost of commercially available platforms, which range from \$5000 to over \$1 000 000.<sup>187,189</sup> Apart from that most of them rely on proprietary software and closed hardware ecosystems, restricting compatibility with novel biomaterials and customization for specific research needs.<sup>175</sup> To overcome this problem, researchers and innovators have focussed on the



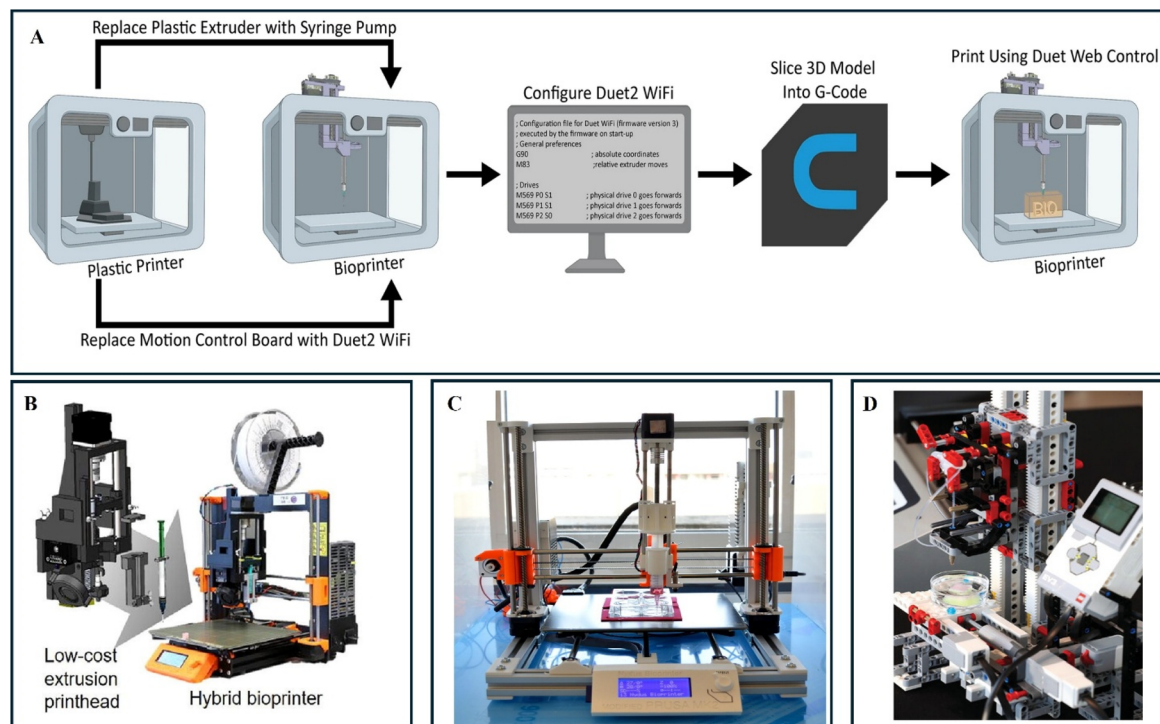


**Fig. 19** (A) Workflow for transforming a standard 3D printer into a bioprinter. The process involves replacing the plastic extruder with a syringe pump for material deposition and upgrading the motion control board with a Duet2 WiFi for enhanced control. The Duet2 WiFi board is configured using custom firmware. A 3D model is then sliced into G-code using appropriate software, followed by printing the bioprinted structure using Duet Web Control. Reproduced with permission. Copyright 2022, *Nature Scientific Reports*.<sup>180</sup> (B) Pictorial view of the modified hybrid 3D bioprinter built on the Prusa i3 MK3 3D printer. A syringe-based micro extruder was incorporated as a modular secondary printhead, while preserving the functionality of the fused deposition modelling (FDM) printing process. Reproduced with permission. Copyright 2021, Elsevier.<sup>169</sup> (C) FDM 3D Printer repurposed into a bio printer. Reproduced with permission. Copyright 2019, Elsevier.<sup>182</sup> (D) A 3D bioprinter built using commercially available LEGO components, including Technic and Mindstorm precision modular construction kits. The system integrates a microfluidic droplet generator, assembled using readily available ETFE T-junctions and FEP tubing. Reproduced with permission. Copyright 2023, *Advanced Materials Technologies*.<sup>179</sup>

development of open-source, low-cost bioprinter designs, leveraging off-the-shelf components and customizable platforms.<sup>173,175,190–192</sup> Open source bioprinters offer an affordable alternative to proprietary systems, democratizing access to bioprinting technologies as shown in the Table 6. The transparency and collaborative nature of open-source platforms have further fuelled innovation, fostering an active global community of developers who continually improve designs and share resources freely.<sup>169</sup> This approach enhances reproducibility and minimizes lab-to-lab variability, addressing critical limitations in conventional proprietary systems. The integration of low-cost, open-source 3D bioprinters into self-driving labs is revolutionizing biomedical research by combining affordability, adaptability, and automation. Moreover, the modularity of open source bioprinters allows seamless integration with autonomous systems, making them scalable and versatile for various research applications. Real-time optimization of bio fabrication processes in self-driving labs not only democratizes access to advanced bioprinting technology but also accelerates innovation in regenerative medicine and personalized healthcare. Konstantinos Ioannidis *et al.* developed an ultra-low cost bioprinter (\$230) by modifying the Anet A8 FDM 3D printer by

integrating a lightweight syringe pump and developing alginate-gelatin bioinks suitable for stem cells.<sup>190</sup> The open-source design allows for further modifications and upgrades by the research community. Similarly, Melanie Kahl *et al.* developed a low cost (\$150) bioprinter by designing a 3D-printed syringe holder and incorporating into Anet A8 FDM 3D printer to accommodate a 1 mL sterile syringe with a luer lock fitting, enabling compatibility with various nozzle types and flexibility for different bioink viscosities.<sup>174</sup> Joshua W. Tashman *et al.* converted a FlashForge Finder 3D printer into a high-performance, low-cost bioprinter using open-source components like the Duet 2 WiFi motion control board and the Replistruder 4 syringe pump extruder as shown in the Fig. 19(A).<sup>180</sup> The modified printer achieved travel errors as low as 35  $\mu\text{m}$ , enabling the fabrication of geometrically complex constructs with high dimensional accuracy, comparable to commercial bioprinters. John A Reid *et al.* explored the adaptation of a low-cost, commercially available 3D printer (Felix 3.0) into a functional bioprinter capable of precise cell placement and differentiation of human induced pluripotent stem cells (hiPSCs).<sup>177</sup> Semyon I. Koltsov *et al.* addressed the need for versatility by modifying standard FDM printers to enable



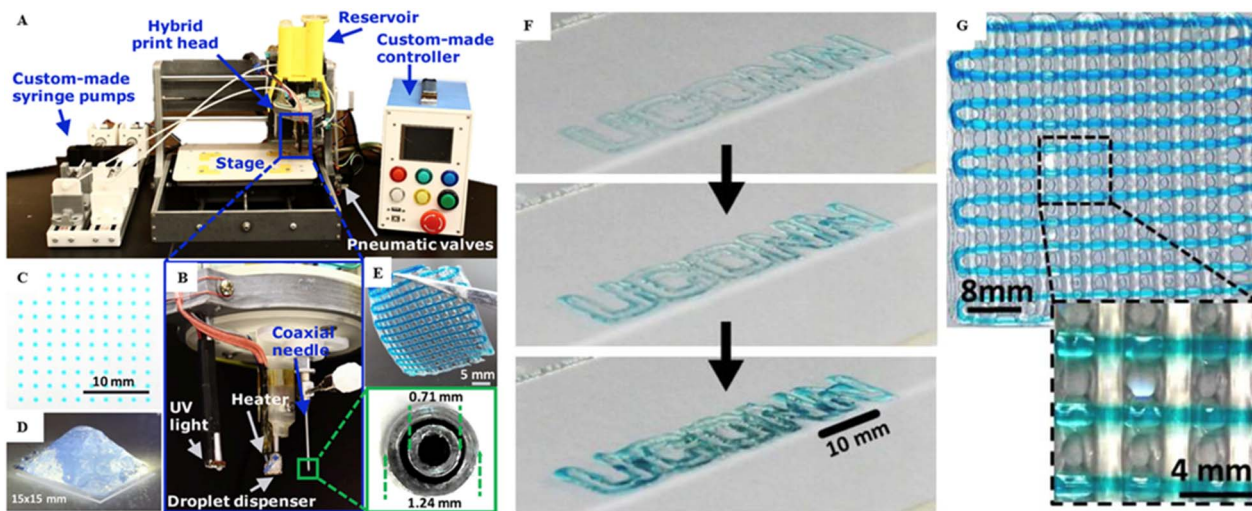


Fig. 20 (A) Pictorial view of a Hybrid Bio Printer, (B) Printing heads, which include a droplet dispenser for inkjet printing, a UV light for bioink crosslinking post-deposition, and a coaxial nozzle for extrusion printing. (C–G) Printing demonstration showing (C) individual droplets, (D) a 3D 21-layer pyramid, (E) a printed mat with the second layer-oriented perpendicular to the first, dyed blue for enhanced visualization, (F) multi-layer inkjet print of the “UConn” logo, demonstrating a complex-design 3D print. (G) Two-layer extrusion print where the second layer is printed perpendicular to the first and dyed blue. Reproduced with permission. Copyright 2019, Elsevier.<sup>173</sup>

extrusion printing of hydrogels and viscous solutions while preserving the printer's original functionality, offering dual capabilities (hard plastic and hydrogel printing).<sup>193</sup> Their approach involves minimal modifications, including a plunger driven extrusion system and Python-based G-code generation, offering flexibility in both droplet and continuous printing modes. The system achieves resolutions comparable to bioprinters, with droplet diameters as small as 100  $\mu\text{m}$  and line thicknesses ranging from 300 to 2000  $\mu\text{m}$ . Similarly, Fritz Koch *et al.* modified the Prusa i3 MK3 to incorporate syringe-based microextrusion alongside traditional FDM, enabling alternating printing of thermoplastics and hydrogels for hybrid constructs as shown in the Fig. 19(B).<sup>169</sup> The inclusion of a 3D-printed extrusion heater allows for multi-material printing at both room and elevated temperatures, increasing versatility. Ralf Zgeib *et al.* advanced the field of multi-material 3D bioprinting by developing a low-cost, quad-extrusion bioprinter based on a modified Creality Ender 3 Pro desktop 3D printer as shown in the Fig. 21(C).<sup>181</sup> This innovative system facilitates the production of diverse multi-material structures using both in-air and support bath printing paradigms. However, challenges such as handling high-viscosity inks and the lack of integrated heating or UV cross-linking remain areas for future improvement. Kazim K. Moncal *et al.* who developed a 3D-printed, thermally controlled extruder head for performing thermally driven crosslinking of collagen bioinks which achieves real-time control over gelation and crosslinking during printing, expanding the range of compatible bioinks and improving structural integrity.<sup>194</sup> Bekir Yenilmez *et al.* further advanced the hybrid bioprinter by combining inkjet and extrusion heads as shown in the Fig. 20.<sup>173</sup> It offered temporal control over material properties using UV crosslinking. It achieves high resolution through inkjet printing and high throughput *via* extrusion-

based printing. The bioprinter can perform direct-write bioprinting of hydrogel materials in multiple layers, achieving a balance between high resolution through the inkjet head with photochemical crosslinking and high throughput using the extrusion head with chemical crosslinking. Similarly, Adolf Krige *et al.* developed an affordable (\$300) bioprinter by performing simple modification to a low-cost Prusa i3 FDM 3D printer.<sup>167</sup>

The modifications allow the printer to maintain its original FDM (plastic printing) capabilities while enabling gel-based bioprinting as shown in the Fig. 21(B). It can print two materials simultaneously, with UV-curing capability for applications requiring bio-inks. Kevin D Roehm *et al.* demonstrated a novel approach to bioprinting by developing a low-cost (\$800) modified 3D printer with syringe-based extrusion and an integrated heated bed to maintain gelation conditions.<sup>172</sup> The study focuses on chitosan-gelatin (CG) hydrogels, however its generalizability to other bioinks or more complex tissue engineering scenarios remains untested. Iek Man Lei *et al.* developed “Printer.HM”, a modular, low cost (\$900 to \$1900) and customizable extrusion-based 3D printer designed for soft materials.<sup>171</sup> As shown in the Fig. 21(A), it includes multi-printhead capability, compatibility with various bioinks, integrated auxiliary tools (*e.g.*, heaters, UV module), and flexible geometry inputs (coordinates, equations, CAD models, and pictures). David Chimene *et al.* demonstrated the conversion of low-cost (\$400) thermoplastic 3D printers, such as the Ender 3 Pro, into cost-effective, open source multi head bioprinters for advanced tissue engineering.<sup>178</sup> However, the limited build volume may restrict its use for larger tissue constructs or industrial-scale applications. Andres Sanz-Garcia and his team converted a FDM 3D printers into micro extrusion based bioprinters (MEBB), that accommodates syringes of varying



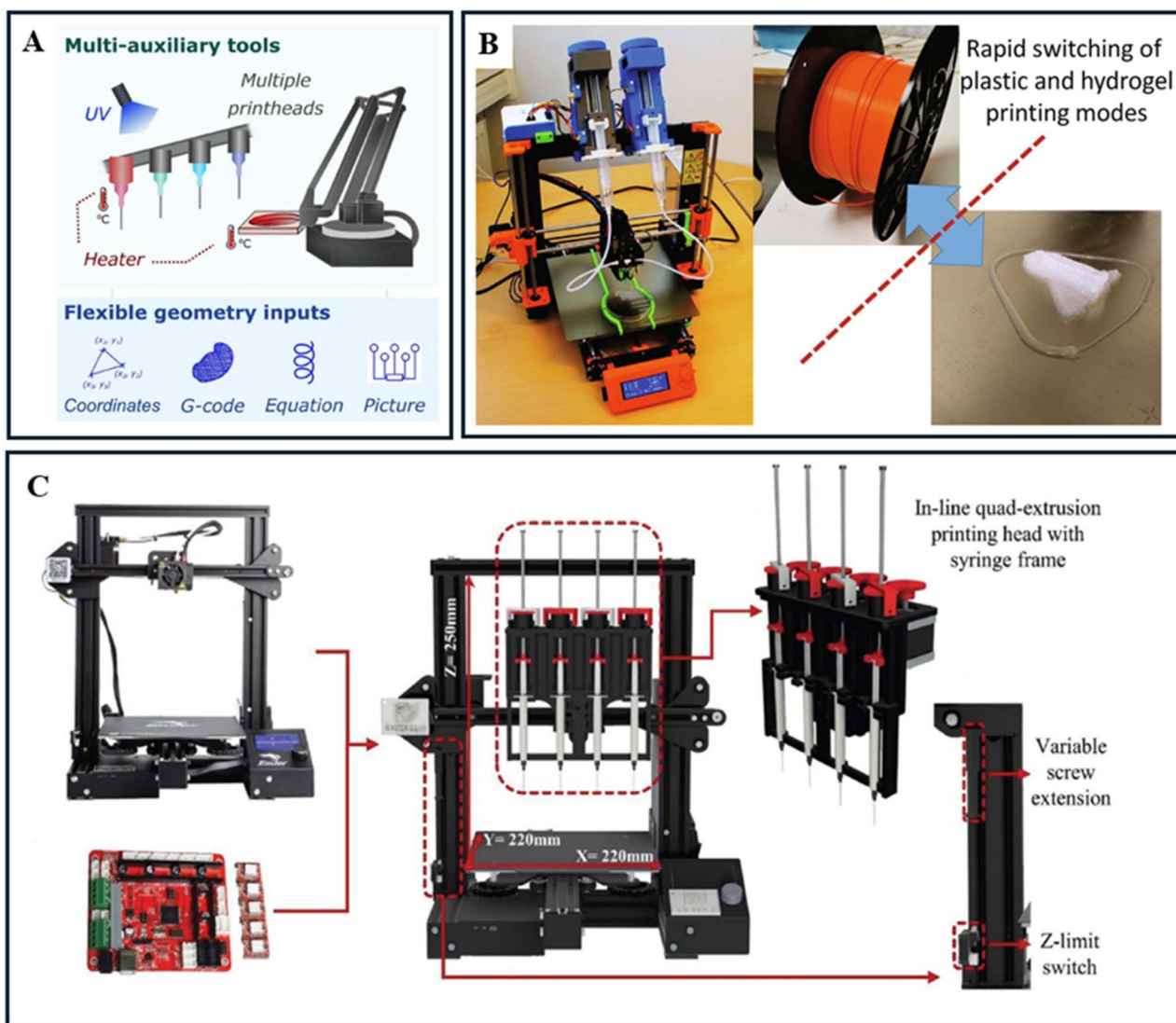


Fig. 21 (A) Features and capabilities of the multi-functional modular extrusion 3D printer. The system includes multi-auxiliary tools, such as multiple printheads, UV curing modules, and heating elements, enabling versatile operations. Flexible geometry inputs, including coordinates, G-code, equations, and images, allow for customizable and precise control. Reproduced with permission. Copyright 2022, *Nature Scientific Reports*.<sup>171</sup> (B) Dual-mode 3D bioprinter for rapid switching between plastic and hydrogel printing. The system integrates syringe-based extruders for hydrogel printing and a filament-based extruder for plastic printing, enabling seamless transitions between printing modes. Reproduced with permission. Copyright 2021, Elsevier.<sup>167</sup> (C) Design and configuration of a low-cost quad-extrusion 3D bioprinter. Base structure derived from the Ender 3 3D printer. Customized control board integrated for managing multiple extrusion functions. Modified frame accommodating the quad-extrusion setup with a build area of  $220 \times 220 \times 250$  mm. In-line quad-extrusion printhead featuring a syringe-based frame for precise deposition of bioinks or materials. Adjustable screw extension and Z-limit switch to enhance compatibility with the quad-extrusion configuration. This system showcases scalability and modularity for multi-material bioprinting applications. Reproduced with permission. Copyright 2023, ACCSCIENCE Publishing.<sup>181</sup>

volumes and can be configured for multi-material printing with minimal modifications.<sup>170</sup> The authors successfully installed on three different open-source 3D printers (Witbox2, Sigma, and BCN3D+), demonstrating compatibility and versatility. It provides a better modular design which supports syringes of varying volumes (3, 5, and 10 mL) and can be configured for multi-material printing with minimal modifications. However, both bioprinting and 3D printing encounter technological hurdles, particularly when creating overhanging or geometrically complex structures, which often require support materials

that must be removed post-printing. The FRESH (Freeform Reversible Embedding of Suspended Hydrogels) printing method, introduced by Thomas J. Hinton, revolutionized the way overhanging or geometrically complex structures are printed.<sup>195</sup> By using a gelatin-based support bath instead of a flat print surface, FRESH provides a thermo-responsive scaffold that can be liquefied and removed by heating to  $37^\circ\text{C}$ . This method allows for the printing of materials with an elastic modulus under 500 kPa and facilitates the creation of intricate, hollow structures without causing cellular damage. Nils Bessler *et al.*



implemented this technology by modifying the Prusa i3 3D printer with the Nydus One Syringe Extruder (NOSE) as shown in the Fig. 19(C), which achieves high cell survival rates of 81% for HEK293 cells and 85% for mESCs.<sup>182</sup> Despite its success, improvements such as a screw-based extruder for better adaptability and the addition of thermal or UV controls could enhance hydrogel compatibility and overall performance. Robert H. Utama *et al.* developed a bespoke drop-on-demand bioprinter for high-throughput (HTP) production of matrix-embedded multicellular spheroids, which is optimized for applications like drug screening, allowing control over spheroid size, cell number, and embedding.<sup>176</sup> It has high-throughput capability of printing 96-well plates rapidly with consistent results. Adam Feinberg and his team modified a commercial FDM 3D printer to create a low-cost (\$500), open-source bioprinter capable of large volume syringe pump extruder (LVE) compatible.<sup>175</sup> However, the system has limited resolution compared to high-end bioprinters and is primarily compatible with soft hydrogels like alginate, lacking versatility for handling higher viscosity bioinks. Mass-produced construction kits like LEGO and K'NEX offer modular and reconfigurable platforms for creating custom laboratory equipment.<sup>179</sup> Advances in commercial LEGO robotics, such as Mindstorms, and programmable control interfaces now allow for the development of smart, automated systems at a low cost and with minimal technical expertise. Ahmad Moukchar *et al.* designed an affordable, open-source 3D bioprinter using LEGO bricks as shown in the Fig. 19(D), which is capable of printing live cells in hydrogel scaffolds.<sup>179</sup> Priced at around \$350, the familiar LEGO platform serves as an engaging tool for teaching bioprinting principles. Similarly, Dominik T. Schmieden *et al.* used K'NEX and DIY electronics to create an affordable bacterial bioprinter, printing *E. coli* biofilms using alginate-based bioinks.<sup>196</sup> While ideal for educational purposes, these systems can be enhanced by integrating automated calibration and real-time monitoring to improve precision and reproducibility. Controlling extrusion printing parameters is critical in bioprinting to ensure precision and success. Amedeo Franco Bonatti and his team developed a theoretical model that serves as a rapid, user-friendly, and open-source tool which helps users identify optimal printing parameters for extrusion-based bioprinting, predicting the printability of a material using specific equipment and parameter settings.<sup>197</sup> The model comprehensively addresses the different stages of extrusion-based bio printing involving extrusion, line formation and scaffold stabilization. The model facilitates real-time parameter optimization, reduces material wastage, and minimizes reliance on trial-and-error experiments by leveraging material rheological properties. Additionally, the model encourages reproducibility in bioprinting by enabling standardized parameterization, making it especially valuable for researchers with limited resources. Its ability to predict outcomes based on material behaviour provides a significant advantage in extrusion-based bioprinting workflows. Machine learning (ML) stands as a transformative technology poised to revolutionize 3D bioprinting. While ML has already made significant strides in traditional 3D printing, enhancing process optimization, dimensional accuracy, defect detection, and

material property prediction, its application in bioprinting remains relatively unexplored. Integrating ML into 3D bioprinting can optimize critical parameters such as pressure, speed, and temperature, thereby predicting the best conditions for specific bioinks and minimizing the reliance on trial-and-error experimentation.<sup>198</sup> In the complex and dynamic environment of bioprinting, achieving reproducible results is a significant challenge due to the variability in bioink properties and environmental conditions. By feeding variables like nozzle size, gas flow, voltage, and bioink viscosity into neural networks, ML algorithms can be trained to evaluate and refine process outcomes, including cell viability, structural integrity, cost efficiency, and fabrication time. This predictive capability allows for the fine-tuning of bioprinting processes to meet specific requirements, enhancing both efficiency and reliability. Real-time defect detection is another area where ML can make a substantial impact. Techniques such as convolutional neural networks (CNNs) can analyse data from sensors and imaging systems to identify errors like misaligned cells, irregular layers, or structural defects during the printing process. By detecting these anomalies as they occur, the system can make immediate adjustments or halt the process to prevent waste and ensure high-quality outputs. This level of control is essential for maintaining the integrity of tissue constructs and for applications where precision is paramount. ML also enhances the dimensional accuracy of fabricated bio-parts by predicting geometric deviations and analyzing scaffold structures to ensure alignment with intended designs. One of the most promising applications of ML in bioprinting lies in material property prediction and scaffold design. Precise scaffold architecture is vital for supporting cell growth and functionality, especially in tissue engineering where the mechanical and biological properties of the scaffold can significantly influence cell behaviour. By accurately predicting how a scaffold will form under certain conditions, ML enables the creation of more effective and reliable tissue constructs. ML algorithms can analyze vast datasets to predict how different bioink formulations and printing parameters will affect the final product's properties. This capability not only accelerates the development of new bioinks but also reduces experimental costs and time by limiting the need for extensive laboratory testing.

The integration of ML into bioprinting paves the way for the development of self-driving laboratories. These self-driving labs can design experiments, adjust parameters in real-time based on sensor feedback, and learn from each iteration to continually improve performance. By automating these processes, researchers can focus on higher-level analysis and innovation rather than routine optimization tasks. However, the widespread application of ML in bioprinting does face challenges. The limited availability of large, standardized bioprinting datasets hampers the training of robust ML models. Additionally, the inherent variability of biological systems adds complexity to predictive modelling. Despite these hurdles, advancements in data collection techniques and collaborative efforts to share data can mitigate these issues over time.



## 4 Conclusions and perspectives

SDLs have been significantly enhanced by advancements in 3D printing technology, which enable the low-cost fabrication of components and the creation of affordable equipment. These innovations are driving the automation of laboratory instruments, enhancing throughput, and expanding opportunities for resource optimization, ultimately contributing to the broader adoption and accessibility of SDLs. The various developments of SDL with low-cost equipment utilizing 3D printing technology have been made as reported in this paper for performing fundamental and applied research in material science, biological science, chemical science and manufacturing engineering and further research is also demanded for providing an economic and scientific solution to industrial problems. Various low-cost 3D printers especially FDM 3D printers are available for producing parts of low-cost materials and for its easy access to convert it into various automated equipment like automated liquid handing device, automated microscope, automated samplers, tools for automatic sample preparation and testing *etc.* required for carrying out experiment at low cost and time which is the major objective of SDL. The advances in 3D printing technology enhance the scope of development of automated sample preparation and detection through automated liquid handlers, auto samplers, automated imaging devices *etc.* at competitive cost which can automate the repetitive task and eliminate human error and make the robotized instrument operative in hazardous environment efficiently with high safety and security. The easy customization and modularity of these devices enhances the decentralization and interconnection of different SDL labs across the globe. The applications of 3D printing technology are remarkable for making low-cost chemical reaction ware for chemical synthesis which is one of the basic requirements of SDL for advancing fundamental research in the chemical and material science. The developments of 3D bio-printer using open-source hardware and software led to the reduction of cost of experimentation in SDL for generating data, modelling and conducting the analysis which is very much effective and fruitful who are working in the field of bio-medical science. The present review and discussions made on the results of research and developments conducted by researchers in this paper in development of low-cost automated experimental setup for SDL utilizing low-cost open-source 3D printing technology will generate the scope of further research interest for democratizing SDL considering different aspects of laboratory automation and digitization at economic and sustainable way. By highlighting the versatility, cost-effectiveness, and accessibility of 3D printing technology, this review aims to inspire a broader audience within the scientific community to actively adopt and innovate with these technologies. Researchers, educators, and industry professionals are encouraged to leverage 3D printing for the development of customized, low-cost laboratory equipment tailored to specific experimental needs. Furthermore, the modular nature of these devices offers opportunities for interconnecting SDLs across diverse disciplines and geographical

boundaries, fostering collaborative research networks. Ultimately, this democratization of SDLs through 3D printing has the potential to accelerate scientific discoveries, improve resource optimization, and make advanced research methodologies accessible to laboratories with limited funding and infrastructure.

## Data availability

As this is a review article, no primary research results, data, software, or code have been included.

## Author contributions

S. D. and L. N. W. T. conceptualized the study. S. D. prepared the initial manuscript draft. M. D., Y. L., Z. H. C., X. X., J. H., and M. O. contributed to manuscript preparation and review. L. N. W. T. provided supervision and resources. All authors reviewed and approved the final version of the manuscript.

## Conflicts of interest

There are no conflicts to declare.

## Acknowledgements

L. N. W. T. acknowledges funding from the Singapore Ministry of Education Tier 1 grants (RS14/23 and RG86/23).

## References

- 1 S. Back, A. Aspuru-Guzik, M. Ceriotti, G. Gryn'ova, B. Grzybowski, G. H. Gu, J. Hein, K. Hippalgaonkar, R. Hormázabal, Y. Jung, S. Kim, W. Y. Kim, S. M. Moosavi, J. Noh, C. Park, J. Schrier, P. Schwaller, K. Tsuda, T. Vegge, O. A. Von Lilienfeld and A. Walsh, *Digital Discovery*, 2024, 3, 23–33.
- 2 R. W. Epps, A. A. Volk, M. Y. S. Ibrahim and M. Abolhasani, *Chem*, 2021, 7, 2541–2545.
- 3 H. G. Martin, T. Radivojevic, J. Zucker, K. Bouchard, J. Sustarich, S. Peisert, D. Arnold, N. Hillson, G. Babnigg, J. M. Marti, C. J. Mungall, G. T. Beckham, L. Waldburger, J. Carothers, S. Sundaram, D. Agarwal, B. A. Simmons, T. Backman, D. Banerjee, D. Tanjore, L. Ramakrishnan and A. Singh, *Curr. Opin. Biotechnol.*, 2023, 79, 102881.
- 4 S. Bräse, *Digital Discovery*, 2024, 3, 1923–1932.
- 5 H. Hysmith, E. Foadian, S. P. Padhy, S. V. Kalinin, R. G. Moore, O. S. Ovchinnikova and M. Ahmadi, *Digital Discovery*, 2024, 3, 621–636.
- 6 C. C. Rupnow, B. P. MacLeod, M. Mokhtari, K. Ocean, K. E. Dettelbach, D. Lin, F. G. L. Parlane, H. N. Chiu, M. B. Rooney, C. E. B. Waizenegger, E. I. De Hoog, A. Soni and C. P. Berlinguette, *Cell Rep. Phys. Sci.*, 2023, 4, 101411.
- 7 B. P. MacLeod, F. G. L. Parlane, T. D. Morrissey, F. Häse, L. M. Roch, K. E. Dettelbach, R. Moreira, L. P. E. Yunker, M. B. Rooney, J. R. Deeth, V. Lai, G. J. Ng, H. Situ, R. H. Zhang, M. S. Elliott, T. H. Haley, D. J. Dvorak,



- A. Aspuru-Guzik, J. E. Hein and C. P. Berlinguette, *Sci. Adv.*, 2020, **6**, eaaz8867.
- 8 R. B. Canty, B. A. Koscher, M. A. McDonald and K. F. Jensen, *Digital Discovery*, 2023, **2**, 1259–1268.
- 9 M. Abolhasani and E. Kumacheva, *Nat. Synth.*, 2023, **2**, 483–492.
- 10 G. Tom, S. P. Schmid, S. G. Baird, Y. Cao, K. Darvish, H. Hao, S. Lo, S. Pablo-García, E. M. Rajaonson, M. Skreta, N. Yoshikawa, S. Corapi, G. D. Akkoc, F. Strieth-Kalthoff, M. Seifrid and A. Aspuru-Guzik, *Chem. Rev.*, 2024, **124**, 9633–9732.
- 11 O. Bayley, E. Savino, A. Slattery and T. Noël, *Matter*, 2024, **7**, 2382–2398.
- 12 S. Lo, S. G. Baird, J. Schrier, B. Blaiszik, N. Carson, I. Foster, A. Aguilar-Granda, S. V. Kalinin, B. Maruyama, M. Politi, H. Tran, T. D. Sparks and A. Aspuru-Guzik, *Digital Discovery*, 2024, **3**, 842–868.
- 13 A. A. Volk and M. Abolhasani, *Nat. Commun.*, 2024, **15**, 1378.
- 14 J. M. Pearce, *Sci. Publ. Pol.*, 2016, **43**, 192–195.
- 15 P. M. Maffettone, P. Friederich, S. G. Baird, B. Blaiszik, K. A. Brown, S. I. Campbell, O. A. Cohen, R. L. Davis, I. T. Foster, N. Haghmoradi, M. Hereld, H. Jores, N. Jung, H.-K. Kwon, G. Pizzuto, J. Rintamaki, C. Steinmann, L. Torresi and S. Sun, *Digital Discovery*, 2023, **2**, 1644–1659.
- 16 M. B. Rooney, B. P. MacLeod, R. Oldford, Z. J. Thompson, K. L. White, J. Tungjunyatham, B. J. Stankiewicz and C. P. Berlinguette, *Digital Discovery*, 2022, **1**, 382–389.
- 17 B. C. Batista, A. S. Vayakkoth, J. Yan, B. B. Dangi and O. Steinbock, *Digital Discovery*, 2025, **4**, 1030–1041.
- 18 G. Pegoraro and T. Misteli, *Trends Genet.*, 2017, **33**, 604–615.
- 19 J. Lee, P. Mulay, M. J. Tamasi, J. Yeow, M. M. Stevens and A. J. Gormley, *Digital Discovery*, 2023, **2**, 219–233.
- 20 M. Seifrid, R. Pollice, A. Aguilar-Granda, Z. Morgan Chan, K. Hotta, C. T. Ser, J. Vestfrid, T. C. Wu and A. Aspuru-Guzik, *Acc. Chem. Res.*, 2022, **55**, 2454–2466.
- 21 G. Lippi and G. Da Rin, *Clin. Chem. Lab. Med.*, 2019, **57**, 802–811.
- 22 V. Saggiomo, *Adv. Sci.*, 2022, **9**, 2202610.
- 23 D. Naranbat, B. Phelps, J. Murphy and A. Tripathi, *SLAS Technol.*, 2025, **30**, 100239.
- 24 F. Barthels, U. Barthels, M. Schwickert and T. Schirmeister, *SLAS Technol.*, 2020, **25**, 190–199.
- 25 A. Faiña, B. Nejati and K. Stoy, *Appl. Sci.*, 2020, **10**, 814.
- 26 M. C. Carvalho, *HardwareX*, 2021, **10**, e00215.
- 27 M. C. Carvalho and B. D. Eyre, *Methods in Oceanography*, 2013, **8**, 23–32.
- 28 J. P. Efromson, S. Li and M. D. Lynch, *HardwareX*, 2021, **9**, e00177.
- 29 S. A. Longwell and P. M. Fordyce, *Lab Chip*, 2020, **20**, 93–106.
- 30 M. C. Carvalho and R. H. Murray, *HardwareX*, 2018, **3**, 10–38.
- 31 M. Dyga, C. Oppel and L. J. Gooßen, *HardwareX*, 2021, **10**, e00211.
- 32 M. S. Cubberley and W. A. Hess, *J. Chem. Educ.*, 2017, **94**, 72–74.
- 33 J. M. Pearce, N. C. Anzalone and C. L. Heldt, *SLAS Technol.*, 2016, **21**, 510–516.
- 34 S. Eggert, P. Mieszczanek, C. Meinert and D. W. Huttmacher, *HardwareX*, 2020, **8**, e00152.
- 35 K. C. Dhankani and J. M. Pearce, *HardwareX*, 2017, **1**, 1–12.
- 36 D. Trivedi and J. Pearce, *Appl. Sci.*, 2017, **7**, 942.
- 37 A. Maia Chagas, L. L. Prieto-Godino, A. B. Arrenberg and T. Baden, *PLoS Biol.*, 2017, **15**, e2002702.
- 38 J. T. Collins, J. Knapper, J. Stirling, J. Mduda, C. Mkindi, V. Mayagaya, G. A. Mwakajinga, P. T. Nyakyi, V. L. Sanga, D. Carbery, L. White, S. Dale, Z. Jieh Lim, J. J. Baumberg, P. Cicuta, S. McDermott, B. Vodenicharski and R. Bowman, *Biomed. Opt. Express*, 2020, **11**, 2447.
- 39 H. Li, C. J. Ford, M. Bianchi, M. G. Catalano, E. Psomopoulou and N. F. Lepora, *IEEE Robot. Autom. Lett.*, 2022, **7**, 8745–8751.
- 40 X. Zhou and A. J. Spiers, in *2023 IEEE/RSJ International Conference on Intelligent Robots and Systems (IROS)*, IEEE, Detroit, MI, USA, 2023, pp. 4555–4561.
- 41 M. Coakley and D. E. Hurt, *SLAS Technol.*, 2016, **21**, 489–495.
- 42 J. Courtemanche, S. King and D. Bouck, *SLAS Technol.*, 2018, **23**, 448–455.
- 43 C. Zhang, B. Wijnen and J. M. Pearce, *SLAS Technol.*, 2016, **21**, 517–525.
- 44 M. D. M. Dryden, R. Fobel, C. Fobel and A. R. Wheeler, *Anal. Chem.*, 2017, **89**, 4330–4338.
- 45 A. Vriza, H. Chan and J. Xu, *Chem. Mater.*, 2023, **35**, 3046–3056.
- 46 J. A. Bennett and M. Abolhasani, *Curr. Opin. Chem. Eng.*, 2022, **36**, 100831.
- 47 J. M. Granda, L. Donina, V. Dragone, D.-L. Long and L. Cronin, *Nature*, 2018, **559**, 377–381.
- 48 B. Burger, P. M. Maffettone, V. V. Gusev, C. M. Aitchison, Y. Bai, X. Wang, X. Li, B. M. Alston, B. Li, R. Clowes, N. Rankin, B. Harris, R. S. Sprick and A. I. Cooper, *Nature*, 2020, **583**, 237–241.
- 49 N. J. Szymanski, B. Rendy, Y. Fei, R. E. Kumar, T. He, D. Milsted, M. J. McDermott, M. Gallant, E. D. Cubuk, A. Merchant, H. Kim, A. Jain, C. J. Bartel, K. Persson, Y. Zeng and G. Ceder, *Nature*, 2023, **624**, 86–91.
- 50 N. J. Szymanski, P. Nevatia, C. J. Bartel, Y. Zeng and G. Ceder, *Nat. Commun.*, 2023, **14**, 6956.
- 51 J. T. Rapp, B. J. Bremer and P. A. Romero, *Nat. Chem. Eng.*, 2024, **1**, 97–107.
- 52 J. Jumper, R. Evans, A. Pritzel, T. Green, M. Figurnov, O. Ronneberger, K. Tunyasuvunakool, R. Bates, A. Židek, A. Potapenko, A. Bridgland, C. Meyer, S. A. A. Kohl, A. J. Ballard, A. Cowie, B. Romera-Paredes, S. Nikolov, R. Jain, J. Adler, T. Back, S. Petersen, D. Reiman, E. Clancy, M. Zielinski, M. Steinegger, M. Pacholska, T. Berghammer, S. Bodenstein, D. Silver, O. Vinyals, A. W. Senior, K. Kavukcuoglu, P. Kohli and D. Hassabis, *Nature*, 2021, **596**, 583–589.
- 53 R. Shimizu, S. Kobayashi, Y. Watanabe, Y. Ando and T. Hitosugi, *APL Mater.*, 2020, **8**, 111110.



- 54 M. A. Soldatov, V. V. Butova, D. Pashkov, M. A. Butakova, P. V. Medvedev, A. V. Chernov and A. V. Soldatov, *Nanomaterials*, 2021, **11**, 619.
- 55 B. P. MacLeod, F. G. L. Parlane, C. C. Rupnow, K. E. Dettelbach, M. S. Elliott, T. D. Morrissey, T. H. Haley, O. Proskurin, M. B. Rooney, N. Taherimakhsoosi, D. J. Dvorak, H. N. Chiu, C. E. B. Waizenegger, K. Ocean, M. Mokhtari and C. P. Berlinguette, *Nat. Commun.*, 2022, **13**, 995.
- 56 M. Hamedirad, R. Chao, S. Weisberg, J. Lian, S. Sinha and H. Zhao, *Nat. Commun.*, 2019, **10**, 5150.
- 57 G. N. Kanda, T. Tsuzuki, M. Terada, N. Sakai, N. Motozawa, T. Masuda, M. Nishida, C. T. Watanabe, T. Higashi, S. A. Horiguchi, T. Kudo, M. Kamei, G. A. Sunagawa, K. Matsukuma, T. Sakurada, Y. Ozawa, M. Takahashi, K. Takahashi and T. Natsume, *eLife*, 2022, **11**, e77007.
- 58 T. Si, R. Chao, Y. Min, Y. Wu, W. Ren and H. Zhao, *Nat. Commun.*, 2017, **8**, 15187.
- 59 <https://opentrons.com/>.
- 60 <https://www.hamiltoncompany.com/>.
- 61 <https://hylandscientific.com/product/thermo-cellinsight-cx7-lzr-imaging-system/>.
- 62 <https://conquerscientific.com/>.
- 63 [https://www.bmglabtech.com/en/microplate-reader/?utm\\_source=chatgpt.com#productfinder](https://www.bmglabtech.com/en/microplate-reader/?utm_source=chatgpt.com#productfinder).
- 64 <https://www.emeraldcloudlab.com/>.
- 65 R. A. Smaldone, K. A. Brown, G. X. Gu and C. Ke, *Device*, 2023, **1**, 100014.
- 66 M. Elbadawi, H. Li, S. Sun, M. E. Alkahtani, A. W. Basit and S. Gaisford, *Appl. Mater. Today*, 2024, **36**, 102061.
- 67 J. E. Johnson, I. R. Jamil, L. Pan, G. Lin and X. Xu, *Light:Sci. Appl.*, 2025, **14**, 56.
- 68 A. E. Gongora, B. Xu, W. Perry, C. Okoye, P. Riley, K. G. Reyes, E. F. Morgan and K. A. Brown, *Sci. Adv.*, 2020, **6**, eaaz1708.
- 69 P. Q. Velasco, K. Hippalgaonkar and B. Ramalingam, *Beilstein J. Org. Chem.*, 2025, **21**, 10–38.
- 70 W. Hou, A. Bubliskas, P. J. Kitson, J.-P. Francoia, H. Powell-Davies, J. M. P. Gutierrez, P. Frei, J. S. Manzano and L. Cronin, *ACS Cent. Sci.*, 2021, **7**, 212–218.
- 71 J. S. Manzano, W. Hou, S. S. Zalesskiy, P. Frei, H. Wang, P. J. Kitson and L. Cronin, *Nat. Chem.*, 2022, **14**, 1311–1318.
- 72 V.-H. Vu, K.-H. Bui, K. D. D. Dang, M. Duong-Tuan, D. D. Le and T. Nguyen-Dang, *J. Sci.:Adv. Mater. Devices*, 2025, **10**, 100818.
- 73 E. Kargar and A. Ghasemi-Ghalebahman, *Sci. Rep.*, 2023, **13**, 18194.
- 74 J. P. M. Pragma, R. F. V. Sampaio, I. M. F. Bragança, C. M. A. Silva and P. A. F. Martins, *Adv. Ind. Manuf. Eng.*, 2021, **2**, 100032.
- 75 *Advances in Additive Manufacturing and Metal Joining: Proceedings of AIMTDR 2021*, N. Ramesh Babu, ed. S. Kumar, P. R. Thyla and K. Sriprayan, Springer Nature Singapore, Singapore, 2023.
- 76 M. Lalegani Dezaki, M. K. A. Mohd Ariffin and S. Hatami, *Rapid Prototyp. J.*, 2021, **27**, 562–582.
- 77 N. A. S. Mohd Pu'ad, R. H. Abdul Haq, H. Mohd Noh, H. Z. Abdullah, M. I. Idris and T. C. Lee, *Mater. Today: Proc.*, 2020, **29**, 228–232.
- 78 D. A. Sawant, B. M. Shinde and S. J. Raykar, *Mater. Today: Proc.*, 2023, DOI: [10.1016/j.matpr.2023.09.202](https://doi.org/10.1016/j.matpr.2023.09.202).
- 79 M. R. Khosravani, M. R. Ayatollahi and T. Reinicke, *J. Manuf. Process.*, 2023, **107**, 98–114.
- 80 A. Kantaros, T. Ganetsos, F. Petrescu, L. Ungureanu and I. Munteanu, *Processes*, 2024, **12**, 595.
- 81 S. Wickramasinghe, T. Do and P. Tran, *Polymers*, 2020, **12**, 1529.
- 82 E. Petersen and J. Pearce, *Technologies*, 2017, **5**, 7.
- 83 T. Baden, A. M. Chagas, G. Gage, T. Marzullo, L. L. Prieto-Godino and T. Euler, *PLoS Biol.*, 2015, **13**, e1002086.
- 84 J. M. Pearce, *Organic Farming*, 2015, **1**, 19–35.
- 85 FINDUS, An Open-Source 3D Printable Liquid-Handling Workstation for Laboratory Automation in Life Sciences - ScienceDirect, <https://www.sciencedirect.com/science/article/pii/S2472630322010251>, accessed 24 October 2024.
- 86 R. Keeseey, R. LeSuer and J. Schrier, *HardwareX*, 2022, **12**, e00319.
- 87 M. R. Behrens, H. C. Fuller, E. R. Swist, J. Wu, Md. M. Islam, Z. Long, W. C. Ruder and R. Steward, *Sci. Rep.*, 2020, **10**, 1543.
- 88 K. Pusch, T. J. Hinton and A. W. Feinberg, *HardwareX*, 2018, **3**, 49–61.
- 89 İ. Ağır, *AKU J. Sci. Eng.*, 2024, **24**, 749–757.
- 90 A. J. Capel, R. P. Rimington, M. P. Lewis and S. D. R. Christie, *Nat. Rev. Chem.*, 2018, **2**, 422–436.
- 91 E. E. A. W. Councill, N. B. Axtell, T. Truong, Y. Liang, A. L. Aposhian, K. G. I. Webber, Y. Zhu, Y. Cong, R. H. Carson and R. T. Kelly, *SLAS Technol.*, 2021, **26**, 311–319.
- 92 K. C. Wells, N. Kharma, B. B. Jaunky, K. Nie, G. Aguiar-Tawil and D. Berry, *HardwareX*, 2024, **18**, e00516.
- 93 A. Kopyl, Y. Yew, J. W. Ong, T. Hiscox, C. Young, M. Muradoglu and T. W. Ng, *J. Chem. Educ.*, 2024, **101**, 640–646.
- 94 T. Kassis, P. M. Perez, C. J. W. Yang, L. R. Soenksen, D. L. Trumper and L. G. Griffith, *HardwareX*, 2018, **4**, e00034.
- 95 A. Gervasi, P. Cardol and P. E. Meyer, *HardwareX*, 2021, **9**, e00199.
- 96 S. Baas and V. Saggiomo, *HardwareX*, 2021, **10**, e00219.
- 97 R. Rogosic, M. Poloni, R. Marroquin-Garcia, D. Dimech, J. Passariello Jansen, T. J. Cleij, K. Eersels, B. Van Grinsven and H. Diliën, *Med. Phys.*, 2022, **14**, 100051.
- 98 M. Kujawa, S. Motała, M. Gonet, R. Pietrzyk, T. Czechowski and M. Baranowski, *HardwareX*, 2021, **9**, e00194.
- 99 J. R. Lake, K. C. Heyde and W. C. Ruder, *PLoS One*, 2017, **12**, e0175089.
- 100 V. E. Garcia, J. Liu and J. L. DeRisi, *HardwareX*, 2018, **4**, e00027.
- 101 D. C. Florian, M. Odziomek, C. L. Ock, H. Chen and S. A. Guelcher, *Sci. Rep.*, 2020, **10**, 13663.
- 102 J. M. Neumaier, A. Madani, T. Klein and T. Ziegler, *Beilstein J. Org. Chem.*, 2019, **15**, 558–566.



- 103 M. Del Rosario, H. S. Heil, A. Mendes, V. Saggiomo and R. Henriques, *Adv. Biol.*, 2022, **6**, 2100994.
- 104 B. Diederich, R. Lachmann, S. Carlstedt, B. Marsikova, H. Wang, X. Uwurukundo, A. S. Mosig and R. Heintzmann, *Nat. Commun.*, 2020, **11**, 5979.
- 105 P. Dettinger, T. Kull, G. Arekatla, N. Ahmed, Y. Zhang, F. Schneider, A. Wehling, D. Schirmacher, S. Kawamura, D. Loeffler and T. Schroeder, *Nat. Commun.*, 2022, **13**, 2999.
- 106 G. O. T. Mercedes, C. Kennedy, B. Lenoci, E. G. Reynaud, N. Burke and M. Pickering, *HardwareX*, 2021, **9**, e00189.
- 107 N. Burke, G. Müller, V. Saggiomo, A. R. Hassett, J. Mutterer, P. Ó Súilleabháin, D. Zakharov, D. Healy, E. G. Reynaud and M. Pickering, *Philos. Trans. R. Soc., A*, 2024, **382**, 20230214.
- 108 R. Parton and M. Wincott, *Zenodo*, 2020, DOI: [10.5281/ZENODO.3701602](https://doi.org/10.5281/ZENODO.3701602).
- 109 H. Li, H. Soto-Montoya, M. Voisin, L. F. Valenzuela and M. Prakash, *bioRxiv*, 2019, preprint, DOI: [10.1101/684423](https://doi.org/10.1101/684423).
- 110 A. R. Miller, G. L. Davis, Z. M. Oden, M. R. Razavi, A. Fateh, M. Ghazanfari, F. Abdolrahimi, S. Poorazar, F. Sakhaie, R. J. Olsen, A. R. Bahrmand, M. C. Pierce, E. A. Graviss and R. Richards-Kortum, *PLoS One*, 2010, **5**, e11890.
- 111 R. A. A. Campbell, R. W. Eifert and G. C. Turner, *PLoS One*, 2014, **9**, e88977.
- 112 J. P. Sharkey, D. C. W. Foo, A. Kabla, J. J. Baumberg and R. W. Bowman, *Rev. Sci. Instrum.*, 2016, **87**, 025104.
- 113 B. Berg, B. Cortazar, D. Tseng, H. Ozkan, S. Feng, Q. Wei, R. Y.-L. Chan, J. Burbano, Q. Farooqui, M. Lewinski, D. Di Carlo, O. B. Garner and A. Ozcan, *ACS Nano*, 2015, **9**, 7857–7866.
- 114 Y. Lee, B. Kim, I. Oh and S. Choi, *Small*, 2018, **14**, 1802769.
- 115 D. Schneidereit, L. Kraus, J. C. Meier, O. Friedrich and D. F. Gilbert, *Biosens. Bioelectron.*, 2017, **92**, 472–481.
- 116 O. Hilsenbeck, M. Schwarzfischer, D. Loeffler, S. Dimopoulos, S. Hastreiter, C. Marr, F. J. Theis and T. Schroeder, *Bioinformatics*, 2017, **33**, 2020–2028.
- 117 R. C. Lagoy and D. R. Albrecht, *Sci. Rep.*, 2018, **8**, 6217.
- 118 G. Murray, S. Bednarski, M. Hall, S. W. Foster, S. Jin, J. J. Davis, W. Xue, E. Constans and J. P. Grinias, *HardwareX*, 2021, **10**, e00220.
- 119 M. C. Carvalho, *HardwareX*, 2020, **8**, e00142.
- 120 M. Růžička, M. Kaljurand, J. Gorbatšova and J. Mazina-Šinkar, *J. Chromatogr. A*, 2022, **1685**, 463619.
- 121 K. Chan, P.-Y. Wong, C. Parikh and S. Wong, *Anal. Biochem.*, 2018, **545**, 4–12.
- 122 S. Byrnes, A. Fan, J. Trueb, F. Jareczek, M. Mazzochette, A. Sharon, A. F. Sauer-Budge and C. M. Klapperich, *Anal. Methods*, 2013, **5**, 3177.
- 123 M. Ponzetti, G. Chinna Rao Devarapu, N. Rucci, A. Carlone and V. Saggiomo, *HardwareX*, 2022, **12**, e00370.
- 124 K. Chan, M. Coen, J. Hardick, C. A. Gaydos, K.-Y. Wong, C. Smith, S. A. Wilson, S. P. Vayugundla and S. Wong, *PLoS One*, 2016, **11**, e0158502.
- 125 A. E. Siemenn, B. Das, E. Aissi, F. Sheng, L. Elliott, B. Hudspeth, M. Meyers, J. Serdy and T. Buonassisi, *Digital Discovery*, 2025, **4**, 896–909.
- 126 B. Iglehart, *SLAS Technol.*, 2018, **23**, 423–431.
- 127 M. C. Carvalho and J. M. Oakes, *Hardware*, 2023, **1**, 29–53.
- 128 D. A. V. Medina, L. F. Rodriguez Cabal, F. M. Lanças and Á. J. Santos-Neto, *HardwareX*, 2019, **5**, e00056.
- 129 J. M. Neumaier, A.-L. Renz and F. Menzel, *J. Open Hardw.*, 2024, **8**(1), DOI: [10.5206/joh.v8i1.18995](https://doi.org/10.5206/joh.v8i1.18995).
- 130 R. L. Schrader, S. T. Ayrton, A. Kaerner and R. G. Cooks, *Analyst*, 2019, **144**, 4978–4984.
- 131 A. Chaturvedi and S. S. Gorthi, *SLAS Technol.*, 2017, **22**, 73–80.
- 132 M. Belka, L. Konieczna, M. Okońska, M. Pyszka, S. Ulenberg and T. Bączek, *Anal. Chim. Acta*, 2019, **1081**, 1–5.
- 133 T. M. Farris, J. P. Humes and M. A. Nussbaum, *Anal. Chem.*, 2020, **92**, 3522–3527.
- 134 G. Anzalone, A. Glover and J. Pearce, *Sensors*, 2013, **13**, 5338–5346.
- 135 B. P. MacLeod, F. G. L. Parlane, T. D. Morrissey, F. Häse, L. M. Roch, K. E. Dettelbach, R. Moreira, L. P. E. Yunker, M. B. Rooney, J. R. Deeth, V. Lai, G. J. Ng, H. Situ, R. H. Zhang, M. S. Elliott, T. H. Haley, D. J. Dvorak, A. Aspuru-Guzik, J. E. Hein, C. P. Berlinguette and B. P. MacLeod, *Sci. Adv.*, 2020, **6**, eaaz8867.
- 136 J. Boyd, *Science*, 2002, **295**, 517–518.
- 137 R. Siemasz, K. Tomczuk and Z. Malecha, *Procedia Comput. Sci.*, 2020, **176**, 3741–3750.
- 138 R. R. Ma, L. U. Odhner and A. M. Dollar, in *2013 IEEE International Conference on Robotics and Automation*, IEEE, Karlsruhe, Germany, 2013, pp. 2737–2743.
- 139 S. Mick, M. Lapeyre, P. Rouanet, C. Halgand, J. Benois-Pineau, F. Paquet, D. Cattaert, P.-Y. Oudeyer and A. De Ruyg, *Front. Neurobot.*, 2019, **13**, 65.
- 140 A. Laron, E. Sne, Y. Perets and A. Sintov, *arXiv*, 2024, preprint, arXiv:arXiv:2401.16463, DOI: [10.48550/arXiv.2401.16463](https://doi.org/10.48550/arXiv.2401.16463).
- 141 F. Salman, Y. Cui, Z. Imran, F. Liu, L. Wang and W. Wu, *Sens. Actuators, A*, 2020, **309**, 112004.
- 142 P. Mannam, A. Rudich, K. Zhang, M. Veloso, O. Kroemer and F. Temel, in *Robotics: Science and Systems XVII, Robotics: Science and Systems Foundation*, 2021.
- 143 A. Imran, W. Escobar and F. Barez, in *Volume 6: Design, Systems, and Complexity*, American Society of Mechanical Engineers, Virtual, Online, 2021, p. V006T06A017.
- 144 A. Murali, T. Chen, K. V. Alwala, D. Gandhi, L. Pinto, S. Gupta and A. Gupta, *arXiv*, 2019, preprint, arXiv:arXiv:1906.08236, DOI: [10.48550/arXiv.1906.08236](https://doi.org/10.48550/arXiv.1906.08236).
- 145 S. Patil, S. C. Alvares, P. Mannam, O. Kroemer and F. Z. Temel, in *2022 IEEE/RSJ International Conference on Intelligent Robots and Systems (IROS)*, 2022, pp. 13213–13219.
- 146 A. Canizares, J. Pazos and D. Benitez, in *2017 IEEE International Autumn Meeting on Power, Electronics and Computing (ROPEC)*, IEEE, Ixtapa, 2017, pp. 1–6.
- 147 F.-F. Răduică and I. Simion, *Appl. Sci.*, 2024, **14**, 8929.
- 148 H. Zwirnmann, D. Knobbe, U. Culha and S. Haddadin, in *2023 IEEE/RSJ International Conference on Intelligent Robots and Systems (IROS)*, IEEE, Detroit, MI, USA, 2023, pp. 6823–6830.
- 149 S. I. Ansary, S. Deb and A. K. Deb, *J. Intell. Rob. Syst.*, 2023, **109**, 13.



- 150 P. Tymkiv, A. Kłos-Witkowska, Z. Babiak, V. Koshelyuk and A. Holovko, *2nd International Workshop on Computer Information Technologies in Industry 4.0 (CITI'2024)*, 2024, pp. 1–12.
- 151 T. Bárány and L. Rónai, *Acta Mech. Slovaca*, 2023, **27**, 12–17.
- 152 C. M. A. Vasques and F. A. V. Figueiredo, in *The 2nd International Electronic Conference on Applied Sciences*, MDPI, 2021, p. 43.
- 153 P. J. Kitson, R. J. Marshall, D. Long, R. S. Forgan and L. Cronin, *Angew. Chem., Int. Ed.*, 2014, **53**, 12723–12728.
- 154 P. J. Kitson, S. Glatzel, W. Chen, C.-G. Lin, Y.-F. Song and L. Cronin, *Nat. Protoc.*, 2016, **11**, 920–936.
- 155 M. D. Symes, P. J. Kitson, J. Yan, C. J. Richmond, G. J. T. Cooper, R. W. Bowman, T. Vilbrandt and L. Cronin, *Nat. Chem.*, 2012, **4**, 349–354.
- 156 A. Bubliauskas, D. J. Blair, H. Powell-Davies, P. J. Kitson, M. D. Burke and L. Cronin, *Angew. Chem., Int. Ed.*, 2022, **61**, e202116108.
- 157 P. J. Kitson, S. Glatzel and L. Cronin, *Beilstein J. Org. Chem.*, 2016, **12**, 2776–2783.
- 158 C. Lin, W. Zhou, X. Xiong, W. Xuan, P. J. Kitson, D. Long, W. Chen, Y. Song and L. Cronin, *Angew. Chem., Int. Ed.*, 2018, **57**, 16716–16720.
- 159 T. Webbe Kerekes, H. Lim, W. Y. Joe and G. J. Yun, *Addit. Manuf.*, 2019, **25**, 532–544.
- 160 K. Günaydın and H. S. Türkmen, *International Congress on 3D Printing (Additive Manufacturing) Technologies and Digital Industry*, 2018, 1–7.
- 161 M. Baechle-Clayton, E. Loos, M. Taheri and H. Taheri, *J. Compos. Sci.*, 2022, **6**, 202.
- 162 J. S. Mathieson, M. H. Rosnes, V. Sans, P. J. Kitson and L. Cronin, *Beilstein J. Nanotechnol.*, 2013, **4**, 285–291.
- 163 V. Dragone, V. Sans, M. H. Rosnes, P. J. Kitson and L. Cronin, *Beilstein J. Org. Chem.*, 2013, **9**, 951–959.
- 164 P. J. Kitson, M. D. Symes, V. Dragone and L. Cronin, *Chem. Sci.*, 2013, **4**, 3099–3103.
- 165 P. J. Kitson, M. H. Rosnes, V. Sans, V. Dragone and L. Cronin, *Lab Chip*, 2012, **12**, 3267.
- 166 R. D. Johnson, *Nat. Chem.*, 2012, **4**, 338–339.
- 167 A. Krige, J. Haluška, U. Rova and P. Christakopoulos, *HardwareX*, 2021, **9**, e00186.
- 168 M. Lanaro, A. Luu, A. Lightbody-Gee, D. Hedger, S. K. Powell, D. W. Holmes and M. A. Woodruff, *Int. J. Adv. Manuf. Technol.*, 2021, **113**, 2539–2554.
- 169 F. Koch, O. Thaden, K. Tröndle, R. Zengerle, S. Zimmermann and P. Koltay, *HardwareX*, 2021, **10**, e00230.
- 170 A. Sanz-Garcia, E. Sodupe-Ortega, A. Pernía-Espinoza, T. Shimizu and C. Escobedo-Lucea, *Polymers*, 2020, **12**, 2346.
- 171 I. M. Lei, Y. Sheng, C. L. Lei, C. Leow and Y. Y. S. Huang, *Sci. Rep.*, 2022, **12**, 12294.
- 172 K. D. Roehm and S. V. Madihally, *Biofabrication*, 2017, **10**, 015002.
- 173 B. Yenilmez, M. Temirel, S. Knowlton, E. Lepowsky and S. Tasoglu, *Bioprinting*, 2019, **13**, e00044.
- 174 M. Kahl, M. Gertig, P. Hoyer, O. Friedrich and D. F. Gilbert, *Front. Bioeng. Biotechnol.*, 2019, **7**, 184.
- 175 3-DIY: Printing your own bioprinter, Carnegie Mellon University College of Engineering, <https://engineering.cmu.edu/news-events/news/2018/03/23-bioprinter-feinberg.html>, accessed 17 May 2025.
- 176 R. H. Utama, L. Atapattu, A. P. O'Mahony, C. M. Fife, J. Baek, T. Allard, K. J. O'Mahony, J. C. C. Ribeiro, K. Gaus, M. Kavallaris and J. J. Gooding, *iScience*, 2020, **23**, 101621.
- 177 J. A. Reid, P. A. Mollica, G. D. Johnson, R. C. Ogle, R. D. Bruno and P. C. Sachs, *Biofabrication*, 2016, **8**, 025017.
- 178 D. Chimene, K. A. Deo, J. Thomas, L. Dahle, C. Mandrona and A. K. Gaharwar, *GEN Biotechnol.*, 2022, **1**, 386–400.
- 179 A. Moukachar, K. Harvey, E. Roke, K. Sloan, C. Pool, S. Moola, A. Alshukri, D. Jarvis, P. Crews-Rees, G. McDermott, L. Evans, J. Li, C. Thomas, S. Coulman and O. Castell, *Adv. Mater. Technol.*, 2023, **8**, 2100868.
- 180 J. W. Tashman, D. J. Shiwerski and A. W. Feinberg, *Sci. Rep.*, 2022, **12**, 22652.
- 181 R. Zgeib, X. Wang, A. Zaeri, F. Zhang, K. Cao and R. C. Chang, *Int. J. Bioprint.*, 2023, **10**, 0159.
- 182 N. Bessler, D. Ogiermann, M.-B. Buchholz, A. Santel, J. Heidenreich, R. Ahmmed, H. Zaehres and B. Brand-Saberi, *HardwareX*, 2019, **6**, e00069.
- 183 E. Prianto, H. Herianto, M. K. Herliansyah, H. S. Pramono, A. F. Husna, R. Adam and A. E. Raditya, *J. Phys.: Conf. Ser.*, 2022, **2406**, 012005.
- 184 A. M. E. Arefin, N. R. Khatri, N. Kulkarni and P. F. Egan, *Polymers*, 2021, **13**, 1499.
- 185 A. M. Bejoy, K. N. Makkithaya, B. B. Hunakunti, A. Hegde, K. Krishnamurthy, A. Sarkar, C. F. Lobo, D. V. S. Keshav, D. Gopal, D. S. Dharshini, S. Mascarenhas, S. Chakrabarti, S. R. R. D. Kalepu, B. Paul and N. Mazumder, *Bioprinting*, 2021, **24**, e00176.
- 186 A. Mazzocchi, S. Soker and A. Skardal, *Applied Physics Reviews*, 2019, **6**, 011302.
- 187 G. Huang, Y. Zhao, D. Chen, L. Wei, Z. Hu, J. Li, X. Zhou, B. Yang and Z. Chen, *Biomater. Sci.*, 2024, **12**, 1425–1448.
- 188 F. Ali, S. N. Kalva and M. Koc, *Discover Mater.*, 2024, **4**, 53.
- 189 X. Yuan, Z. Wang, L. Che, X. Lv, J. Xu, D. Shan and B. Guo, *Int. J. Bioprint.*, 2024, 1752.
- 190 K. Ioannidis, R. I. Danalatos, S. Champeris Tsaniras, K. Kaplani, G. Lokka, A. Kanellou, D. J. Papachristou, G. Bokias, Z. Lygerou and S. Taraviras, *Front. Bioeng. Biotechnol.*, 2020, **8**, 580889.
- 191 J. D. Weiss, A. Mermin-Bunnell, F. S. Solberg, T. Tam, L. Rosalia, A. Sharir, D. Rüttsche, S. Sinha, P. S. Choi, M. Shibata, Y. Palagani, R. Nilkant, K. Paulvannan, M. Ma and M. A. Skylar-Scott, *Adv. Mater.*, 2025, **37**, e2414971.
- 192 M. Wagner, A. Karner, P. Gattringer, B. Buchegger and A. Hochreiner, *Bioprinting*, 2021, **23**, e00142.
- 193 S. I. Koltsov, T. G. Statsenko and S. M. Morozova, *Polymers*, 2022, **14**, 5539.
- 194 K. K. Moncal, V. Ozbolat, P. Datta, D. N. Heo and I. T. Ozbolat, *J. Mater. Sci.: Mater. Med.*, 2019, **30**, 55.



- 195 T. J. Hinton, Q. Jallerat, R. N. Palchesko, J. H. Park, M. S. Grodzicki, H.-J. Shue, M. H. Ramadan, A. R. Hudson and A. W. Feinberg, *Sci. Adv.*, 2015, **1**, e1500758.
- 196 D. T. Schmieden, S. J. Basalo Vázquez, H. Sangüesa, M. van der Does, T. Idema and A. S. Meyer, *ACS Synth. Biol.*, 2018, **7**, 1328–1337.
- 197 A. F. Bonatti, I. Chiesa, G. Vozzi and C. De Maria, *Bioprinting*, 2021, **24**, e00172.
- 198 C. Yu and J. Jiang, *Int. J. Bioprint.*, 2020, **6**, 253.

